PB83-107953

U.S. Department
of Transportation
**Federal Railroad
Administration**

Improvement of Railroad Roller Bearing Test Procedures and Development of Roller Bearing Diagnostic Techniques

Office of Research and
Development
Washington, DC 20590

Volume II - Diagnostics

W.D. Waldron
J.M. McGrew
A.I. Krauter

Shaker Research Corporation
Northway 10 Executive Park
Ballston Lake, New York 12019

DOT/FRA/ORD-81/28.11

April 1982
Final Report

This document is available to the U.S. Public through the National Technical Information Service, Springfield, Virginia 22161.

Technical Report Documentation Page

1. Report No. FRA/ORD-81/28,II	2. Government Accession No.	3. Recipient's Catalog No. PB83 107953
4. Title and Subtitle IMPROVEMENT OF RAILROAD ROLLER BEARING TEST PROCEDURES AND DEVELOPMENT OF ROLLER BEARING DIAGNOSTIC TECHNIQUES (Volume II - Diagnostics)		5. Report Date April 1982
		6. Performing Organization Code
7. Author(s) W. D. Waldron, J. L. Frarey, A. I. Krauter		8. Performing Organization Report No. DOT-TSC-FRA-81-15,II
9. Performing Organization Name and Address Shaker Research Corporation Northway 10 Executive Park Ballston Lake, N. Y. 12019		10. Work Unit No. (TRAIS) RR028/R1309
		11. Contract or Grant No. DOT-TSC-917
12. Sponsoring Agency Name and Address U.S. Department of Transportation Federal Railroad Administration Office of Research and Development Washington DC 20590		13. Type of Report and Period Covered Final Report October 1974-April 1977
		14. Sponsoring Agency Code

15. Supplementary Notes

Under contract to: U.S. Department of Transportation
Research and Special Programs Administration
Transportation Systems Center
Cambridge MA 02142

16. Abstract A comprehensive review of existing basic diagnostic techniques applicable to the railcar roller bearing defect and failure problem was made. Of the potentially feasible diagnostic techniques identified, high frequency vibration was selected for experimental evaluation because it showed the most promise for implementation over a wide range of railroad deployment location requirements (from certification laboratory to trackside) and because it showed promise of being cost-effective while still providing a great deal of quantitative information regarding bearing condition. Tests were conducted in the laboratory on new and known faulty bearings and in a railroad wheel shop on bearings of unknown quality. It was found that minute defects in new bearings could be accurately identified using envelope detection and spectrum analysis techniques of the high frequency vibration signature and that simple peak detection was adequate to identify the "typical"grossly defective bearing. The degree of diagnostic system sophistication to cover the range from new to grossly defective was identified.

A mathematical model was developed to perform cost-benefit analyses of railcar roller bearing diagnostic approaches and procedural innovations. Results of the cost-benefit analyses that were made set the ground rules for allowable diagnostic system costs.

17. Key Words Railcar Roller Bearings, Bearing Diagnostics, High Frequency Vibration, Bearing Failure, Bearing Defects, Bearing Failure Progression, Envelope Detection.	18. Distribution Statement DOCUMENT IS AVAILABLE TO THE PUBLIC THROUGH THE NATIONAL TECHNICAL INFORMATION SERVICE, SPRINGFIELD, VIRGINIA 22161

19. Security Classif. (of this report)	20. Security Classif. (of this page)	21. No. of Pages	22. Price
Unclassified	Unclassified	165	

Form DOT F 1700.7 (8-72) Reproduction of completed page authorized

PREFACE

This study was conducted for the Federal Railroad Administration through the Transportation Systems Center (TSC) in Cambridge, Massachusetts. Mr. Roger K. Steele was the initial technical monitor. He was succeeded by Mr. James M. Morris.

New York State derailment data was provided and explained by Mr. Wallace R. Klefbeck of the New York State Division of Traffic and Safety.

Data from several railroads were made available to us in this study. Acknowledgement is made to Mr. R. F. Tuve of the Southern Railway System, Dr. P.E. Rhine of the Union Pacific and Mr. Dale Harrison of the Santa Fe. Southern Railway data formed the basis of the analysis conducted in Appendix D of this report. Mr. Tuve, furthermore, reviewed a draft of this report and made many suggestions for modifications. Acknowledgement of his help in reviewing this report does not imply that he or Southern Railway necessarily agrees with the contents, conclusions, or recommendations presented in this report.

The Southern Railway System made their Coster Shop available for diagnostic testing of bearings while installed on wheel sets. Acknowledgement is made to Messrs, Bible, Hayes, and Trollinger, whose tolerance of our intrusion allowed us to complete the tests successfully.

This study could not have been completed without the active cooperation of the staff of Brenco, Inc., who provided bearing defect data from three of their rework shops. Dr. Gerald Moyar, Vice President, Research and Development for Brenco, Inc., provided invaluable technical guidance.

Mr. O. W. Knoblock of the Association of American Railroads made available all relevant certification data and procedures.

The Southern Railway System, Norfolk and Western Railway, Delaware and Hudson and New Departure Hyatt also supplied valuable information and guidance. Messrs. R. F. Tuve and C. M. Scott of the Southern, Mr. H. Miller of the N&W, and Mr. J. T. Colpoys of the D&H were particularly helpful.

METRIC CONVERSION FACTORS

Approximate Conversions to Metric Measures

Symbol	When You Know	Multiply by	To Find	Symbol
		LENGTH		
in	inches	*2.5	centimeters	cm
ft	feet	30	centimeters	cm
yd	yards	0.9	meters	m
mi	miles	1.6	kilometers	km
		AREA		
in^2	square inches	6.5	square centimeters	cm^2
ft^2	square feet	0.09	square meters	m^2
yd^2	square yards	0.8	square meters	m^2
mi^2	square miles	2.6	square kilometers	km^2
	acres	0.4	hectares	ha
		MASS (weight)		
oz	ounces	28	grams	g
lb	pounds	0.45	kilograms	kg
	short tons (2000 lb)	0.9	tonnes	t
		VOLUME		
tsp	teaspoons	5	milliliters	ml
Tbsp	tablespoons	15	milliliters	ml
fl oz	fluid ounces	30	milliliters	ml
c	cups	0.24	liters	l
pt	pints	0.47	liters	l
qt	quarts	0.95	liters	l
gal	gallons	3.8	liters	l
ft^3	cubic feet	0.03	cubic meters	m^3
yd^3	cubic yards	0.76	cubic meters	m^3
		TEMPERATURE (exact)		
°F	Fahrenheit temperature	5/9 (after subtracting 32)	Celsius temperature	°C

*1 in = 2.54 (exactly). For other exact conversions and more detailed tables, see NBS Misc. Publ. 286, Units of Weights and Measures, Price $2.25, SD Catalog No. C13.10:286.

Approximate Conversions from Metric Measures

Symbol	When You Know	Multiply by	To Find	Symbol
		LENGTH		
mm	millimeters	0.04	inches	in
cm	centimeters	0.4	inches	in
m	meters	3.3	feet	ft
m	meters	1.1	yards	yd
km	kilometers	0.6	miles	mi
		AREA		
cm^2	square centimeters	0.16	square inches	in^2
m^2	square meters	1.2	square yards	yd^2
km^2	square kilometers	0.4	square miles	mi^2
ha	hectares (10,000 m^2)	2.5	acres	
		MASS (weight)		
g	grams	0.035	ounces	oz
kg	kilograms	2.2	pounds	lb
t	tonnes (1000 kg)	1.1	short tons	
		VOLUME		
ml	milliliters	0.03	fluid ounces	fl oz
l	liters	2.1	pints	pt
l	liters	1.06	quarts	qt
l	liters	0.26	gallons	gal
m^3	cubic meters	35	cubic feet	ft^3
m^3	cubic meters	1.3	cubic yards	yd^3
		TEMPERATURE (exact)		
°C	Celsius temperature	9/5 (then add 32)	Fahrenheit temperature	°F

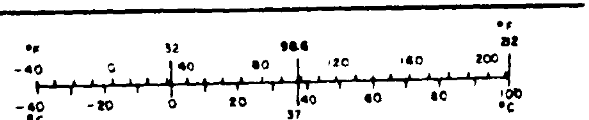

TABLE OF CONTENTS

Section		Page
1.	INTRODUCTION AND SUMMARY	
1.1	Background	1
1.2	Summary	2
1.3	Summary of Work and Report Organization	4
2.	DIAGNOSTIC SYSTEM REQUIREMENTS	6
2.1	Bearing Defect Modes Critical to Railroad Industry	10
2.2	Implications of Roller Bearing Diagnostic Systems	11
2.3	Concepts Selected for Evaluation	15
2.3.1	Bearing Temperature Rise	17
2.3.2	High Frequency Vibration	18
2.3.3	Ultrasonic Crack Detector	25
2.3.4	Grease Ferrography	25
2.3.5	Bearing Electrical Contact Resistance	27
3.	EXPERIMENTAL EVALUATION	32
3.1	Overview of Bearing Tests and Objectives	32
3.1.1	Shaker Research/NASA Component Tests	32
3.1.2	Failure Progression Tests	33
3.1.3	Certification Demonstration Tests	37
3.1.4	Wheel Shop Tests	38
3.2	Summary of Bearing Performance and Degradation	40
3.2.1	Temperature and Temperature Rise	40
3.2.1.1	Bearing Steady State Temperatures	43
3.2.1.2	Bearing Overgreased Temperatures	45
3.2.1.3	Undergreased Bearing Temperature	48
3.2.2	Progression of Defects and Failures	51
3.2.2.1	Progression Test Procedures	51
3.2.2.2	Test Bearings	52
3.2.2.3	Test Results	52
3.2.2.4	Failure Progression	54

			Page
3.3	Diagnostic System Effectiveness		61
3.3.1	High Frequency Vibration		61
3.3.1.1	Preliminary Vibration Analysis Tests		61
3.3.1.2	Failure Progression Test Results		64
3.3.1.3	Certification Demonstration Tests		67
3.3.1.4	Railroad Wheel Shop Tests		81
3.3.1.5	Summary of High Frequency Vibration Technique Results		90
3.3.2	Ultrasonic Crack Detection		96
3.3.3	Grease Ferrography		98
3.3.4	Electrical Contact Resistance		103
4.	COST MODELING		105
4.1	Description of the Technique		105
4.1.1	Schematic Diagram		105
4.1.2	Computer Model		109
4.1.3	Data		110
4.2	Results		110
4.3	Examples of Cost-Benefit Analysis		121
4.3.1	Derailed Bearing Diagnostic System		121
4.3.2	Improved Safety		124
4.4	Example of Time Dependence		132
5.	CONCLUSIONS AND RECOMMENDATIONS		136
5.1	Conclusions		136
5.1.1	Bearing Temperature Rise		136
5.1.2	Failure Progression		136
5.1.3	High Frequency Vibration		136
5.1.4	Ultrasonic Crack Detector		138
5.1.5	Grease Ferrography		139
5.1.6	Bearing Electrical Contact Resistance		139
5.1.7	Diagnostic System Deployment		139
5.1.8	Proposed Diagnostic System		140
5.2	Recommendations		140
6.	REFERENCES		142
APPENDIX A - COST MODEL COMPUTER PROGRAM			A-1
APPENDIX B - REPORT OF NEW TECHNOLOGY			B-1

LIST OF ILLUSTRATIONS

Figure		Page
1.	Comparison of Percent of Population Defective Under Different Inspection Criteria	12
2.	Relative Sensitivity of Four Bearing Diagnostic Systems	16
3.	High Frequency Vibration Peak Amplitude Detector	20
4.	Typical Signals from Defective Bearings	21
5.	Modified Crest Factor System Block Diagram	22
6.	Vibration Envelope Detector Block Diagram	24
7.	Summary of Diagnostic Systems Versus Complexity and Sensitivity	26
8.	Railcar Roller Bearing Lubricant Film Thickness	28
9.	Contact Resistance Signal	30
10.	Electrical Contact Diagram	30
11.	Constant Current Bearing Resistance System for Linear Output	31
12.	Bearing Component Test Rig	34
13.	Roller Bearing Test Rig for Failure Progression and Certification Demonstration Testing	36
14.	Testing for Bearing Defects at Southern Railway Wheel Shop	39
15.	Thermocouple Location Tests 2,3	41
16.	Steady State Temperatures, Test No. 6 (Bearings 112, 101, 110)	44
17.	Test Rig Bearing Temperature Rise (55 mph, 6 x 11 tapered roller)	46
18.	Effect of Overgreasing Bearing on Outer Race (Cup) Temperature Rise	47
19.	Temperature Rise Versus Time for Undergreased Bearing	49
20.	Bearing 104 Water-etched Cup (no damage progression from 100-hour test)	55
21.	Cracked Roller from Bearing 105A after 97.7 Hours	56

LIST OF ILLUSTRATIONS (CONTINUED)

Figure		Page
22.	Bearing 106, Spalled (no significant progression)	57
23.	Bearing 108, Spalled (severe cup and moderate roller damage progression)	58
24.	Bearing 110, Split Roller (no significant progression)	59
25.	Appearance of Brinelled and Water-Etched Bearing Surfaces Before and After 5000-Mile Failure Progression	60
26.	Progression of Race Spalls During Equivalent of 5000 Miles at 65 mph under 26,000 lb. Load (Bearing No. 113)	62
27.	Spalled Bearing Components for Test C3A	70
28.	Low Frequency Spectra Demodulated from 39.7 kHz	71
29.	Low Frequency Spectra Demodulated from 37.1 kHz	72
30.	Low Frequency Spectra Demodulated from 10 to 50 kHz	74
31.	Roller from Bearing 204 Following Test C4A	77
32.	Inner Race from Bearing 212 Following Test C5A	78
33.	Inner Race from Bearing 214 Following Test C4B	80
34.	Proportion of Condemnable Bearings Versus Vibration Characteristic Amplitude	83
35.	Proportion of Defective Bearings Vs. Characteristic Vibration Amplitude	84
36.	Results of Tests at Southern Railroad Wheel Shop Showing Typical Defects	85
37.	Bearing 204 Defect and Low Frequency Spectra Following Test C4A	87
38.	Demodulated Low Frequency Spectra from Bearing 212 Following Test C5A Using Bearing Turning Device	88
39.	Demodulated Low Frequency Spectra from Bearing 214 Following Test C4B Using Bearing Turning Device	89
40.	Summary of Single Component Tests	91

LIST OF ILLUSTRATIONS (CONTINUED)

Figure		Page
41.	Summary of Defect Variety	92
42.	Condition and Amplitude - Failure Progression Tests	93
43.	Condition and Amplitude - Wheel Shop Tests	94
44.	Condition and Amplitude - Certification Tests	95
45.	Mode of Operation - Ultrasonic Cup Crack Detector	97
46.	Ultrasonic Detection of Cracked Cups	99
47.	Roller Bearing Schematic	106
48.	Cost-Benefit Analysis - Derailment Diagnostic System	123
49.	Saving Effected by Roller Bearing Failure Reduction	128
50.	Effect of Increased Bearing Cost on Total Cost Saving for Various Failure Reductions	130
51.	Projected Total Population and Population of "Old" Bearings Assuming a Constant 18.8% Removal Rate	131
52.	Allowable Wayside Sensor and Increased Bearing Costs to Achieve a 61% Reduction in Catastrophic Bearing Failures and Hot-Box Sellouts by 1986 and 20×10^6 per-Year Cost Benefit by 1986	133
53.	Effects of Bearing Shop Reject Rate on Average Age of Bearing Population	134

LIST OF TABLES

Table		Page
1.	Review of Diagnostic Techniques	7
2.	Thermocouple Locations for Failure Progression Tests 4 Through 7 and Certification Tests 1 Through 5	42
3.	Failure Progression Test Result Summary	53
4.	Relative Ranking of Defects	64
5.	Progression Test Vibration Measurements	65
6.	Imperfection Frequencies	68
7.	Amplitude and Overall Noise Level at 12.04 Hz	73
8.	Amplitude and Overall Noise Level at 110.8 Hz	75
9.	Summary of Ferrographic Analysis	101
10.	Input Data	111
11.	Input Data Continued	112
12.	Cost Input Data	113
13.	System Costs - 1975 Base Case	117
14.	Branch Cost Sensitivity - 1975 Base Case	119
15.	Path Cost Sensitivity - 1986 Base Case	125
16.	Branch Cost Sensitivity - 1986 Base Case	127

NOMENCLATURE

Avg	Average	
C	Proportion	
F	Farenheit	
g	Gravitational Unit of Acceleration	$386.4 in/sec^2$
h	Film Thickness	in.
h	Hour	
HR	Hour	
Hz	Frequency	cycles/sec
K	Kilo (1000)	
L	Component Life	hours, years, miles
Lbs	Pounds	
L_n	Life for Which (1-n)% of All Components Will Survive	hours, years, miles
Mi	Mile	
Min	Minute	
mm	Millimeter	
mph	Miles Per Hour	
N	Number	
P-P	Peak-to-Peak	
Oz	Ounce	
RPM	Revolutions Per Minute	
T	Temperature	^oF
ΔT	An Increment of Temperature	^oF
δ	Surface Finish	in.
γ	Film Thickness	in.

1. INTRODUCTION AND SUMMARY

1.1 Background

The roller bearing was introduced into freight car journal use in the U. S. in 1954 and its numbers have risen so that today approximately 60 percent of the freight car fleet of U.S. railroads ride upon roller bearings. The change to roller bearings has led to a marked decrease in the number of set-outs for overheated axles (1). However, in the period from 1965 through 1971, there was an increase in the rate at which roller bearing equipped cars were reported to have hot bearings (2). The number of train accidents attributable to overheated roller bearings has remained a small portion of the total (near 1%). The observation of increased roller bearing setouts prompted the Federal Railroad Administration to caution "that the roller bearings become less effective with age" (2).

At the request of the Federal Railroad Administration (FRA), the Transportation Systems Center (TSC) initiated a program to explore the possibility of achieving improved railroad roller bearing testing and diagnostic procedures. The stimulus for this effort had been the problem encountered with service performance of a bearing design after it had satisfactorily passed the Association of American Railroads (AAR) dynamic tests as well as the observation based on a review of statistics that "roller bearings become less effective with age . . ."

In an effort to examine roller bearing failure and defect behavior in a most detailed fashion and to ascertain whether improved testing and diagnostic techniques could have a substantial cost-beneficial impact on bearing serviceability, a three-phase program was devised. The first phase, of four months' duration, had as its objectives: (a) the analysis of railroad roller bearing failure and defect behavior and the identification of failure modes; and (b) conception of improved cost-beneficial approach(es) to testing and diagnostics based on the results of (a). In phases II and III (one year each): (a) improvements in the test process were to be proposed and tested, leading to establishment of guidelines for improved cost-beneficial practices, and (b) potentially useful diagnostic approaches were to be developed and tested, leading to the definition of performance specificatior for one or more methods.

The results of the work performed by Shaker Research under Contract DOT-TSC-917 "Improvement of Railroad Rolier Bearing Test Procedures and Development of Roller Bearing Diagnostic Techniques -- Phase I and II" are contained in two volumes. Volume I (3) presents the test procedure aspects of the work, and Volume II the diagnostic aspects. This report (Volume II) describes the work directed at the development of roller bearing diagnostic techniques.

1.2 Summary

The initial approach to the design of a defective bearing diagnostic system was one of simplicity of operation designed to detect the more gross defects primarily deep spalls, brinells and cracked cups. The rationale for this approach was the fact that most bearings are removed from service for non-bearing-related causes, i.e. wheel defects and non-bearing-caused derailmen It was reasoned and shown analytically that considerable (several million dollars per year) money could be saved if a diagnostic system could identify those defects (brinells and cracks) that reasonably could result from a derailment and thus save the removal and rework shop costs for those bearings not suffering derailment damage. To this end, a system was built that coulc be used by a repair crew at a rip track or in a wheel shop. The capability of the system to adequately sense moderately gross condemnable defects was demonstrated both in a railroad rework shop and in the laboratory during the 600-mile failure progression tests.

However, during the course of the reliability analyses conducted for the certification effort, it became clear that the current practice of bearing removal for derailment and wheel-related reasons is the only effective meth the railroad industry has for inspecting bearings and subsequently removing defective bearings from the population. Without this vehicle for thorough inspection (approximately 8% of the population each year), the bearing fail rate will increase even faster than currently projected.

Thus, it became clear that any diagnostic system intended to replace current derailment and wheel-related bearing removal practices must be sensitive (and accurate) enough to detect defects of the size near that currently defined as "condemnable" per the AAR rules.

During the course of demonstration testing, the vibration-based diagnostic system (previously used for failure progression and wheel shop tests) was employed with added sophistication which included demodulation (envelope detection) of the high frequency vibration amplitude and real time spectrum analysis of the demodulated signal. By employing the more sophisticated vibration analysis techniques, defects that developed during the demonstration tests were readily detected. Furthermore, the detection level was sensitive enough to discern defects considerably smaller than defined as "condemnable" by the AAR.

Thus, it was demonstrated that a diagnostic system could be built to detect bearing defects of the size defined as just "condemnable" without removing the bearing from the axle, and this could be done in a "field" environment -- i.e., at a rip track or in a wheel shop. Furthermore, methods of achieving this objective short of employing complex and expensive laboratory-type analysis equipment have been identified.

Although a means of detecting bearing defects without removing the bearings from the axle has been defined, new and/or improved diagnostic system deployment schemes will have to be developed if the future roller bearing failure rate is to be reduced without imposing new bearing removal and inspection rules. That is to say, merely using diagnostic systems to check bearings on the axle following derailment or in a normal wheel shop environment will only save the industry the <u>cost</u> of current-practice bearing removal and inspection -- it will not reduce the number of failures. Apart from improving quality, the only way to reduce the failure rate is to increase the frequency of bearing inspection.

One attractive approach would be to develop a less sophisticated system designed to detect the more gross defects that could be expected to lead to failure in several hundreds or thousands of miles. Such a system might be a wayside type or could be deployed at classification yards. It could be vibration or temperature based and could employ primary sensors (in the case of being temperature based) integral with the bearings.

However, before such a development is undertaken, two things must be very seriously considered -- investment cost and accuracy of failure prediction. Preliminary cost-benefit anaylses based on 1986 failure, setout, and population projections showed that the added cost to a new bearing either for improved quality or for the addition of a primary diagnostic sensor must be kept to a few dollars if the added investment cost is to be paid for by savings accrued from reduced failures and setouts. The study further showed that, depending upon the ability of a system to predict failures, thousands to tens of thousands of dollars could be spent on a wayside or yard-type diagnostic system.

As a prelude to the development of a wayside or yard-type diagnostic system, it is recommended that additional failure-progression-type tests similar to those conducted on the subject program be conducted. For these tests, bearings which are more severely damaged than those employed on the subject program should be considered so as to shorten the test time and to provide a vehicle for studying the final stages of failure. Furthermore, all available prototype diagnostic approaches -- both vibration and temperature -- should be employed. Following such a test program, the various approaches could be better evaluated and more rational specifications prepared.

1.3 Summary of Work and Report Organization

The work was divided into two basic tasks: a test procedure task, and a diagnostic task. The test procedure task was covered separately in Volume I (3). This volume covers the diagnostic task.

The diagnostics portion of the program was initiated by a literature search for available diagnostic techniques that might be applicable to the broad railcar roller bearing failure problem. Although the search did not turn up any obvious solutions, it brought into focus the variety of techniques that might be useful in addressing a particular failure mode of interest. Based upon this literature search, the actual bearing failure and defect analysis work being conducted concurrently in the certification area, and a study of actual railroad operations pertaining to roller bearings, a rationale for evaluating selected diagnostic approaches was developed. This part of the work is covered in Section 2 of this volume.

Section 3 addresses the experimental work that was accomplished. The experimental work had two main thrusts - evaluation of selected diagnostic techniques and evaluation of the rate at which selected bearing defects progress to failure. The latter (failure progression tests) were conducted on bearings having a variety of classical defects (spalls, brinells, cracks, water etches, etc.) under full load, high speed conditions for a period equivalent to 6000 miles. The evaluation of selected diagnostic techniques included bench testing, testing under simulated operating conditions, and testing of bearings while installed on actual railcar axles. Section 3 also addresses itself to the sensitivity (i.e., the ability to detect and distinguish defects) of the various diagnostic approaches evaluated experimentally during the course of the program.

To determine the cost effectiveness of various ideas and approaches developed during the work, a cost model was developed early in the program. This cost model was used a number of times to test hypothesized situations and proved to be a valuable tool in weeding out ideas that were not cost effective early in the program. The cost model, which is described in Section 4, attempts to consider all possible cost factors and bearing location situations between the time a bearing is manufactured and the time it is finally scrapped.

The report concludes in Section 5 with a description of the conclusions reached in the program and recommendations for further work.

2. DIAGNOSTIC SYSTEM REQUIREMENTS

The initial task in the investigation of diagnostic techniques applicable to railroad roller bearings was to conduct an extensive literature search of the subject. The search, as is normally the case, turned up some references that were directly related or applicable to railroad roller bearings and also unearthed sources that might be related in some way.

Over 100 detection concepts were reviewed for possible application to the railway roller bearing problem. These concepts were initially separated into six categories:

1. Mechanically Actuated
2. Optically Related
3. Electromagnetic
4. Vibration Associated
5. Resistance Element
6. Magnetic Types.

In order to make a better evaluation of the applicability of each detection concept, each was further categorized. The categories were:

1. Failure Mode Application
2. Diagnostic Systems Deployment Site
3. Railroad Experience in Use of the Technique
4. The State of the Development.

Table 1 is a summary listing of some of the most pertinent techniques reviewed.

Those techniques which are presently used by the rail industry are noted by the darkened circles in the table. Although several techniques are employed by the industry (vide first column of circles), very few are used in determining failure conditions in bearings. Only five techniques were found to be used at the present time (vide the columns under "Defects Sensed") in establishing bearing defect conditions.

TABLE 1. REVIEW OF DIAGNOSTIC TECHNIQUES

● Now in Use
0 Possible Tool
x Maybe
y Yes

DIAGNOSTIC TECHNIQUE		Present Rail Tech.	In Development	Where Applicable: Railyard	Shop	Trackside	Wayside	Ride Along	Certification	Defects Sensed: Surface Defects	Lubricant	Seal	Broken Parts	Size Over/Under	Improper Lateral	Bolt Integrity	Backing Ring	Adapter	Passive
MECHANICAL	Feeler Gages	●		0	0	0			0	●			0	0	0		●	0	y
	Flow Sensors				0			0	0	0	0	0	0	0		0	x		
	Inspection Gages - Dial	●		0	0	0			0	0		0	0	0	●		0	0	y
	Electronic				0				0	0				0	0		0		
	Air				0				0					0	0				
	Load Cells				0				0						0	0	0		
	Phase Change		●					0	0		0	0							y
	Pressure Sensors				0			0	0		0	0	0						
	Hardnass Detection	●		0	0	0			0										y
OPTICAL	Chromographic				0				0		0								
	Dye Penetrants	●			0				0	0		0	0						y
	Encoders			0	0	0		0	0			0							
	Fiber Optic			0	0	0		0	0	0	0	0	0	0	0				y
	Fluoroscopy									0	0	0	0						y
	Grazing Angle Illum.	0	●		0				0	●									
	Laser				0		0		0	0			0						
	Photoelectric	●		0	0	0	●	0	0				0			0			
	Radiometers (Hotbox)	●		0		0	●				●	0							
	Reflectivity Change	●		0	0	0		0	0		0	0				0			y
	Spectrographic								0		0								
	Microscopes				0				0	0			0						y
ELECTRO-MAGNETIC	Capacitive			0	0	0		0	0	0	0	0	0	0					
	Conductive (Thermal)	●		0	0	0		0	0		0	0							
	Eddy Current	●		0	0	0		0	0	●			0	0	0	0			
	LVDI				0				0	0			0	0					
	Piezoelectronic			0	0	0	0	0	0	0			0						
	Radiographic								0	0			0						
	Thermistors			0	0	0		0	0		0	0							
	Thermovision®			0	0	0	0		0		0	0							
VIBRATION	Sonic								0	0	x		0						
	Ultrasonic	●		0	0	0	●	●	0	0	x	0	0						
	Resonant Rocking		●					0											
RESISTANCE	Continuity Meas.	●		0	0	0	0	0	0	0	0		0		0	0			
	Humidity Sensors			0		0		0			0								y
	Strain Gage			0	0	0		0	0	0	0		0			0			
	Thermocouple				0			0	0	0	0								
	Wear Detector			0	0	0		0	0			0						0	y
MAGNETIC	Barkhausen								0	0			0						
	Ferrographs		●		0				0	0	0		0						
	Hall Effect				0				0				0						
	Search Coil								0				0						
	Speed Pick-up (pulse)	●		0	0	0	●	●	0		0	0							

Specifically, the five types used in bearing-related detection schemes include feeler gages, dial gages, grazing angle illumination, radiometers, and eddy current detectors. The AAR light stand (4) necessitates use of feeler gages and grazing angle lighting. Dial gages are used in rework facilities for establishing sizes of bearing bores and wheel shafts. Radiometers are used principally in many different forms as "hot-box" detectors. Eddy current sensors are presently utilized by Sante Fe Railway Company (5) in the detection of spalls and brinells in their roller bearing shop. This unit has been in operation since 1973 and is intended to replace the approved AAR light inspection stand.

Non-bearing-related sensing systems employed by the rail industry in fault detection techniques include hardness checkers, dye penetrants, photoelectric sensors, temperature sensors, ultrasonic detectors, continuity measurement and pulsed speed pickups. These sensors are well recognized by the industry in the following areas:

1. Metal hardness checking (Teleweld, Inc.) is performed in wheel and rework facilities as well as on track rails in the field.
2. Dye penetrants are used in metal surface analysis.
3. Photoelectric sensors (6) are deployed in car high and wide checking systems.
4. Temperature indicating is done routinely in engine monitoring.
5. Ultrasonics is used worldwide (7) in rail and wheel crack fault systems.
6. Continuity measurement (8) is used in determining car presence through wheel and axle shunting of electrically energized rails.
7. Pulsed speed pickups are used in determining train velocities and distances traveled.

Additional development areas of diagnostic sensing which were reviewed and may prove useful to the rail industry include phase change alloys, new electronic grazing angle illumination work and ferrography. The Navy, in conjunction with the FRA, is developing a sensor which employs a phase-sensitive alloy to warn of impending derailments (9).

Grazing angle illumination has been used by the Bendix Corporation (10) to scan and sort bearing rollers automatically. An electronic logic system determines the degree of the damage to rollers based upon high angle optical reflectivity. Reflectivity level as well as peak-to-peak variations are considered in establishing the degree of damage. Ferrographs (a trademark of Trans-Sonics, Inc.) have been used successfully (11) in bearing defect analysis.

The conclusion drawn from this initial search was that there are very few directly applicable diagnostic systems available. Even those techniques which,have been applied to bearings in other environments might require great ingenuity to be applied to railroad bearings.

Although the initial search did not bring forth any obvious railcar roller bearing diagnostic solution, it identified possible techniques that could be applied to railroad bearing diagnosis. Along with the listing of possible techniques, Table 1 identified which failure mode might be detected and where such a system might be deployed. These two elements of information are essential to the task of evaluating the usefulness and cost effectiveness of a proposed system.

The deployment of the hot-box detector illustrates this point. The failure mode detected by this system is the elevation of operating temperature of the bearing. It is a secondary failure mode in that if some other failure had not occurred (low grease or broken cage, for example) there would be no reason for the temperature to rise. Indeed, it is suspected that almost all bearing defects progress to failure through this symptom. The problem encountered in detecting this symptom is that the bearing is in the act of catastrophic failure and the time to effect preventative action is short. The hot-box detector has been successful in reducing plain bearing derailments as a result of deployment at intervals of approximately 30 miles on main lines. Recent work (12) indicates that the spacing required for protection against roller bearing defects may approach half of the spacing required for plain bearings. Not only is it necessary to identify the failure mode to be detected, it is also necessary to know how long it takes to progress to catastrophic failure in order to establish system deployment.

2.1 Bearing Defect Modes Critical to Railroad Industry

Initial tasks in the overall program provided bearing defect and failure data from several sources. One source was bearing defect data gathered at rework shops and complemented by a study of the AAR rules pertaining to bearings and several discussions with operating personnel. These data are reviewed in Volume I of this report and show that 18% of the bearings returned for rework have condemnable defects in one or more of their component parts. Defects noted included spalled, brinelled, cracked, etc., internal components such as races or rollers and oversize cone bore sizes. Another source of data was the reports that are made on the causes of confirmed hot-box detector setouts. The causes listed were such things as overgreasing, leaking seals, misplaced adapter, etc., and not the internal components of the bearings. There were, of course, a portion in which the bearing was destroyed and no cause could be ascertained.

While these two sources of data seem to conflict, one should be aware that the number of bearings returned for confirmed hot-box setouts represents less than 1% of the total number of bearings returned for rework. Furthermore, the over-greased condition which represents the majority of the setouts (Table 5, Volume I) causes elevated temperatures in bearings that trigger a hot-box detector. However, tests described in Section 3.2 show that this condition does not necessarily lead to catastrophic failure. It thus seems that procedural changes would be more effective in reducing the exasperating over-greased condition than some diagnostic technique.

Volume I of this report discussed the number of bearings that will be in service in the year 1985 which will contain condemnable defects. At that time most of the population will be roller bearings and the average age of the bearings will reflect the more mature population of bearings in service. It is felt that the percentage of condemnable bearings in service at that time must be reduced. If not, the problem of roller bearing failures will escalate to an unacceptable level. In other words, the problems which are the most obvious today (i.e., overgreased bearings) may mask the more insidious problem for tomorrow (i.e., internal defects).

In reviewing the techniques of Table 1, it is seen that there are no developed techniques that can be used to inspect the internal condition of a roller bearing without disassembling the bearing, clearly an unacceptable solution for the field.

The future importance of detecting the internal condition of a roller bearing coupled with the lack of a noninvasive method of accomplishing this inspection has led Shaker Research to identify failure modes that should be of importance to the railroad industry in the future. These modes would include:

- Surface spalls of rollers and races
- Surface brinelling of rollers and races
- Cracked cup, cone or roller
- Severely water-etched internal surfaces.

2.2 Implications of Roller Bearing Diagnostic Systems

Analysis contained in Section 3.7.2 of Volume I (3) prepared under this contract shows that the two major reasons for bearing removal and return to the rework shop for inspection are derailment and maintenance of wheels. During this inspection, bearings with condemnable defects are scrapped. Figure 1 compares the future percentage of a population of bearings introduced at year 0 ex-

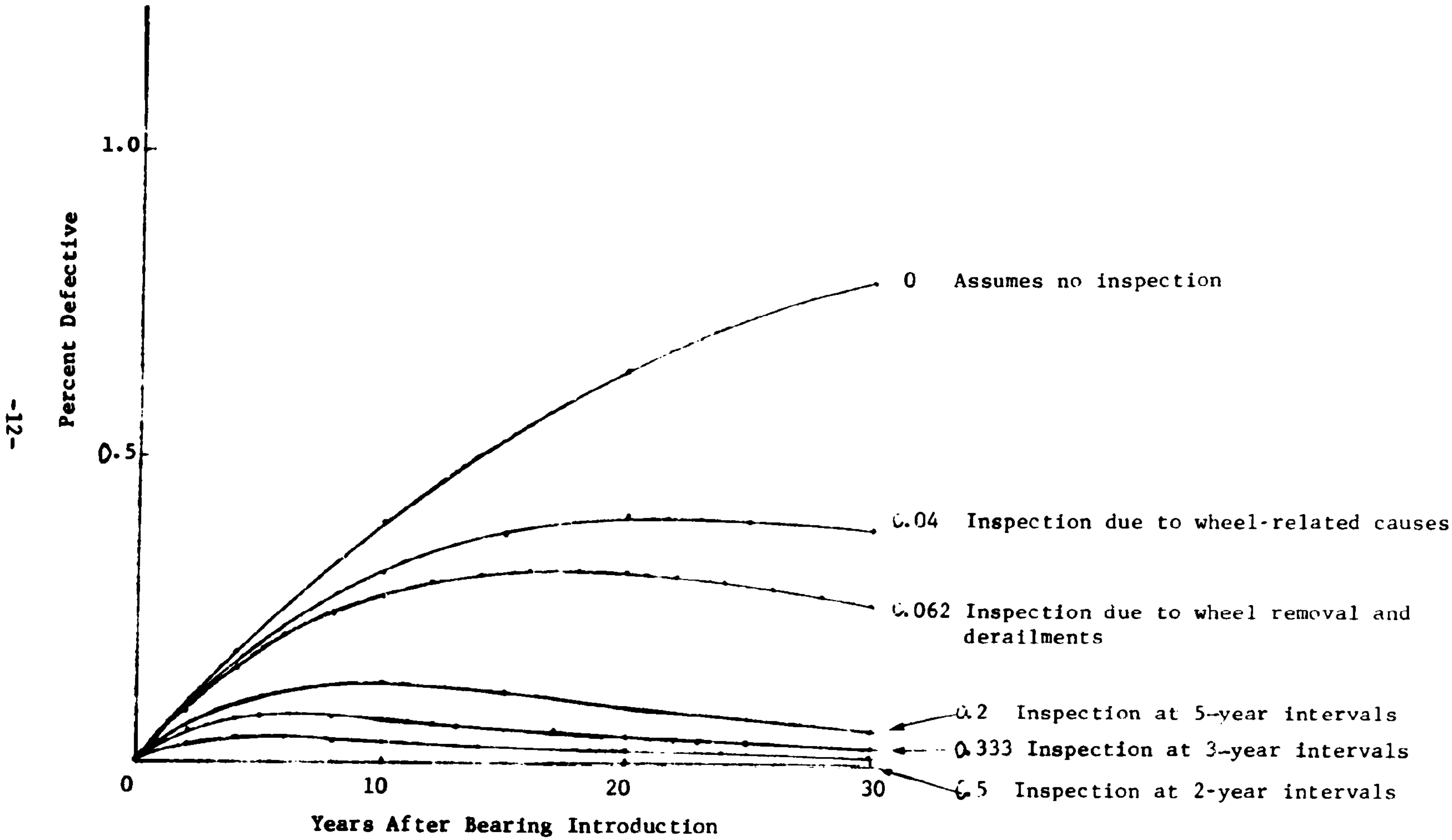

Figure 1 Comparison of Percent of Population Defective Under Different Inspection Criteria

hibiting condemnable defects with and without the inspection allowed by the present AAR derailment rule. It can be seen that the real benefit of the AAR rule is to provide a system by which a random sampling of the bearing population is removed and inspected. Of course, in addition, the rule also accomplishes its primary objective of removing those bearings which were seriously damaged during derailment. However, this number is small.

What the foregoing reasoning leads to is a modification of the requirements for a diagnostic system. If our initial approach is used and a diagnostic system is developed that removes only the seriously damaged bearings following a derailment, then the savings projected in Section 5 and shown in Figure 48 could be realized in the short term. We would pay the additional penalty of an increased defect rate in the future as shown in Figure 1. Interestingly enough, this future penalty does not relate at all to the act of derailment. This means that the system proposed must accomplish two objectives:

1. It must reject those bearings damaged by the derailments.
2. It must reject those bearings with AAR condemnable defects.

Of course, if Objective #2 is accomplished, Objective #1 has also been met. The reverse is not true, i.e., a system designed to accomplish #1 does not automatically accomplish #2.

The interesting result of the AAR rule is that the railroad industry uses freight train derailments as a method of randomly sampling the bearing population for inspection. The other method of sampling the bearing population for inspection involves worn or damaged wheels. For these two inspection selection processes the following number of bearings are inspected per year: (1974)

Derailments	196,000
Wheel-related	395,000.

For these bearings inspected, 18.8% have at least one condemnable component. Data available did not allow determining a percentage for each inspection cause. Inspection of bearings due to derailment is a sample size not set by the industry. In fact, if the industry succeeded in reducing derailments, the sample size would go down and thus the percentage of defective bearings in the population would increase with time.

If the AAR derailment rule is to be modified to allow on-axle inspection, then the diagnostic system to be used to inspect these bearings at a rip track following derailment must be more sophisticated than originally planned. If, however, a different basis were set for the sample of railroad bearings for inspection, then it might be possible to utilize the more sophisticated system for that sample and the simpler system for the derailment sample.

An integrated approach to railcar roller bearing diagnostics involves four elements. Two of these elements have been shown to be feasible during the present program. Additional development or experimentation is required on the other two. A total protective system would include:

1. The establishment of an AAR rule requiring roller bearing inspection at some periodic interval between 2-5 years. It has been shown that an automated diagnostic system could be developed that would allow on-axle bearing inspection quickly and that its sensitivity is comparable to present AAR condemnable defect levels for spalls, cracks, brinells and water-etched bearings.

2. The establishment of an on-axle test procedure to inspect roller bearings following a derailment. The sensitivity of this system must be adequate to identify gross defects caused by the derailment.

3. Search for a system that could be used at widely spaced wayside locations that would be capable of identifying grossly defective bearings prior to the generation of heat and catastrophic failure. The acoustic technique appears to offer promise for this application.

Implied in element 3 is the possibility that an onboard sensor could be substituted for either wayside system.

Available dollars for this system approach would be derived from savings achieved by not removing all derailed bearings for return to the bearing rework facility and from a reduction in the future catastrophic failure rate. These data are presented in Section 4.3.1 and 4.3.3.

Figure 2 relates the four elements of the diagnostic system to the point in the failure progression of a bearing.

2.3 Concepts Selected for Evaluation

The diagnostic concepts selected for evaluation in this program were:

- o Bearing temperature rise
- o Bearing high frequency vibration
- o Grease ferrography
- o Ultrasonic crack detection
- o Bearing electrical contact resistance measurements.

Bearing temperature rise instrumentation was selected because it has been seen that information relating the bearing temperature to internal defects is needed to evaluate the deployment of hot box detectors for roller bearings as well as to obtain data that would allow the evaluation of the failure progression time available for on-board sensors that have been proposed as protective devices for railcar roller bearings.

Based on the experience of Shaker Research in the diagnosis of rolling element bearings utilizing high frequency vibration, this technique was selected for evaluation on all tests run. High frequency vibration techniques may be implemented using several different levels of sophistication. The objective of all testing was to establish a relationship between defect size and data processing equipment required.

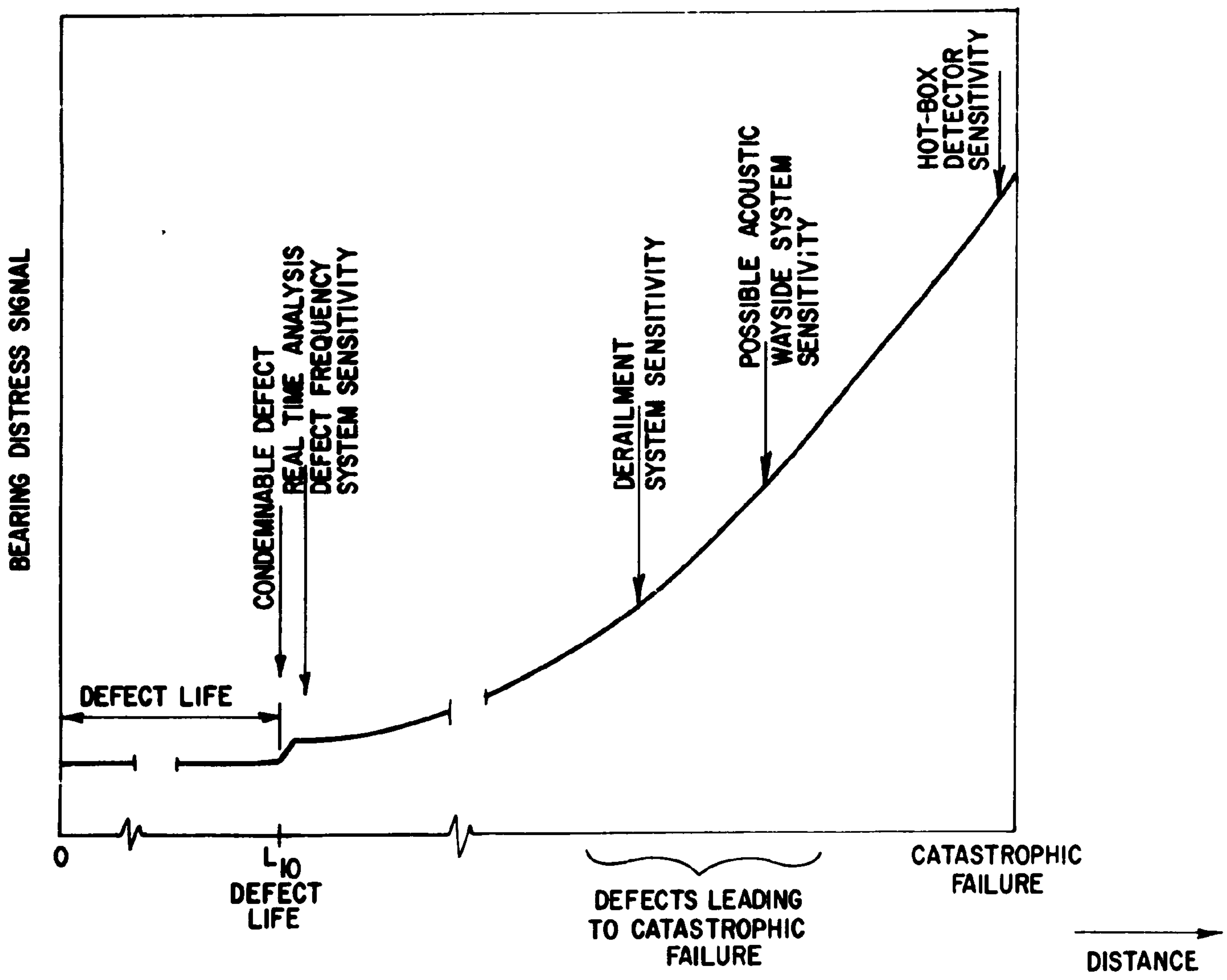

FIGURE 2. RELATIVE SENSITIVITY OF FOUR BEARING DIAGNOSTIC SYSTEMS

The inclusion of ultrasonic crack detection is not to test the validity of the concept since this is a well documented nondestructive testing technique, but rather to evaluate it specifically for detecting cup cracks caused, say by a derailment. In this case the emphasis was on a quick test with an easy to interpret difference between a good and cracked cup.

Ferrography is a technique developed by Trans-Sonics, Inc., that analyzes the magnetic material content of a lubricating oil. Whereas spectrometric oil analysis can provide data on the concentration of all elements, ferrography can provide data on the size distribution of iron contaminants such as those produced by degrading bearings. The technique is, of course, usually applied to bearings located in a circulating oil lubricating system. The technique presents a problem if applied to railcar roller bearings in that a sampling technique would have to be developed to extract grease from the bearing. Not only the method of getting at the grease, but which portion of the bearing collects a greater concentration of contaminants and would thus be the best location, needed to be examined. It was to answer this latter question that ferrography was to be evaluated in closely controlled lab tests.

Bearing electrical contact resistance measurements have been used in conjunction with rolling element bearings to examine the characterization of the lubricating film in the bearing. Preliminary testing demonstrated that added information on bearing condition could be generated by performing a spectral analysis of the resistance waveform in much the same manner as vibration analysis. This technique showed promise of supplementing the high frequency vibration technique and was selected for evaluation during some portions of the testing.

2.3.1 Bearing Temperature Rise

The hot-box detector "looks" at the bottom of the cup as the train passes over. Therefore, it was desired to document the surface temperature of this portion of the bearing. The Naval Surface Weapons Center has been working under contract to the FRA to develop an onboard sensor to warn of impending bearing failure. The phase of the Navy program that developed data and the sensor system, and evaluated the system for plain bearings, has been completed (9). The program phase concerning roller bearings has been initiated. Roller bearing temperatures under operating conditions will be obtained under the present program by NSWC personnel.

The program being run by NSWC and the failure progression tests performed by Shaker Research complement each other. NSWC will obtain temperatures under real conditions but will be limited in its opportunity to operate defective bearings. The test stand used by Shaker Research and described elsewhere in this report will allow defective bearings to be operated; however, the three test bearings in close proximity to each other do not allow for normal heat dissipation and therefore will produce higher temperatures than would normally be obtained. Temperature rise, however, should be more accurate. For this reason, the temperature locations chosen for the test rig were in the same locations as selected by NSWC. Their locations are shown in Figure 17 (Section 3.2.1).

2.3.2 High Frequency Vibration

In a normal rotating machine (not reciprocating), motion should be very smooth with very little part-to-part impacting occurring. As a machine deteriorates, this deterioration is often marked by harsher operation in which component-to-component rubs and impacts occur. When these happen, the component impacted or rubbed will resonate at one of its natural modes. For unrestrained parts, this would normally be the lowest mode that could be excited by the location of the impact. A combination of component restraint (fit) and the fact that at high frequencies, very small motions allowed by this restraint will produce very high acceleration levels results in high level accelerometer signals produced in the frequency range above 15 kHz. For example, a deflection of only one micro-inch at 100 Hz and 50 kHz will result in acceleration levels of 0.001g and 250g, respectively.

When this concept is applied to rolling element bearings, the excitation of the high frequency resonance is due to imperfections in the contacting surfaces that result in an impact. Defects such as spalls, brinells, water etch and cracked or dented rollers are examples of the type of defect that can excite the high frequency vibration.

Several different detection methods may be used to indicate defective bearings. In general, it can be expected that the tradeoffs between detection methods involve simplicity versus complexity of the detection system on the one hand and sensitivity of detection on the other. The systems are described in this section while the results obtained are reviewed in a later section.

The simplest detection scheme involves measuring the peak amplitude in the high frequency region--usually for railroad roller bearings in the 15 kHz to 50 kHz region. Figure 3 shows a block diagram of such a simple system.

A typical signal generated by a defective bearing is shown in Figure 4. Note the short bursts of high frequency data that are generated every time a roller contacts a defect in the outer race or other impact rates for other defects. A peak reading meter will indicate the amplitude of these peaks but will provide no information on their duration or other wave shape characteristics.

Another form of detection attempts to measure this bursting nature of the signal. A measurement is used in electrical engineering called the crest factor that ratios the peak signal amplitude to the true RMS signal amplitude. It can be seen that if the peak increases (in Figure 4), the peak reading goes up directly while the RMS value increases much less due to the fact that the majority of the signal over one period does not change. An approximation of the crest factor may be made if the high frequency vibration signal is envelope-detected as shown in Figure 5. This accom-

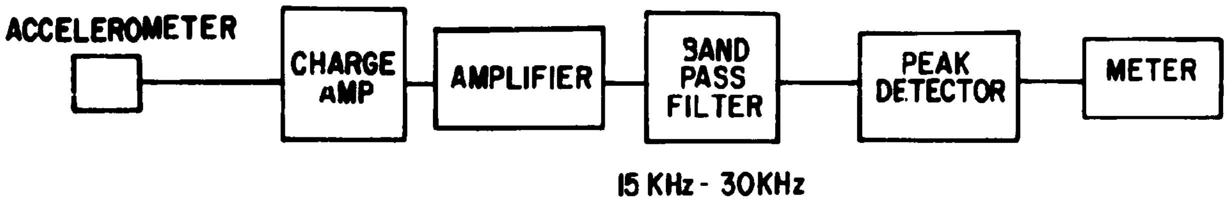

FIGURE 3. HIGH FREQUENCY VIBRATION PEAK AMPLITUDE DETECTOR

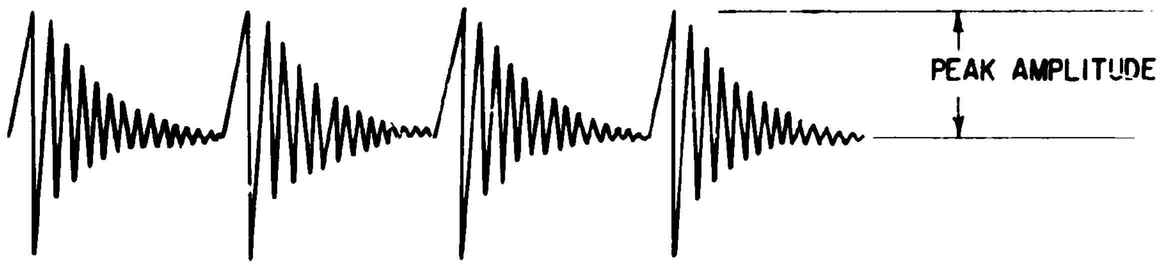

a) FILTERED HIGH FREQUENCY VIBRATION - 15 KHz to 30 KHz

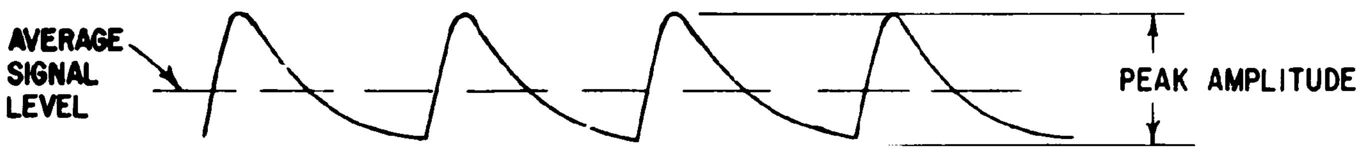

b) DEMODULATED HIGH FREQUENCY VIBRATION SHOWING PEAK & AVERAGE SIGNAL LEVELS

FIGURE 4. TYPICAL SIGNALS FROM DEFECTIVE BEARINGS

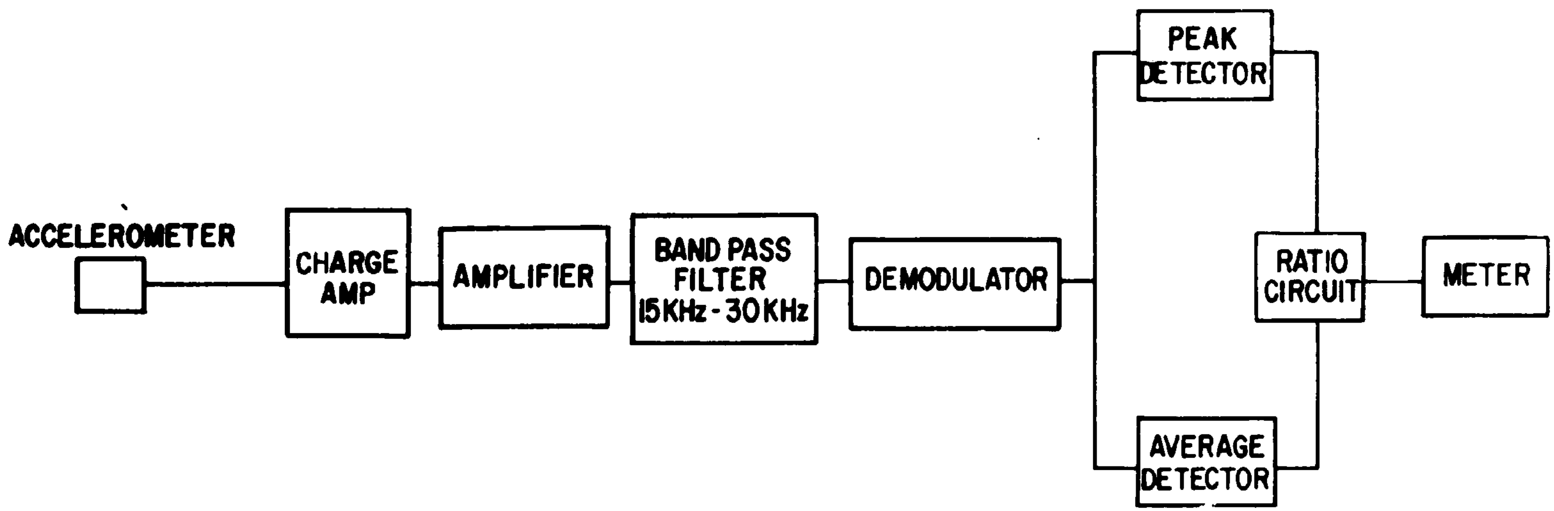

FIGURE 5. MODIFIED CREST FACTOR SYSTEM BLOCK DIAGRAM

plishes two things -- it removes the negative portion of the signal and also removes the high frequency carrier -- leaving a low frequency signal at the impact repetition rate. Removing the negative portion of the signal allows the same type of information as provided by the crest factor to be obtained by ratioing the peak amplitude to the average amplitude. A system configuration that provides the desired ratio is shown in Figure 5. In the detailed diagram of both the simplified system and the ratio system, the time constants selected for the rise time and decay time of both the peak and average detector must be carefully selected or errors will enter the data that reduce the sensitivity of the system to bearing defects.

A conventional vibration technique used for many years analyzes the low frequency vibration using spectrum analyzers of one type or another. The idea is to search the spectra for the presence of roller bearing defect signals. The frequency can be calculated knowing the geometry of the bearing and its rotational speed. The same technique can be used with the envelope-detected data and experience has shown that the detection sensitivity is many times greater than analyzing the low frequency data. Figure 6 is a block diagram of a system in which the frequency spectra at various stages of processing are shown.

The power of modern real time analysis is such that it allows very narrow band analysis to be performed in a short period of time. Figure 6 also shows an alternate method of processing the envelope detector data in which a band pass filter is used to search the data for the bearing defect signals. The sensitivity of the two methods (band pass filter versus real time analyzer) differs due to the band width of the two filters used.

If, for example, a defect signal exists at 150 Hz, and the real time analyzer (500 line) is set for spectra to 200 Hz, then the band width will be 0.4 Hz. If a band pass filter of $\pm$ 5% filter width is tuned to 150 Hz,

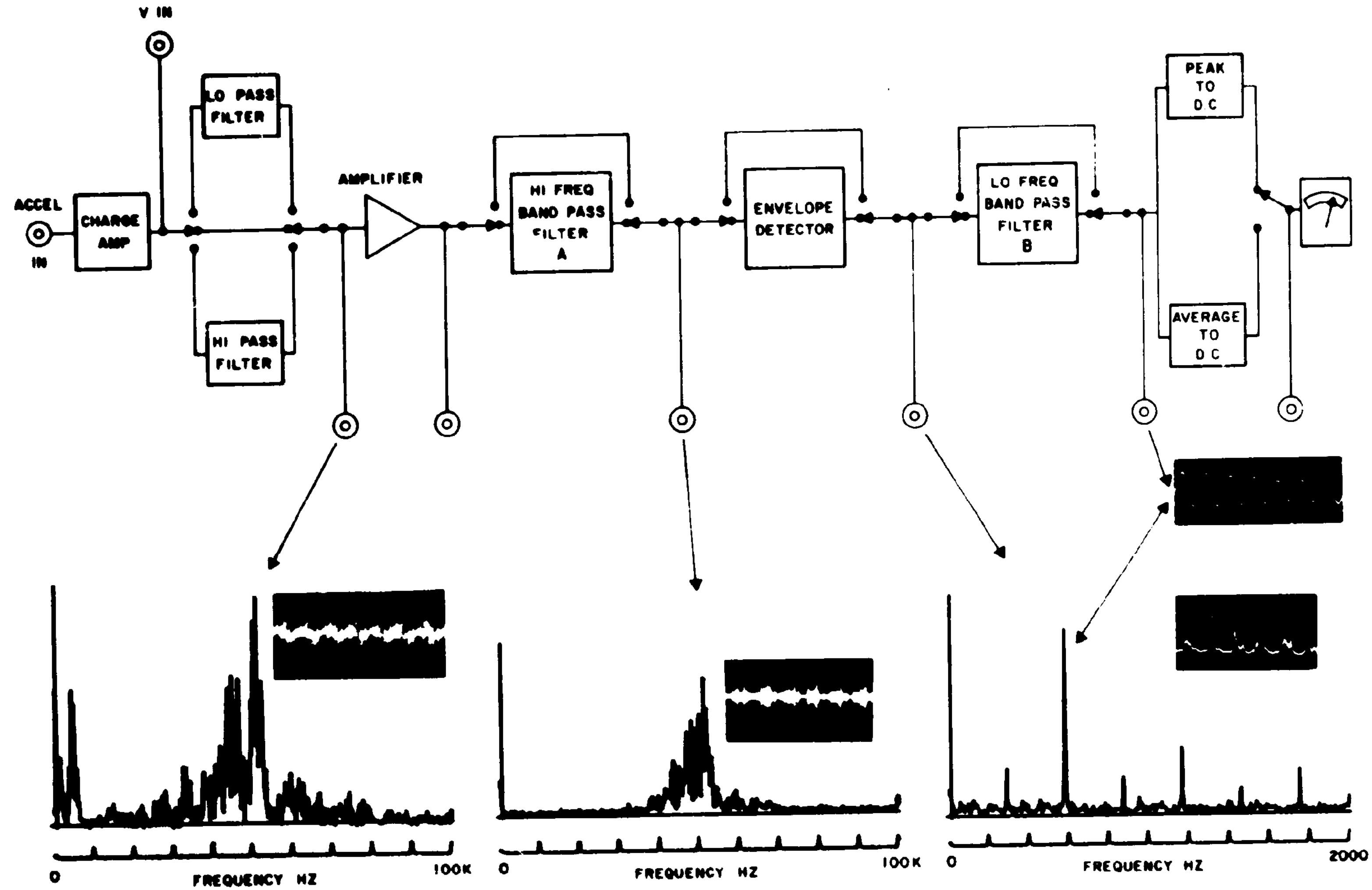

FIGURE 6. VIBRATION ENVELOPE DETECTOR BLOCK DIAGRAM

then its band width will be 15 Hz. The signal to noise ratio of the two filters is proportional to the inverse square root of the filter band width. Theresult is that for this case, the real time analyzer will be over six times as sensitive to the defect signal as the $\pm$ 5% band pass filter.

The above discussion shows that the term "bearing vibration analysis" does not describe an analysis technique. There are other techniques in addition to the few described above that could be and are utilized by other investigators in the field. The important characteristic of any technique is where it is located on the complexity scale and what kind of sensitivity to defective bearings it exhibits. Figure 7 is a block diagram of the techniques discussed, shown in ascending complexity as one moves to the right.

2.3.3 Ultrasonic Crack Detector

Several approaches were reviewed to evaluate a crack detection scheme for bearing cups damaged during derailments. One possibility was to use a modified version of the Wheelfax (13) unit that is being developed to inspect railroad wheels. After review, this was rejected for two reasons. The present unit introduces surface waves into the wheel. To transmit these waves from the transducer to the test item requires a good surface finish. This is normally available for a wheel but definitely not for a bearing. In addition, extensive modification would be required, primarily in a frequency change to accommodate the smaller diameter bearing when compared to a wheel. For this reason it was decided to use standard off-the-shelf equipment described in Section 3.3.2.

2.3.4 Grease Ferrography

This technique (11) involves sampling bearing lubricant at periodic intervals and monitoring the presence of metallic wear particles. A sudden

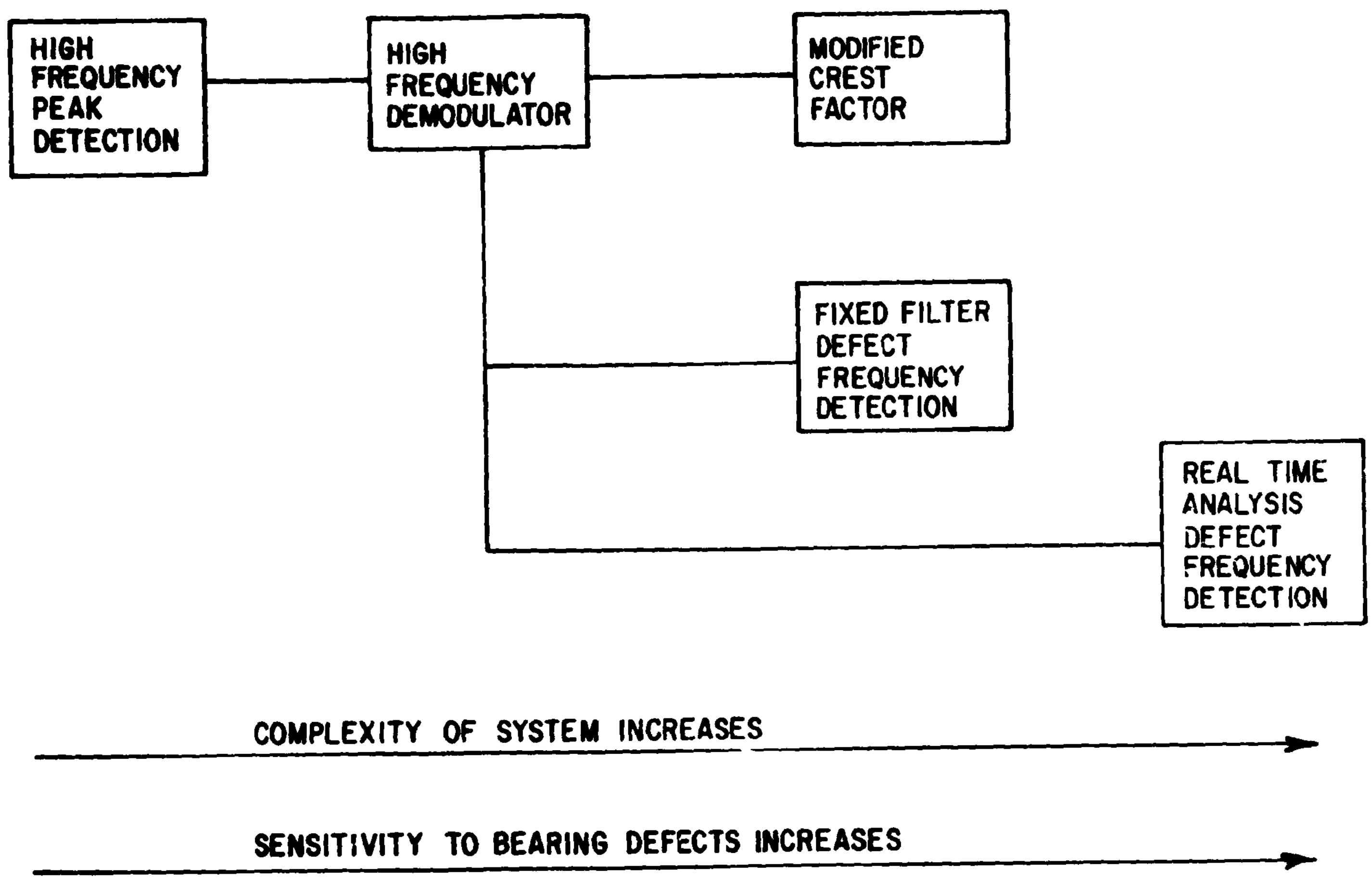

FIGURE 7. SUMMARY OF DIAGNOSTIC SYSTEMS VERSUS COMPLEXITY AND SENSITIVITY

rise of such particles in the lubricant indicates an abnormal wear situation in the bearings. The metal particles, usually iron or steel, are attracted by magnetic fields and can be deposited on specially prepared substrates for microscopic examination. The technique is particularly useful in systems such as jet engines where oil is the lubricant and it is circulated continuously throughout the bearing system.

Samples of grease were taken during the bearing certification tests described in Section 4, Volume I (3). Samples were not taken during the failure progression tests since the degraded bearing was assembled using clean grease. While progression would produce new particles, their number would not relate to the damage which had previously occurred.

Additional development of the ferrography technique is required to apply it to grease lubricated bearings such as the railcar roller bearing. Although the amount of grease needed for sampling is small, the question of exactly where it should be taken from and how to get it out of the bearing is discussed later in Section 3.3.3.

2.3.5 Bearing Electrical Contact Resistance

When rolling element bearings are operated, metal-to-metal contact can occur at the contact interface of the elements. The degree of contact is determined by the lubricant film thickness within the bearing. The lubricant film thickness generated depends primarily upon the load applied to the bearing, the speed of operation and the surface roughness of the rolling element components.

Present day railcar roller bearings operate with a high degree of metallic contact. This is to say that the film generated from rolling is rarely greater than the surface finish of the bearing components. This ratio of film to finish (Lambda) is shown for all loads, speeds, and two temperatures normally encountered in railcar operation in Figure 8. For most operating conditions the Lambda ratio is less than two.

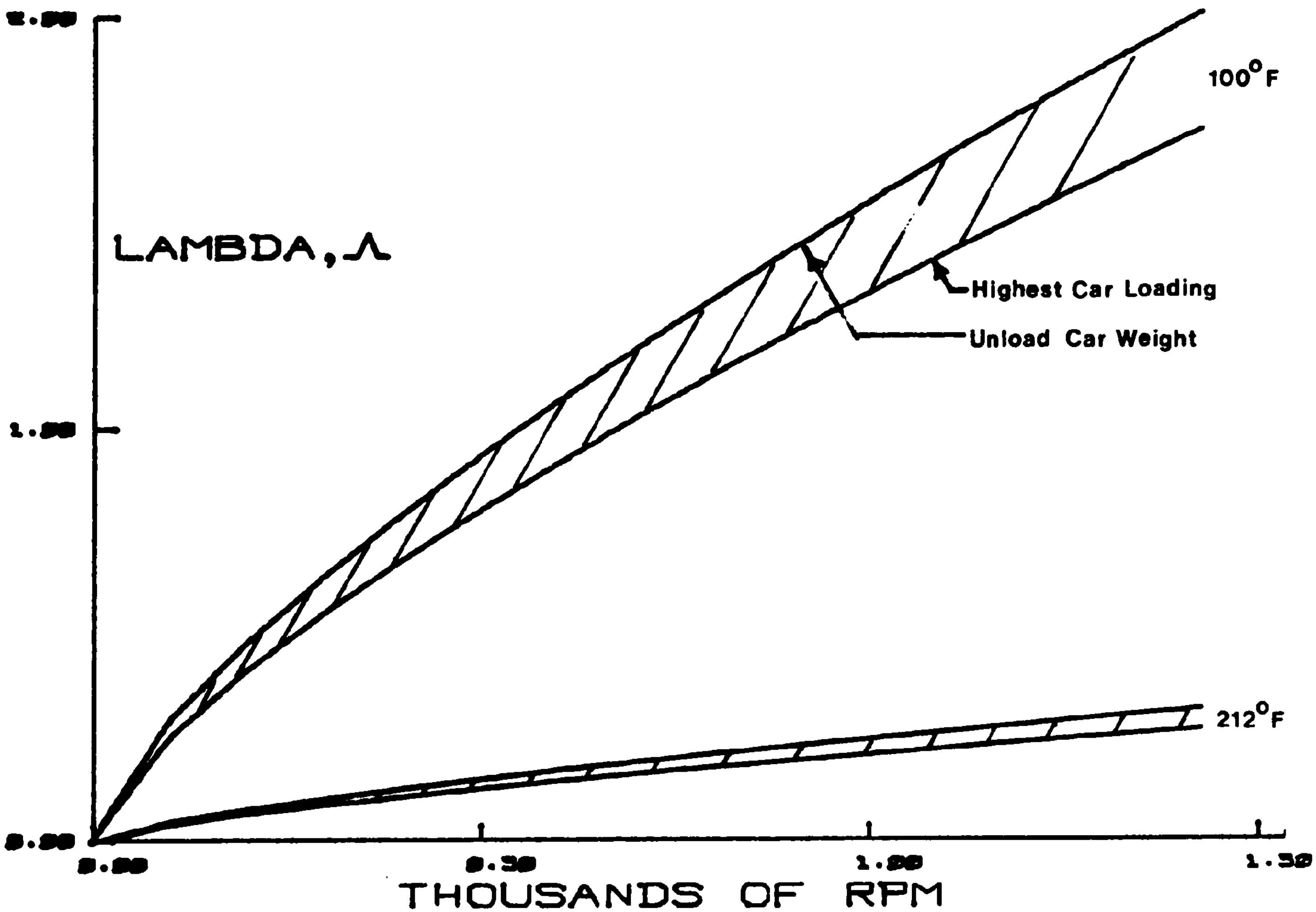

FIGURE 8. RAILCAR ROLLER BEARING LUBRICANT FILM THICKNESS

When a high degree of metallic interaction is present in a bearing, electrical contact analysis has been used to monitor the component "health" of ball bearings.

Variations in bearing electrical resistivity as a result of internal metallic interaction have been observed for many years (14). Photographs similar to that shown in Figure 9 reveal the degree of asperity interaction within an operating railcar bearing. A time varying contact signal can be obtained from a rolling element bearing with the aid of the circuitry and test arrangement shown in Figure 10.

If the circuit of Figure 10 is analyzed it shows that the voltage generated is not a first order function of the variation in bearing resistance. If the amplitude of the signal produced by Figure 10 is to be analyzed either by peak amplitude or by spectral component analysis, it can be seen that it is a function both of the resistance variation and the value of the fixed resistor. This may be done in laboratory situations but would be difficult to implement as an automatic diagnostic device. It was decided, therefore, to change the voltage source to a constant current source and eliminate the fixed resistor. In this way, the voltage measured across the bearing has a direct relationship with bearing resistance variations. A block diagram of the device is shown in Figure 11.

The output of the system is displayed on a meter with four selections possible: minus peak, plus peak, peak-to-peak, and average. The peak-to-peak value was expected to relate to the presence of a defect since the resistance will be driven toward zero when a defect is impacted. The average value will be a measure of the overall film thickness of a bearing. The output of the voltage across the bearing can be analyzed using a real time analyzer. There will be a linear relationship between spectral peaks and resistance variations.

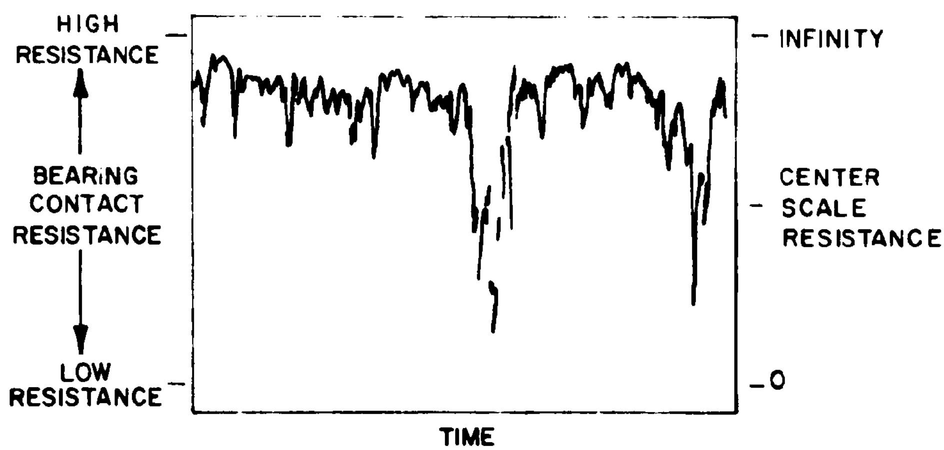

FIGURE 9. CONTACT RESISTANCE SIGNAL

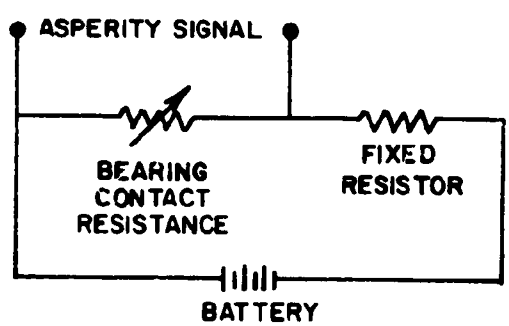

FIGURE 10. ELECTRICAL CONTACT DIAGRAM

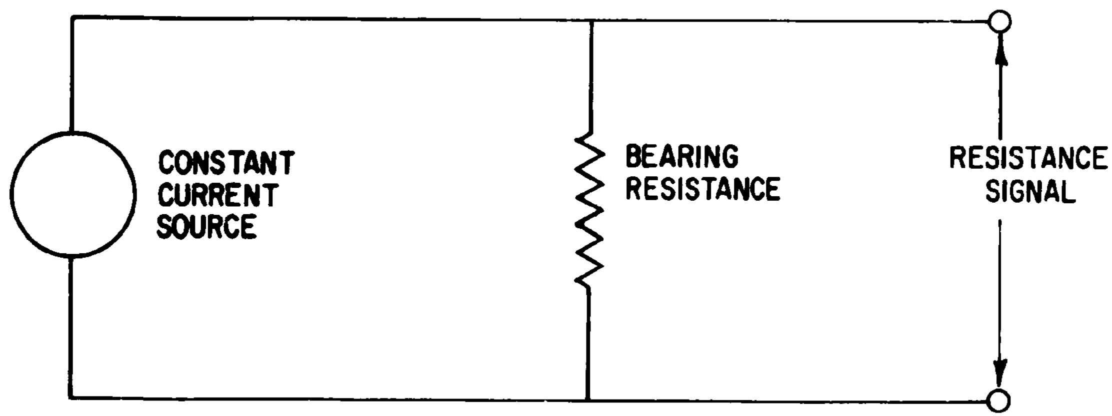

FIGURE 11. CONSTANT CURRENT BEARING RESISTANCE SYSTEM FOR LINEAR OUTPUT

3. EXPERIMENTAL EVALUATION

3.1 Overview of Bearing Tests and Objectives

Three different series of tests pointed toward evaluation of defective bearings, generation and progression of bearing defects, and evaluation of the selected diagnostic techniques were performed during the course of the subject program. These tests were called:

1. failure progression tests
2. certification demonstration tests
3. wheel shop tests.

The first two contained elements of both defective bearing evaluation and assessment of bearing diagnostic techniques. The latter test was strictly diagnostic system oriented.

The diagnostics portion of the work was in part based upon the results of tests of defective bearing components which were conducted on a previous program jointly sponsored by Shaker Research Corporation and NASA (15). For this reason, results from that program that are of significance to the subject work are also included in this report.

The following four subsections describe the objectives of each test series and the test equipment that was utilized. Test results are discussed in Sections 3.2 and 3.3.

3.1.1 Shaker Research/NASA Component Tests

The primary objectives of these tests were to evaluate the feasibility of employing high frequency vibration and high frequency sound monitoring techniques as diagnostic tools for defective bearings and to examine the effect of bearing rotational speed on signal (vibration or sound amplitude) strength.

For these tests, components (cups and cones) from fifty-eight defective, but still operable, bearings were tested in the apparatus shown in

Figure 12. In this rig, the cone (inner race) is held stationary and loaded axially against the rotating cup (outer race). Bearing components were lightly oiled as opposed to being grease-packed due to test rig drive power limitations.

For vibration amplitude evaluation, a miniature high frequency accelerometer was attached to the cone locating fixture. (See Figure 12.) For high frequency sound evaluations, a high frequency microphone was hung directly above the bearing approximately 3 feet away.

The principal conclusions drawn from the component tests were:

1. High frequency vibration and sound amplitude in the 10 to 40 kHz range is a good indicator of grossly defective bearings.

2. The discrimination between new, good, and "marginal" bearings was poor.

3. Both vibration and sound amplitude decreases markedly below 30 mph.

Significant test results are summarized in Section 3.3.1.1.

3.1.2 Failure Progression Tests

In the work that preceded these tests, three basic questions continually surfaced. These were:

1. How reliable is temperature as a harbinger of failure and what is the time (or distance) between an abnormal temperature rise and ultimate (catastrophic) failure?

2. How much useful or safe life is remaining in a bearing that possesses components that are "defective" as defined by the AAR?

3. How sensitive must a practical defective bearing diagnostic system really be? That is to ask, if the objective is to pre-

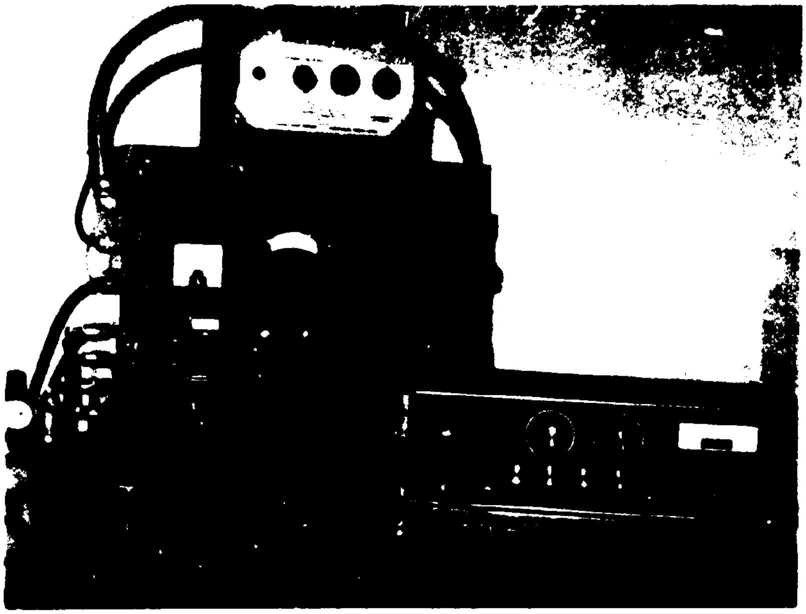

Rig Control Panel and Test Bearing

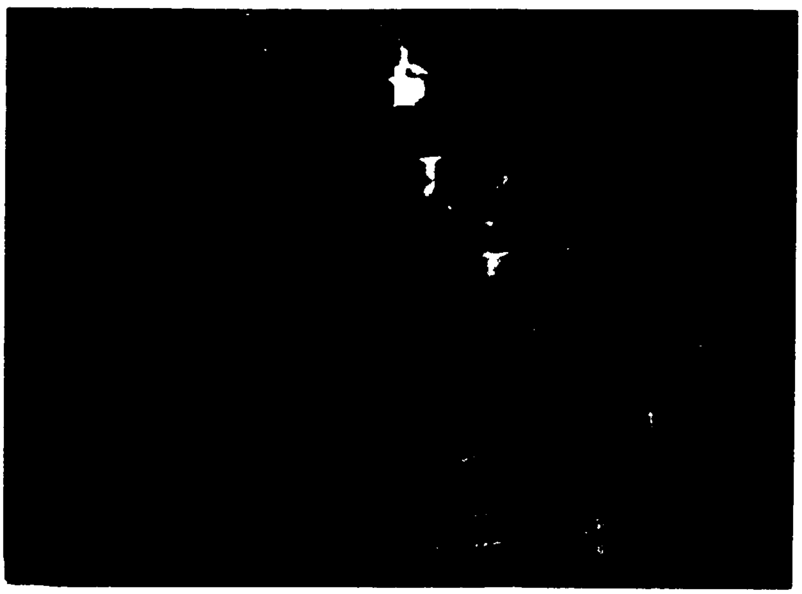

Installed Test Bearing and Accelerometer Pickup

FIGURE 12. BEARING COMPONENT TEST RIG

vent bearing-caused accidents, can a relatively simple diagnostic system which is designed to identify only the severely defective bearing (as opposed to the stringent AAR definition of defective) be deployed?

The failure progression tests were conducted in an effort to begin to answer these questions with the principal objectives being:

1. To gain an understanding as to the manner in which defective bearings progress towards failure;
2. To evaluate high frequency vibration and bearing electrical contact resistance diagnostic techniques in an environment more closely simulating that of an operating railcar bearing.

These tests were accomplished using the test rig shown in Figure 13. Three bearing assemblies are mounted on the common shaft rather closely together. The load is applied to the center bearing from above through a standard railcar roller bearing adapter. The hydraulic cylinder to apply the load is mounted beneath the bearing on the underside of the bed of the machine with the plunger pointing down. Two large connecting rods, one on either side, carry the load to the top of the test bearing. A maximum of some 120,000 pounds radial load can be applied. The shaft is belt driven by a 25 hp, 440 volt motor. The support bearings are covered by sheet metal shrouds (not shown in Figure 13) into which outside air is forced to provide convective cooling.

Laboratory instrumentation utilizes with the test rig included a 24-point temperature recorder, high frequency (50 kHz) accelerometers mounted on each bearing, and electrical contact resistance across the bearings. Automatic shutdown protection is incorporated and is triggered by high temperature, high vibration, or high motor current.

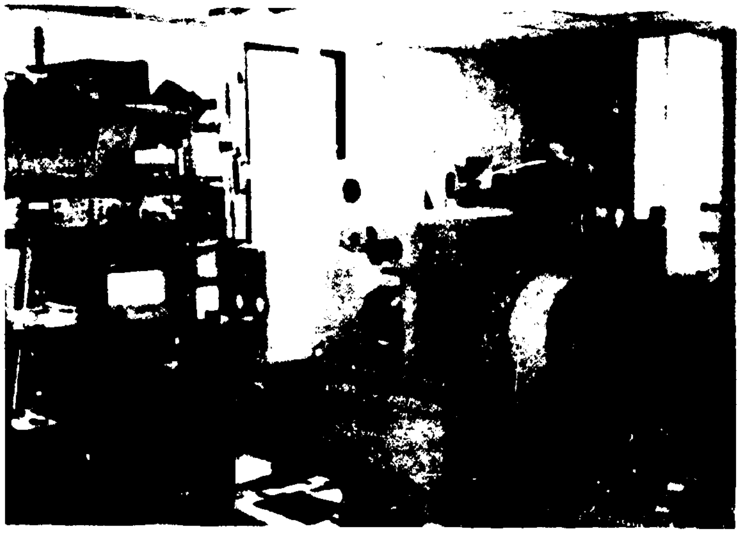

FIGURE 13. ROLLER BEARING TEST RIG FOR FAILURE PROGRESSION AND CERTIFICATION DEMONSTRATION TESTING

Testing was conducted using thirteen 6 x 11 railcar roller bearings at a full freight car load (26,000 lbs) at approximately 666 rpm (equivalent of 65 mph) for a minimum of 92 hours (equivalent of 6,000 track miles). Ten of the bearings contained faults ranging from water-etched cups or rollers to severe spalls, cracked rollers, and brinells. Most of the faulty test bearings had been previously rejected at a rework facility after macroscopic examination.

The principal results and/or conclusions of the failure progression tests are summarized below:

1. Although some bearings were very severely damaged, and some defects (primarily spalls) enlarged during the tests, no catastrophic failures were produced.
2. Temperature by itself is a poor indicator of bearing condition.
3. High frequency vibration amplitude is a good indicator of a grossly defective bearing.
4. High frequency vibration amplitude is a good measurement for tracking the degradation of a single defective bearing, but is an unreliable measurement for rating degree of damage.
5. Bearing electrical contact resistance, in the form used for the subject tests, is an unreliable indicator of bearing condition.

Detailed test results addressing the first aforementioned objective are given in Sections 3.2.1 and 3.2.2. Results concerned with the second objective are discussed in Sections 3.2.1.2 and 3.3.4.

3.1.3 Demonstration Tests

The objectives of the acceptance demonstration tests, which utilized the same test apparatus as was used for the failure progression tests summarized above, were:

1. To evaluate techniques for accelerated life testing, and
2. To evaluate potential bearing diagnostic approaches to identify the "first" signs of a bearing surface defect.

The results of the test activity concerned with the first objective were discussed in Section 4.5 Volume I(3) of this report. The second objective results are discussed in Section 3.3.1.3 of this volume.

In summary, it was found that the creation of a minute surface defect during the course of the demonstration tests could repeatably be identified if spectrum analysis of an envelope-detected high frequency acceleration signature was employed.

3.1.4 Wheel Shop Tests

Early in the program it became clear that a large number of bearings (on the order of 200,000 per year) were being removed because of the AAR Derailment Rule (4). Since there was no evidence that the proportion of these that were defective exceeded the 15 to 20% found for all bearings (Volume I), it appeared that a diagnostic device deployed at a rip track to inspect "derailed" bearings without removal and disassembly could save the industry a considerable amount of money (on the order of millions of dollars per year -- see Section 4.3.1).

To evaluate the high frequency vibration technique for internal surface defect detection in a manner suitable for rip track use, a device was built which rotated the cup on the axle. This device (which is shown in Figure 14) was used to test 90 bearings on wheelsets that had been removed from service at the Southern Railway Coster Wheel Shop in Knoxville, Tennessee. This evaluation was done at the Southern's wheel shop instead of an actual rip track because of the large number of available roller bearing wheelsets and because the bearings were to be removed and inspected as normal routine. Thus, a convenient and natural unbiased

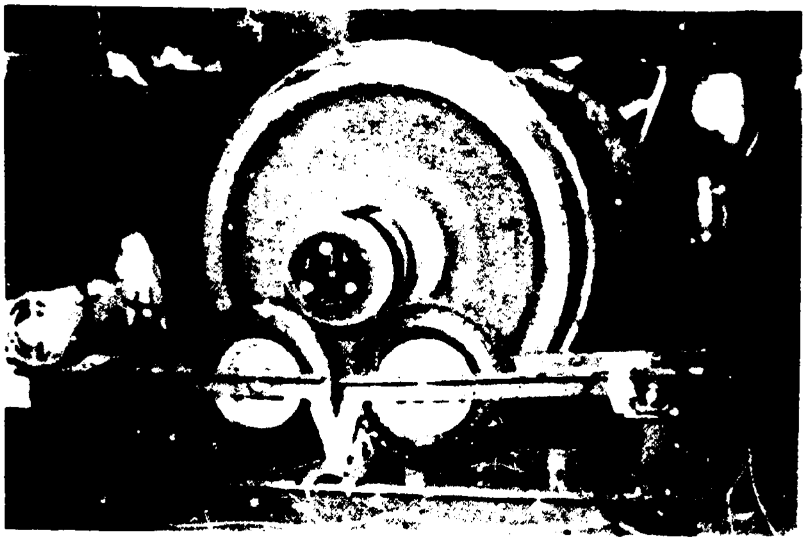

BEARING TURNING FIXTURE

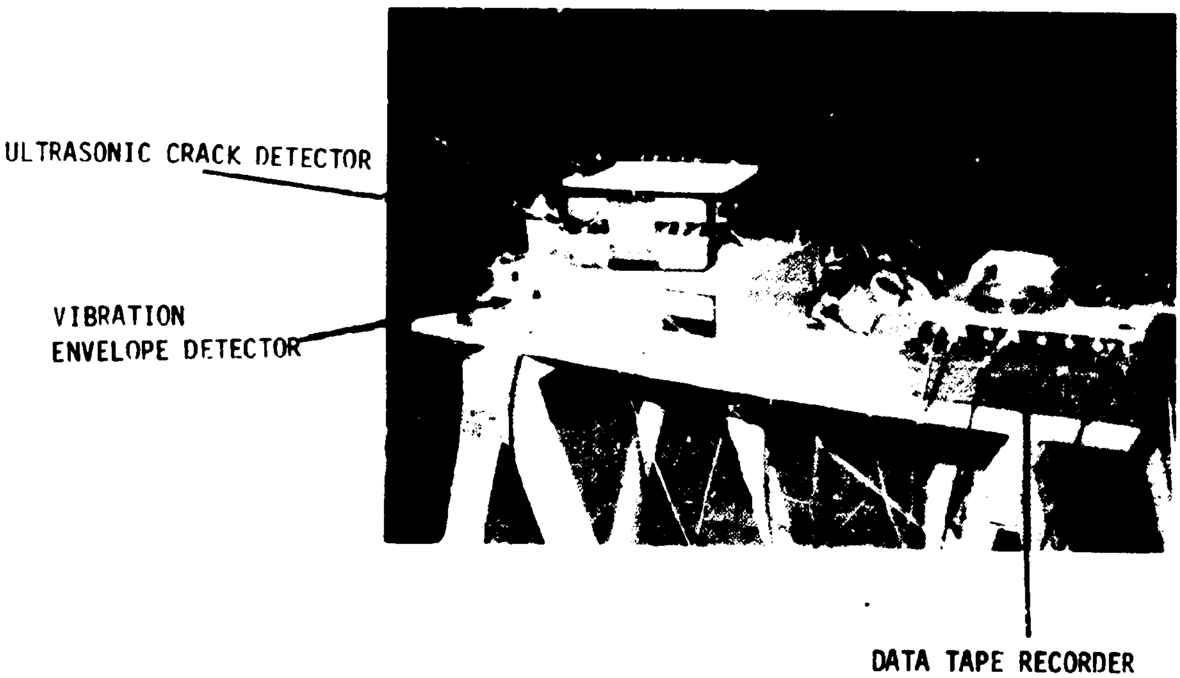

FIGURE 14. TESTING FOR BEARING DEFECTS AT SOUTHERN RAILWAY WHEEL SHOP

inspection (after testing) was automatically provided. The inspection was accomplished by the Brenco Bearing Service Company in Knoxville, Tennessee.

In addition to evaluating the high frequency vibration technique for surface defect identification, ultrasonic detection was also evaluated for cup crack detection.

The results of the wheel shop tests are described in Sections 3.3.1.4 and 3.3.2. In summary, the following conclusions were drawn from these tests:

1. The simple high frequency vibration amplitude technique was clearly adequate for identifying "nonrepairable" bearings.
2. Additional sophistication is required to separate "good" bearings from those near the edge of the AAR condemnable limit (4).
3. The ultrasonic probing technique is suitable for locating grease-filled cracked cups with only minimal surface preparation.

3.2 Summary of Bearing Performance and Degradation

3.2.1 Temperature and Temperature Rise

During the failure progression and acceptance demonstration tests, which employed the test rig previously shown in Figure 14, thermocouples were welded to the cups and seal cases in the locations shown in Figure 15 and Table 2.

The thermocouple locations shown in Figure 15 were chosen to coincide with the locations selected by the U. S. Naval Surface Weapons Center (NSWC) for their separately FRA-funded System for Train Accident Re-

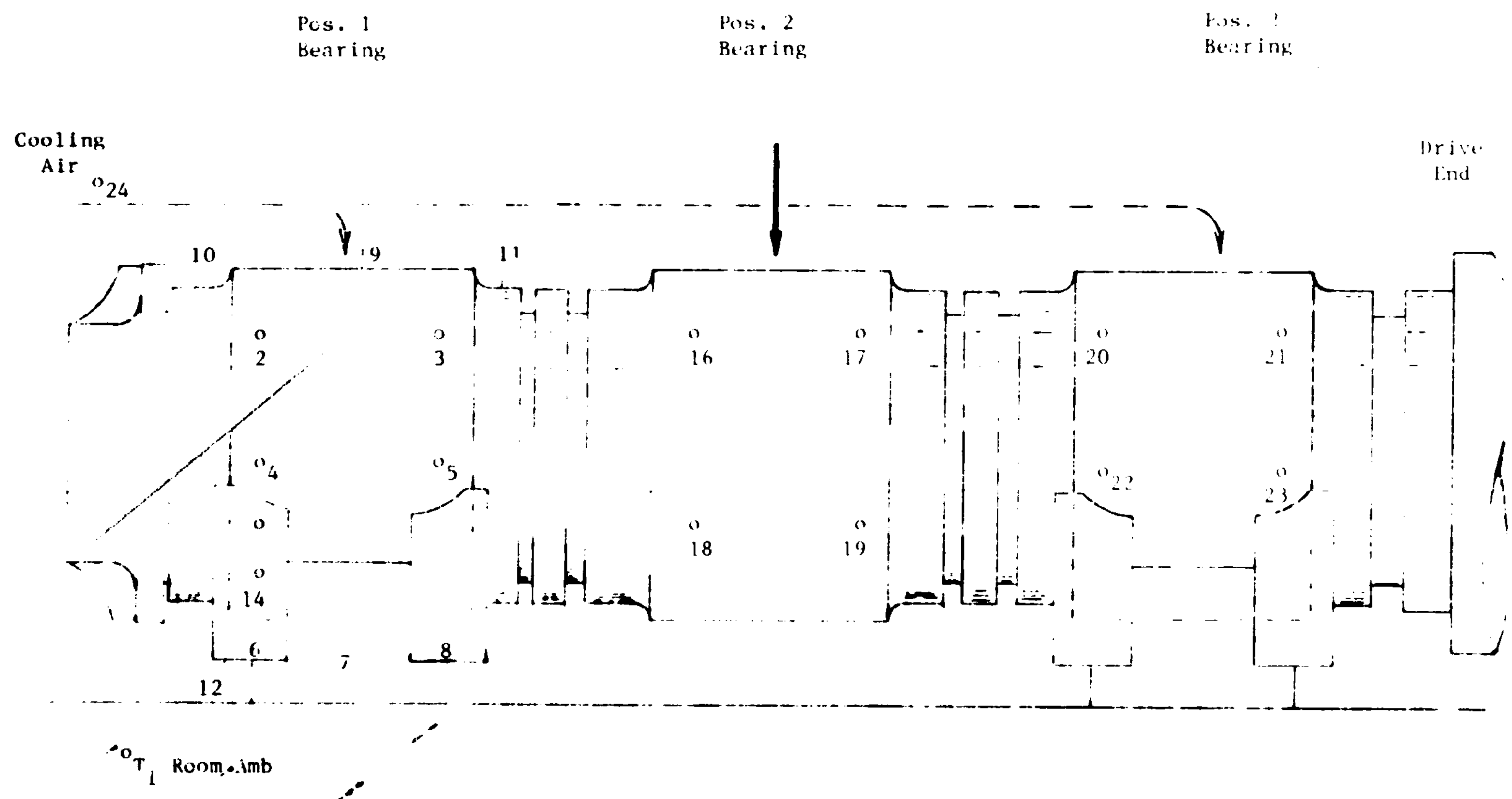

FIGURE 15. THERMOCOUPLE LOCATION TESTS 2,3

TABLE 2.

THERMOCOUPLE LOCATIONS
FOR
FAILURE PROGRESSION TESTS 4 THROUGH 7
AND
ACCEPTANCE TESTS 1 THROUGH 5

Thermocouple Number	Bearing Number	Part of Bearing	Angular Location (o'clock)	Physical Location (see drawing below)	Chart Number
T1	Test environment ambient				1
T1-1	1	cup	6	B	2
T1-2	1	cup	6	A	3
T1-3	1	cup	12	C	4
T1-4	1	cup	3	C	5
T1-5	1	seal	12	A	6
T1-6	1	seal	6	B	7
T2-1	2	cup	12	B	8
T2-2	2	cup	12	A	9
T2-3	2	cup	6	C	10
T2-4	2	cup	3	C	11
T2-5	2	seal	12	A	12
T2-6	2	seal	6	B	13
T3-1	3	cup	6	B	14
T3-2	3	cup	6	A	15
T3-3	3	cup	12	C	16
T3-4	3	cup	3	C	17
T3-5	3	seal	12	A	18
T3-6	3	seal	6	B	19
T in		Air Intake			20

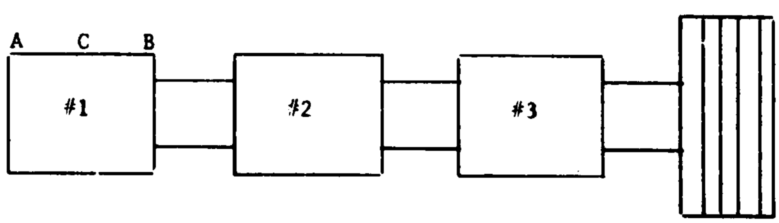

duction (DOT-STAR) program. Since the NSWC intended to measure roller bearing temperatures on an actual operating railcar during the course of the DOT-STAR program, using common thermocouple locations could provide valuable correlation data between the real and laboratory thermal environments. Unfortunately, DOT-STAR temperature data did not become available during the course of the subject program. Thus, the desired correlations were not made.

After the first two failure progression tests (Nos. 2 and 3)*, the thermocouple locations were changed to those shown in Table 2 to give better overall temperature coverage within the limitations of the 24-point temperature logger.

3.2.1.1 Bearing Steady State Temperatures. As previously discussed, thermocouples were used to monitor the bearing temperatures. Figure 16 is a typical plot of steady-state temperature during the test of bearings 112 and 110. As noted, the highest temperatures occur in the load zone of the bearing.

During the operation of the rig, bearings in positions 1 and 3 are shrouded with sheet metal into which the cooling air flows. The gradients noted on the bearings in Figure 16 are due in part to the way the cooling air flows around the bearing. At the drive end (position 3), the air flows around the cup and axially in both directions. At the free end (position 1) the axial flow tends toward the free end.

On Figure 16, it will be noted that the top of the bearing is cool from the incoming air and the free end is cool from the axial flow. The bearing in position 2 is more uniform in temperature since no direct cooling contacts the bearing and only the axial flow of air

*Failure progression test run number 1 was a test rig and instrumentation shakedown test and the results are not reported herein.

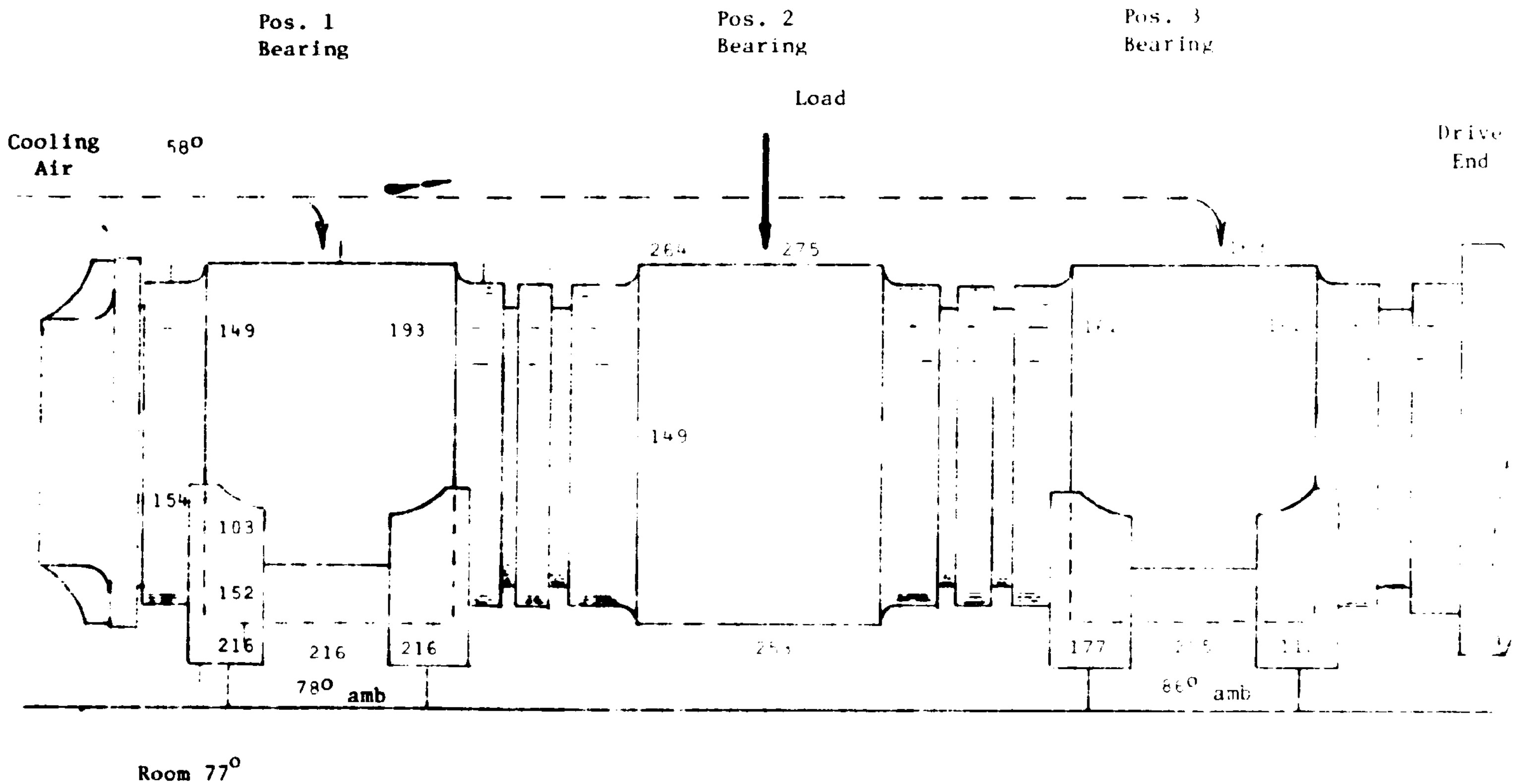

FIGURE 16. STEADY STATE TEMPERATURES, TEST NO. 6 (BEARINGS 112, 101, 110)

from bearings 1 and 2 provides cooling. The thermocouples in the load zone are protected from direct cooling since they are under the adapter. They tend to provide a better indication of temperature. The temperatures in these locations were used to determine the influence of load on temperature rise.

Figure 17 is a plot of temperature rise versus load for all three bearings. The solid dots represent the center bearing and agree closely with the end bearings at reduced load. Also shown is the temperature rise of all bearings with no cooling applied. The average hot spot temperature rise of bearings installed on railroad cars should fall between these limits.

3.2.1.2 Overgreased Bearing Temperatures. Since difficulty is often encountered in controlling the amount of grease added to a bearing during regreasing (since the quantity of grease contained within an assembled bearing is unmeasurable), a test was run to determine the influence of grease quantity on temperature. The normal grease quantity that was applied to the 6 x 11 bearing was 9 ounces between rollers and 4.5 ounces to the cones. The steady-state average cone hot spot temperature rise (in the load zone) was determined on test as 115°F.

The quantity of grease in the bearing was increased to 29.5 ounces total and temperature rise rechecked. The end cap was completely filled to permit adding additional grease through the cap. The temperature rise was not influenced by this additional grease. Finally, an additional 5 ounces of grease was added by pumping through the end cap until grease leakage at the seal lip was observed. This resulted in a total grease quantity in the bearing itself of 34.5 ounces. Figure 18 is a plot of the influence of grease quantity on bearing temperature rise. As noted, when the normal grease load of 18 ounces is increased to 29.5 ounces, a temperature increase of 24 to 25°F is encountered. Increasing the grease quantity to completely filled (34.5 ounces) results in a temperature increase over normal of 39°F.

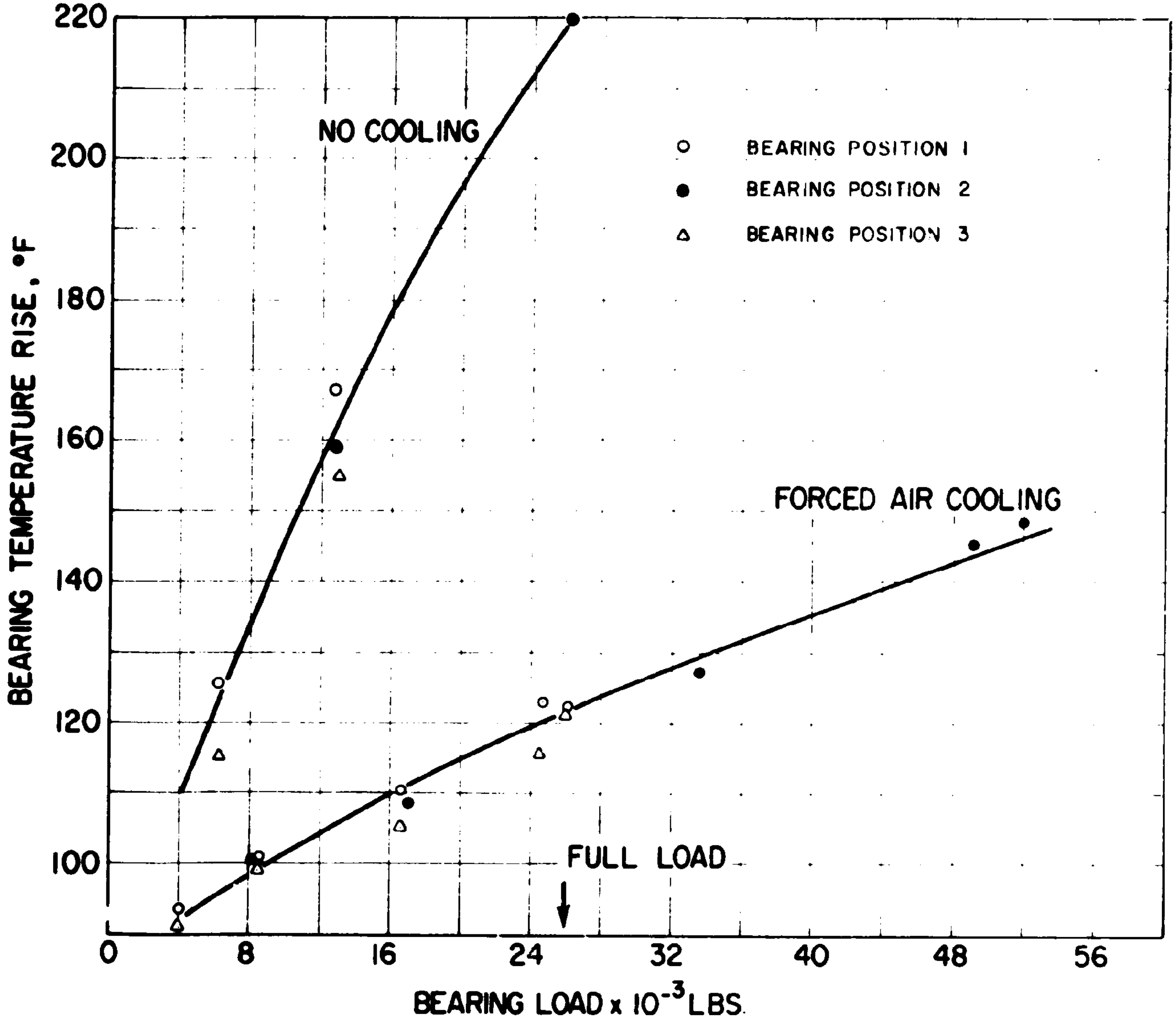

FIGURE 17. TEST RIG BEARING TEMPERATURE RISE (55 MPH, 6 X 11 TAPERED ROLLER)

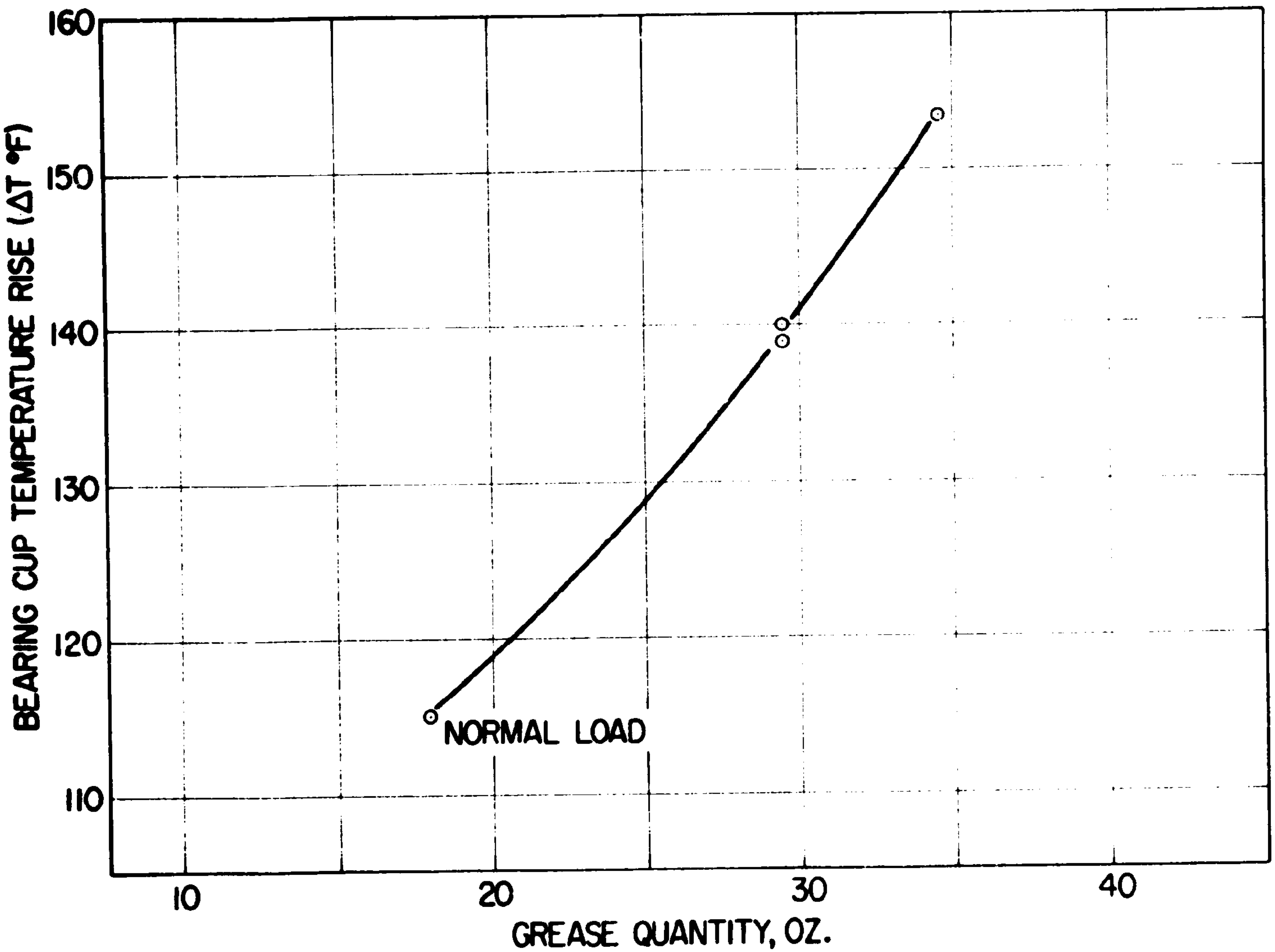

FIGURE 18. EFFECT OF OVERGREASING BEARING ON OUTER RACE (CUP) TEMPERATURE RISE

From a temperature rise standpoint, overgreasing the bearing has a similar effect to overloading the bearing. The effect of increasing load from no load to full load induces an approximate 37°F temperature rise while overgreasing can result in a 39°F rise.

For a fully loaded bearing, the effect of overgreasing the bearing resulted in an additional temperature rise of 39°F. (See Figure 18.) A summary of these operating points is as follows:

Speed	Load	Grease	Temp. Rise
60 mph	Light	Normal (18 oz)	83°F
60 mph	Full	Normal (18 oz)	115°F
60 mph	Full	Overgreased (30 oz)	140°F
60 mph	Full	Overgreased (35 oz)	154°F

3.2.1.3 Undergreased Bearing Temperature. One additional test conducted was to determine the influence of undergreasing the bearing. The purpose of this test was to determine how rapidly a bearing would overheat with insufficient lubricant. In order to conduct this test, a bearing was degreased and lubricant provided only in the seal lip region to prevent seal failure. A small portion of grease remained in the bearing under the cage. This provided a small quantity of lubrication.

The bearing stabilized out at about a 150°F temperature rise after about 1-3/4 hours as shown in Figure 19. Following this point the temperature began a slow rise and then showed an increase followed by a slight decrease and then another increase. During a period of one hour, the temperature rise increased to 230°F. At this point, the temperature rapidly increased in a few seconds and the rig was shut down by the protective devices. From these data, a hot-box detector spaced at 30 miles and an alarm point at a 180°F temperature

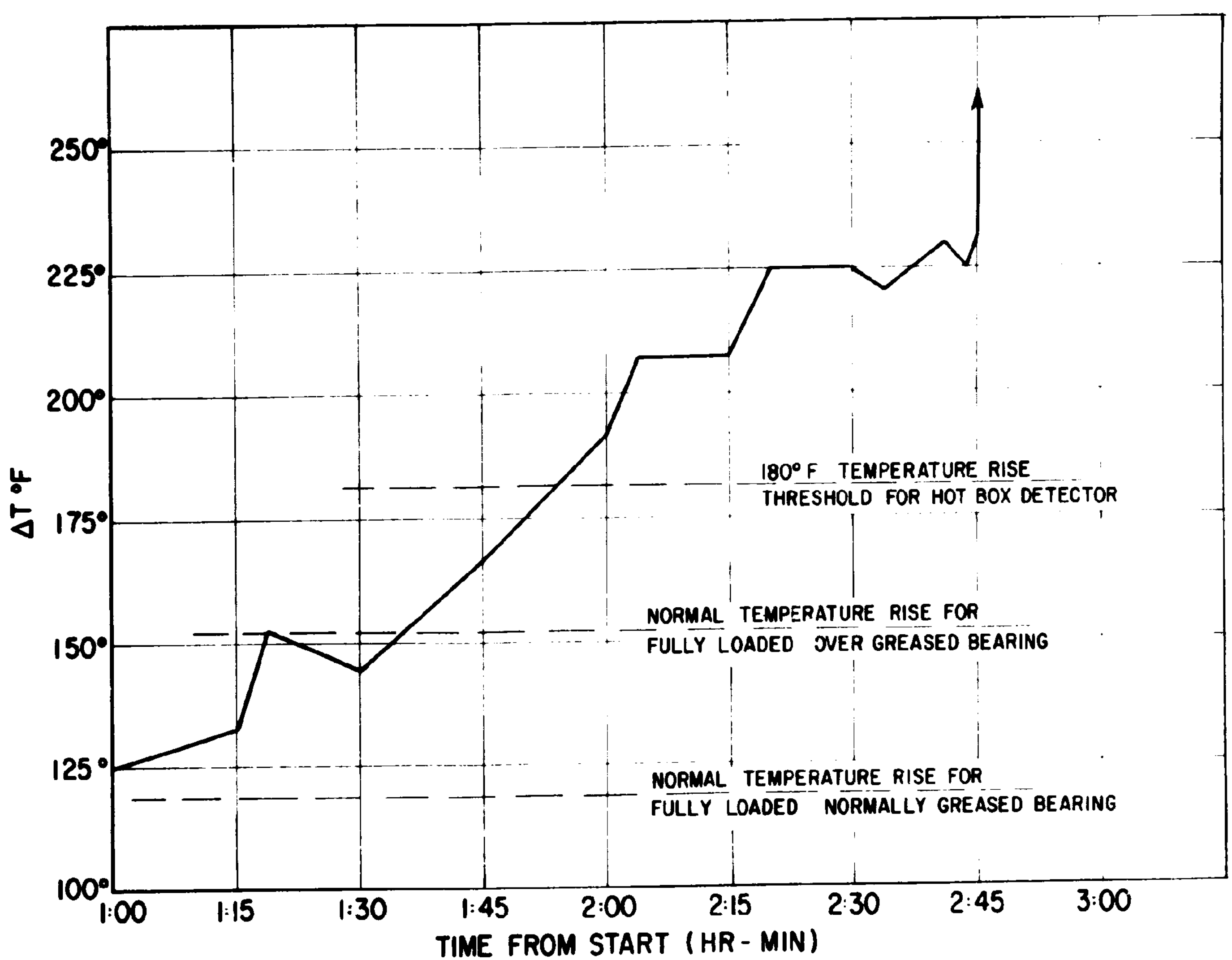

FIGURE 19. TEMPERATURE RISE VERSUS TIME FOR UNDERGREASED BEARING

rise would have succeeded in stopping the train in the case of this particular bearing. Once the temperature reached the point where it was over a 230°F rise, catastrophic failure rapidly ensued.

The bearing ran a total of 2.6 hours in this condition. One end of the bearing contained less grease than the other, causing one end of the bearing to run hot. The resultant gradient across the bearing was 92°F, with the hot end attaining 300°F. Within 40 seconds the hot end temperature jumped to 350°F, which automatically shut down the test rig.

Inspection of the bearing after test indicated the roller temperature had attained 450 to 500°F at one end, as judged from the temper color. A file test indicated that the hot end of the roller was beginning to anneal. Both races (cup and cone) did not show the same high temperature as the rollers and showed no indication of failure. The grease at this end of the bearing had coked, leaving a black deposit on the bearing elements.

The test was stopped in sufficient time to prevent catastrophic failure and permit examination. The failure mechanism for a bearing with insufficient lubrication appears to be a rapid process once a cup temperature in the range of 300 to 350°F is attained. The final insufficient lubricant failure process most likely begins with gross roller race sliding, causing the roller temperature to rise above race temperature (due to poor heat flux from the roller) and resulting in a loss of clearance. This situation causes thermal runaway to a point where the roller annealing temperature (approximately 380°F) is reached and macroscopic welding occurs. At this point the temperature rapidly accelerates and seizure results.

Because of the poor heat transfer out of the roller, it most likely reaches annealing temperature while the cup is still in the 300 – 350°F region.

On the basis of one test, however, it is difficult to determine if the temperature rise, the absolute temperature of 300°F, or the temperature gradient across the bearing is the actual factor that is the harbinger of final catastrophic failure.

3.2.2 Progression of Defects and Failures

When a defect occurs in a bearing, it is not known how long the bearing will continue to operate without failure. To help answer this question, the failure progression tests described in Section 3.1.2 were conducted to determine the life margin of a bearing containing defects. Simulating a full freight car load operating at 65 miles per hour over an equivalent rail mileage of approximately 6,000 miles was considered sufficiently severe a test to establish the marginality of the bearings. One important purpose of the test was to determine spacing deployment of wayside sensors.

3.2.2.1 Progression Test Procedures. The test rig utilized for performing the progression tests was described in Section 3.1.2. Test instrumentation consisted of temperature monitoring, vibration monitoring and electrical resistance monitoring across the bearing.

The test rig requires three bearings for operation. The rig was assembled with a damaged bearing at either end and a new bearing in the center position. Two test shafts were employed during the test program to permit assembly of bearings and one shaft while the second was in operation. The same center bearing, therefore, was used for every other test and accumulated more hours than the test bearing.

Each bearing was assembled with 18 ounces of new grease and new seals. A number of bearings had been used in tests conducted at the Association of American Railroads and had been assembled and greased at Brenco, Inc. These bearings had less than four hours of operation after greasing and new seals and had run at essentially a no-load condition.

Six endurance tests were conducted for a minimum of 92 hours to test all bearings. The first two tests (2 and 3) were in continuous operation, and the last four tests (4 through 7) were shut down and cooled four times during the test.

Following the endurance tests, one of the test bearings was selected for temperature evaluation from overgreasing (test 8) and undergreasing (test 9). A test was also conducted to determine the effect of load on temperature on a properly greased bearing (test 10). The results of these nonendurance tests were previously discussed in Section 3.2.1.

<u>3.2.2.2 Test Bearings.</u> Thirteen bearings were utilized for the failure progression test program. Three of these were new bearings and ten were damaged. Two of the new bearings were installed in the center position of each of two test shafts. One new bearing was installed in the test bearing position to establish a baseline for comparison with damaged bearings.

Table 3 lists the test bearings and the type of damage that was observed prior to test. In all damaged bearings, the damage condition was quite visible. The table also indicates the condition of the bearing after test and references figure numbers of photos taken before and after test of the typical damage.

<u>3.2.2.3 Test Results.</u> All bearings subjected to test operated 92 hours or more without catastrophic failure or significant increase in temperature levels. It should be noted (see Table 3) that bearing 108 was used in two tests resulting in 198 hours of running. Since

TABLE 3. FAILURE PROGRESSION TEST RESULT SUMMARY

Bearing No.	Load (lb)	Running Time (h)	Condition Before Test	Condition After Test	Figure No.
101	54,000	299.4	New bearing	Light brown discoloration on cups, cone and rollers – no damage	-
102	54,000	306.8	New bearing	Light brown discoloration on cups, cone and rollers – fatigue spall 0.25 in. x 1.0 in.; A-side small dents in race of cup A side; B-side: no damage	-
103	26,000	100.6	New bearing	No damage – light brown discoloration over 50 percent of rollers	-
104	26,000	100.6*	A-side: new roller B-side: blued roller Cup - water-etch	*A-side – light heat on rollers at major diameter end; B-side: fatigue of five rollers (0.25 in. x 0.125 in. on small diameter end) Cup – no further damage	20
105	26,000	97.7	A-side: cracked roller B-side: high spot on roller Cup - new	A-side: crack progressed, roller locked; B-side: high spot fatigued (0.125 in.) – five rollers; burnish discoloration and race pitting (B-side) -180°	21
106	26,000	92.1	A-side: spalled rollers B-side: spalled cup and rollers	No significant progression of damage	22
107	26,000	92.1	A-side: brinell cone B-side: roller high spot Cup – new	A-side: no progression of damage; B-side: high spot fatigued (0.125 in.) five rollers; burnish discoloration B side (180°)*	-
108	26,000	198.0	A-side: mod. spall cup, cone and rollers spalled; B-side: cone spalled, rollers spalled	Slight progression of roller spalls, gross progression of light spall on the A-side	23
109	26,000	116.4	A-side: water-etch cup B-side: water-etch cup and cone	No marked progression in damage	25
110	26,000	101.1	A-side: water-etch cup, split roller B-side: no significant damage	A-side: no progression in damage; B-side: rollers rusty brown in color	26
111	26,000	114.4	A-side: light brinell of cup and roller B-side: light brinell of cone	No significant progression of damage	-
112	26,000	101.1	A-side: light spall of cup B-side: light brinell of cup and cone	A-side: gross spalling cup, scoring of rollers B-side: no progression of damage	25
113	26,000	100.3	A-side: several spalled areas of cup B-side: no significant damage	A-side: moderate progression of spalls B-side: no significant damage	26

*Bearing test with grease removed after failure progression tests – overheated in 2.6 hours.

the vibration level of this bearing had increased significantly during the first test, it was felt that an additional 100-hour test might induce a failure. However, no failure was induced.

Bearing 101, located in the center position, was operated for a total of 299.4 hours (approximately 19,500 rail miles) at a load of 52,000 pounds without incident. Bearing 102 operated 306.8 hours (20,300 rail miles) under the same condition as 101.

In the following paragraphs, the results of failure progression tests are discussed. In Section 3.3.1, the results of analysis of vibration levels are reviewed.

<u>3.2.2.4 Failure Progression.</u> In review of Table 3, it will be noted that no significant progression of damage was observed in four of the ten damaged bearings, i.e., 106, 109, 110 and 111. In two bearings (105 and 107) that contained high spots on the roller, fatiguing of the roller resulted. Bearing 104 contained a blued roller before test and spalled rollers after test. Three bearings that contained spalled areas (108, 112 and 113) resulted in moderate to gross spalls after test. Bearing 105 contained a cracked roller prior to test. The crack progressed during test completely across the roller at the large diameter end. The dimensional changes and stress patterns produced by the crack resulted in fatigue failure 90 degrees from the crack, as seen in Figure 21. The roller finally seized in the cage with resulting sliding on the race producing flats on the roller O.D. Despite this sliding under full load, there was no indication of over-heating of the roller or races. In contrast to this experience, bearing 110 contained a split roller before test with no marked degradation in damage after test as seen from Figure 24.

Generally water-etch damage and light brinell damage did not induce further damage during test, as shown in Figure 25. Spalled rollers did not show significant damage progression during test,

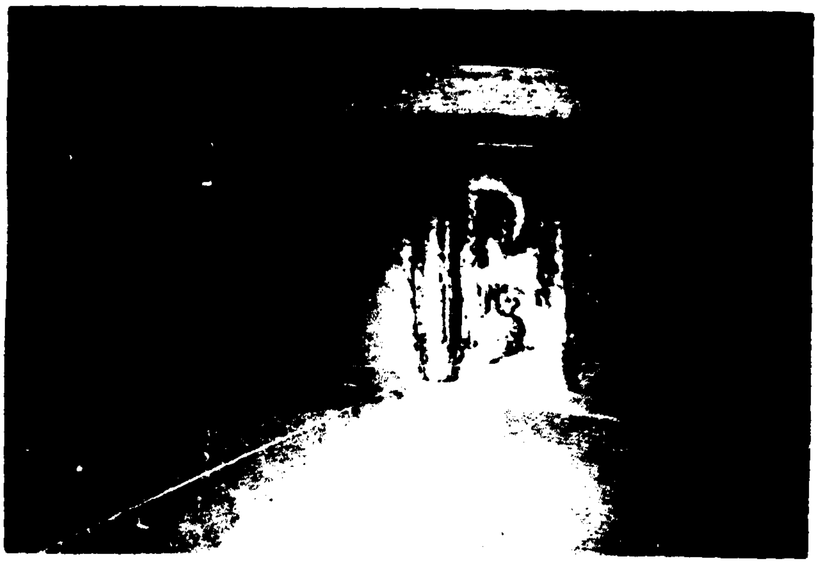

FIGURE 20. BEARING 104 WATER -ETCHED CUP (NO DAMAGE PROGRESSION FROM 100-HOUR TEST)

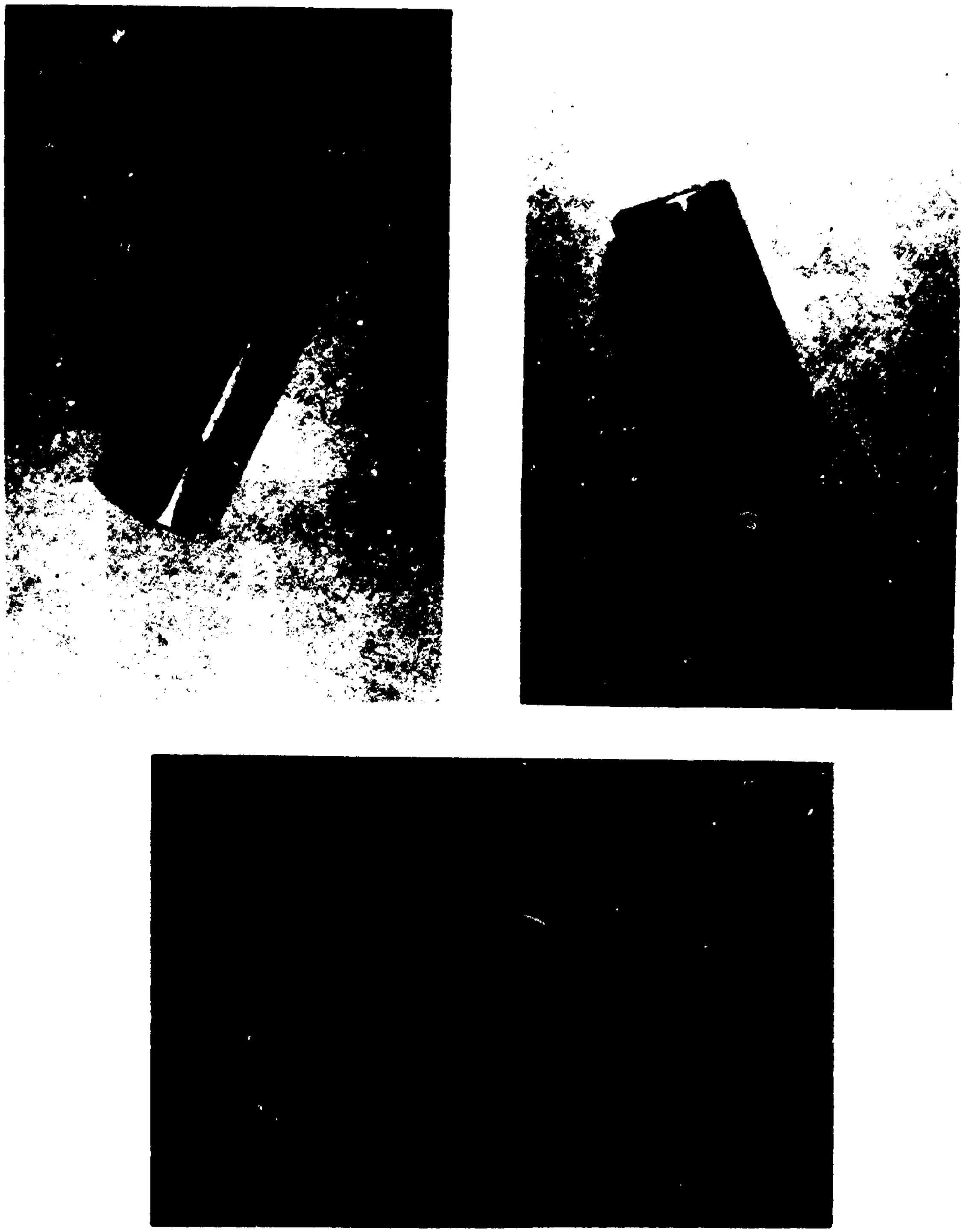

FIGURE 21. CRACKED ROLLER FROM BEARING 105A AFTER 97.7 HOURS

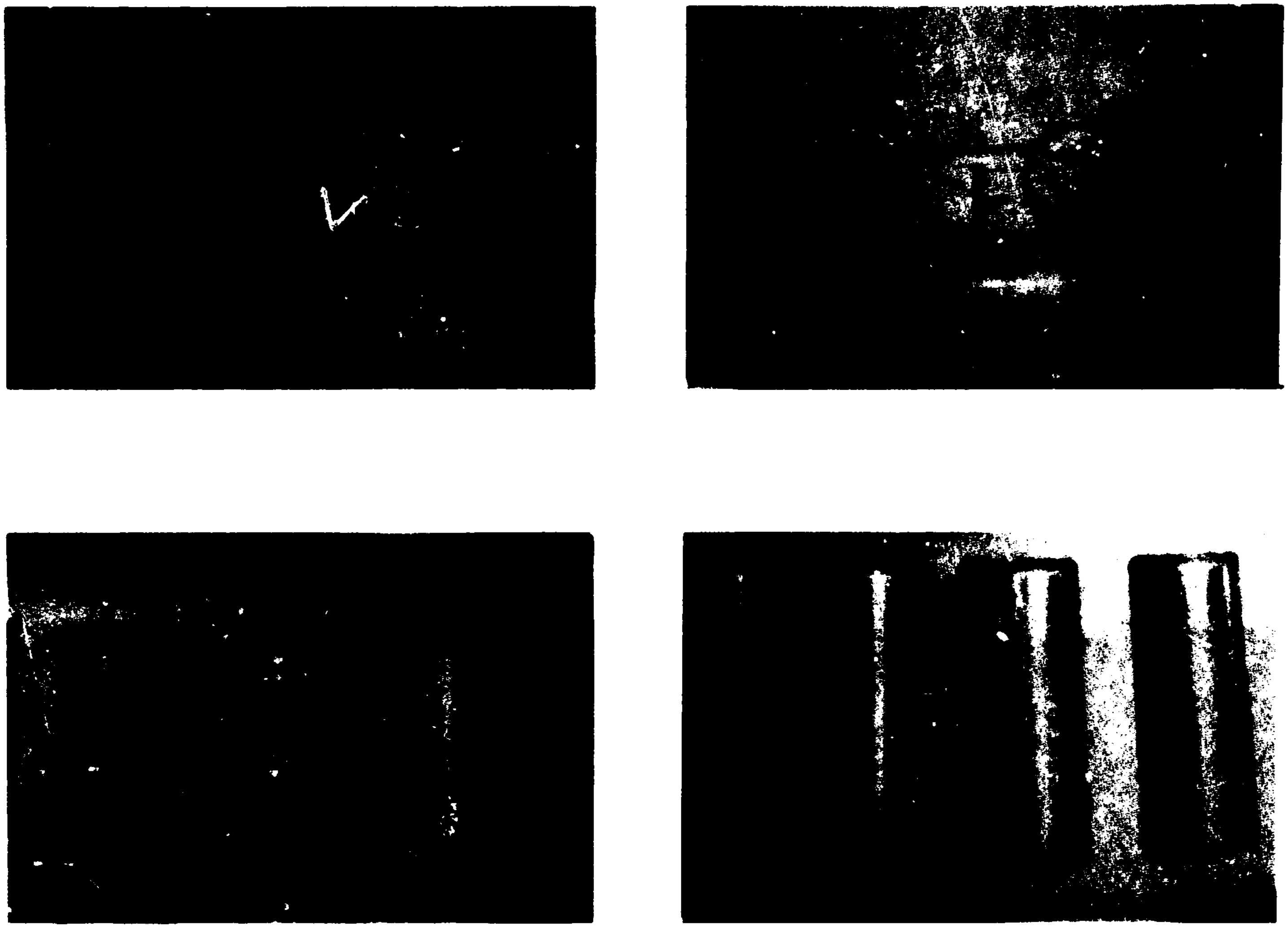

BEFORE AFTER

FIGURE 22. BEARING 106, SPALLED (NO SIGNIFICANT PROGRESSION)

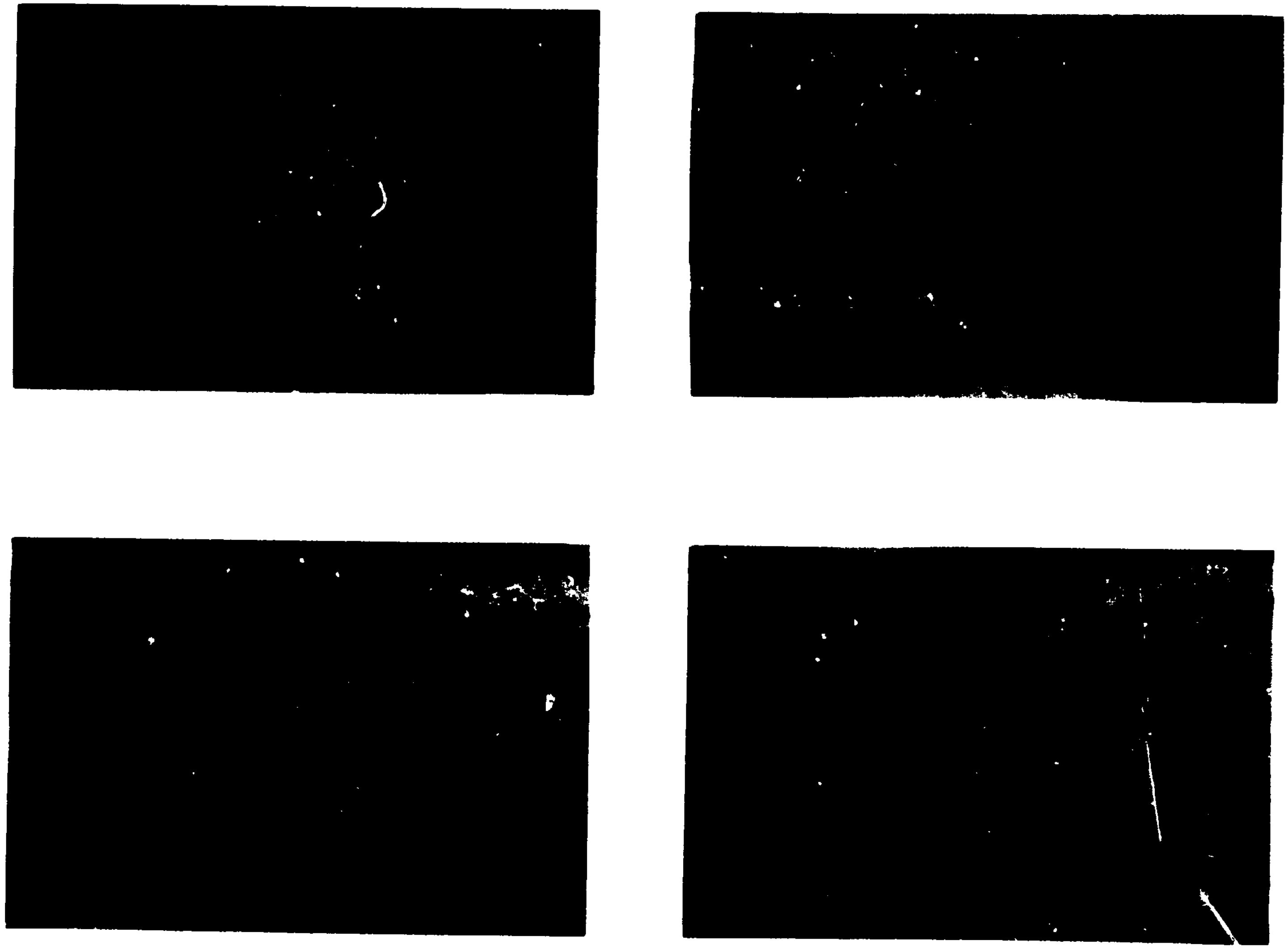

BEFORE AFTER

FIGURE 23. BEARING 108, SPALLED (SEVERE CUP AND MODERATE ROLLER DAMAGE PROGRESSION)

BEFORE

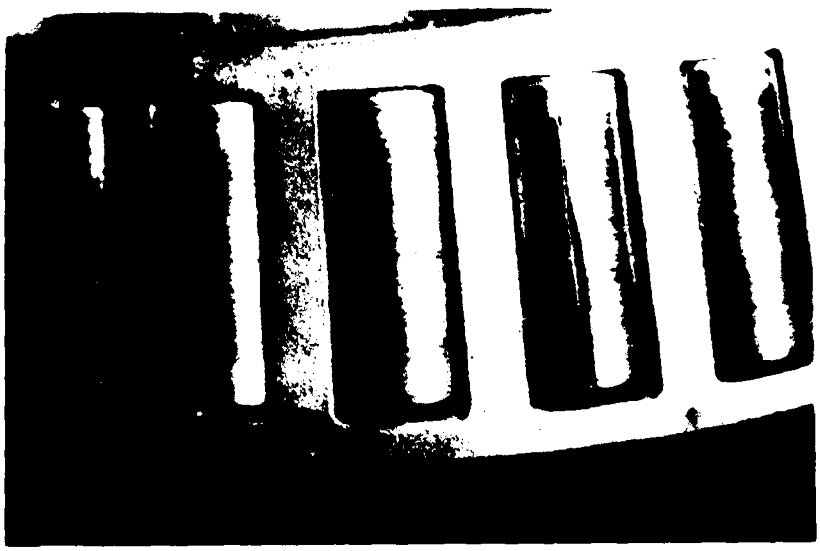

AFTER

FIGURE 24. BEARING 110, SPLIT ROLLER (NO SIGNIFICANT PROGRESSION)

112B BRINELLED

112 BRINELLED

109 WATER-ETCHED

BEFORE TEST

109 WATER-ETCHED

AFTER TEST

FIGURE 25. APPEARANCE OF BRINELLED AND WATER-ETCHED BEARING SURFACES BEFORE AND AFTER 5000-MILE FAILURE PROGRESSION

as noted in Figures 22 and 23. However, spalling of the races generally leads to marked increases in damage as observed in bearings 108 (Figure 23) and 112. Moderate progression in damage on bearing 113 is depicted in Figure 26. The load direction relative to the cup damage was not recorded during test.

It is assumed that the cup spall of Figure 22 was not in the load zone and that the moderate increase in spall damage of Figure 26 was due to a slight orientation out of the load zone.

From these limited tests it would appear that bearings containing light brinelling, water etching and light indentations are not as prone to failure as cone and cup spalls. Rollers containing high spots are quite prone to fatigue, but after spalling further progression appears to be quite slow.

3.3 Diagnostic System Effectiveness

Five diagnostic concepts were chosen for evaluation under this program. The first of these, bearing temperature rise, was selected because of the need to evaluate the deployment of hot-box detectors for roller bearings. Roller bearing temperature rise as a function of load and degree of lubrication has been discussed previously in Section 3.2.1. We now discuss the effectiveness of the remaining concepts studied.

3.3.1 High Frequency Vibration

The high frequency vibration technique, in at one least form, was applied to all tests conducted. Our evaluation of this technique is summarized below.

3.3.1.1 Preliminary Vibration Analysis Tests. Fifty-three used bearings were obtained for conducting initial evaluations. The condition of the bearings ranged from new to large visual defects. These bearings were not complete bearing assemblies but consisted of individual cone (roller, cage, inner race) assemblies.

BEFORE TEST

AFTER TEST

FIGURE 26. PROGRESSION OF RACE SPALLS DURING EQUIVALENT OF 5,000 MILES AT 65 MPH UNDER 26,000 LB. LOAD (BEARING NO. 113)

Each of the assemblies was run in a special rig that drove (rotated) through the cup. The same cup (which was new) was used to test all assemblies. These tests were followed by running a new cone assembly in cups having different degrees of damage. The cone was loaded axially with 600 pounds and run at an equivalent train speed of 70 to 100 mph. A high frequency response accelerometer was installed on the stationary inner cone to measure vibration amplitude to 100 khz. The structural vibration data was analyzed for frequency content utilizing a real time frequency analyzer. The peak amplitude of sixteen spectra of frequency content versus amplitude of the complex vibration and acoustic data were stored in the computer for further analysis.

Analysis of the complex frequency indicated that the maximum amplitudes of vibration occurred in the frequency range from 10 kHz to 30 kHz. The peak amplitude of vibration occurring in this frequency range was used to rank the severity of damage in the bearing. This severity number was compared against the degree of damage existing in the bearing as determined macroscopically. The inspected damage condition was rated as follows:

Large defect - very evident by eye
Medium defect - evident by close inspection
Small defect - very light or difficult to discern.

In the case of medium defects, such things as water etching or bluing are quite evident by eye but were not ranked large since their influence on life was not considered as serious a defect as a cracked roller.

Utilizing this ranking technique, the vibration relative amplitudes shown in Table 4 were attained:

TABLE 4.

RELATIVE RANKING OF DEFECTS

Defect	Number of Bearings	Maximum Amplitude g's	Minimum Amplitude g's	Mean Amplitude g's	Standard Deviation
Large	10	19.93	1.75	6.17	± 6.0
Medium	15	2.08	0.8	1.22	± 0.38
Small	26	1.16	0.21	0.61	± 0.23
New	5	0.95	0.29	0.55	± 0.25

It is noted that the mean amplitudes of all readings rank favorably with the visual ranking of defects. There is some overlap between the minimum amplitude of one category and the maximum of the next. The trend of the data does indicate the suitability of high frequency vibration as a technique of sorting defects by severity. Large defects can be readily discerned. For small and medium defects, refinements of the technique such as demodulation or pulse counting methods could be employed.

3.3.1.2 Failure Progression Test Results. As a result of the preliminary vibration tests described in paragraph 3.3.1.1, evidence indicated that vibration monitoring of the bearing during failure progression tests would prove beneficial in monitoring any further degradation of the test bearings. The test rig and procedures for conducting the tests were previously described in Section 3.1.2. The instrumentation for these tests, included vibration sensors on the bearing cup and resistance measurements through the bearing from cup to cone. The 10 kHz to 40 kHz frequency range of vibration proved to be the most fruitful area to assess bearing damage. Therefore, a 10 KHz to 40 KHz band pass filter was used to filter the bearing vibration. Both peak vibration and electrical resistance were logged during the test using peak reading meters. Table 5 is a summary of the readings recorded for all of the damaged test bearings. The vibration amplitude is given in peak acceleration values expressed in units of gravity (g-values) and the resistance uncalibrated. Since the resistance is the variation in dynamic amplitude, the higher readings indicate a greater percentage of electrical contact in the rolling elements.

TABLE 5. PROGRESSION TEST VIBRATION MEASUREMENTS

Bearing No.	Cumulative Testing Time(h)	Peak Vibration Amplitude (g's)	Peak Resistance Amplitude (g's)	Remarks
104	1.7	1.5	0.012	Contained blued rollers and water-etched cup, fatigue spalls developed on five rollers, no further damage (suspect spalling occurred after this test - during over-temperature test)
	12.4	1.5	-	
	27.5	1.5	-	
	50.0	2.0	0.06	
	100.6	2.0	0.06	
105	1.4	80.0	0.4	Contained cracked roller - roller crack increased and roller locked in cage
	5.0	7.5	--	
	36.0	12.0	0.7	
	69.0	15.0	0.1	
	97.7	18.0	1.5	
106	2.0	6.5	1.3	Contained spalled rollers and spalled up - no progression of damage
	23.5	7.5	-	
	68.0	7.5	1.4	
	92.1	7.5	1.0	
107	2.0	40.0	-	Contained high spot on roller and in cone - five rollers developed fatigue spalls
	23.5	48.0	0.5	
	68.0	48.0	0.7	
	32.1	37.0	1.6	

TABLE 5. PROGRESSION TEST VIBRATION MEASUREMENTS (CONT.)

Bearing No.	Cumulative Testing Time(h)	Peak Vibration Amplitude (g's)	Peak Resistance Amplitude (g's)	Remarks
108	1.4	6.0	0.014	Contained small spalled areas on cup, cone and rollers — cup spall progressed to gross damage
	5.0	6.0	0.4	
	36.0	18.0	1.4	
	69.0	60.0	0.8	
	97.7	60.0	0.8	
	117.0	50.0	0.8	
	160.0	40.0	0.33	
	171.0	40.0	1.4	
	197.0	50.0	1.7	
109	1.0	2.0	.25	Water etched cup and cone — no marked progression in damage
	20.0	4.5	.6	
	68.0	8.0	.72	
	114.4	6.0	.3	
110	0.25	25.0	1.4	Split roller and water etched up — no marked progression of damage
	34.0	25.0	.02	
	50.0	40.0	.13	
	101.0	45.0	.02	
111	1.0	0.2	.012	Tight brinell of cup, cone and roller — no marked progression of damage
	20.0	1.5	1.0	
	68.0	2.1	.88	
	114.4	1.2	2.0	
112	0.25	0.2	.35	Light spall and brinell of cup — gross spalling of cup after test
	34.0	3.5	.08	
	50.0	3.5	.20	
	101.0	10.0	-	
113	0.25	0.2	0.4	Several spalled areas in cup — moderate progression of spalled areas during test
	19.0	0.2	0.8	
	υ2.0	3.0	-	
	83.0	-	-	
	99.0	-	-	

In review of Table 5, the general trend is for increasing vibrational amplitudes with duration of test. In contrast, a new bearing amplitude was 0.1 throughout the test. Bearings with roller high spots, large local spalls or split rollers produced high peak vibrations in the range from 40 to 80 g. For smaller spalled regions and surface damage regions, amplitudes ranged from 2 to 30 g.

Two bearings (105 and 107) indicated a decrease in amplitude during the test. In the case of bearing 105, the roller became locked in the cage and was sliding rather than rolling during the test. This probably occurred during the first few hours of operation.

Bearing 107 had roller high spots on the end of the roller. After test it was noted that these areas had fatigued. It has been postulated that the fatiguing (removal) of the roller high spots was the cause for the amplitude decrease.

3.3.1.3 Acceptance Demonstration Tests. For the acceptance demonstration tests, described in Volume I (3), the test bearings were also instrumented in the same way as were the bearings for the failure progression tests previously discussed; i.e., thermocouples, high frequency accelerometers, and vibration monitor.

The requirements imposed upon the diagnostic instrumentation applied to an acceptance test are significantly more stringent than those imposed by failure progression testing. Failure progression testing involved bearings with gross defects while acceptance tests involved testing new bearings with the instrumentation required to detect the presence and growth of a relatively small defect -- certainly much smaller than any initial defect considered during the failure progression tests.

Following the first two series of acceptance demonstration tests (C1A and C2A), it became clear that the peak amplitude of vibration in the 10 to 40 kHz region did not provide enough information to determine the presence of small defects generated during the test and thus to give reason for terminating the test. The primary reasons for this are that many new bearings produce a relatively high constant overall vibration level and that small discrete frequency disturbances caused by defects cannot be separated from the overall vibration level without utilizing demodulation techniques.

Thus, for the remainder of the series (tests C3A, C4A, C5A, and C4B), a high frequency demodulator and spectrum analyzer was added to the vibration data analysis equipment. Each test was operated until a discrete test bearing defect was identified by means of vibrational frequency analysis and then found to change with time. At this point the test was terminated and the bearings inspected.

The basic analysis technique used was to demodulate, or envelope-detect, the high frequency (10 to 40 khz) vibration amplitude and to perform a low frequency (0 to 200 Hz) spectrum analysis on the demodulated amplitude to identify discrete frequencies associated with imperfections of the bearing component surfaces. For the rotational speed used for the test (666 to 672 rpm) the frequencies shown in Table 6 were of significance in identifying bearing component imperfections:

TABLE 6.

IMPERFECTION FREQUENCIES

5.2 Hz	-	Cage Rotational Frequency
11.2 Hz	-	Inner Race Rotational Frequency
55 Hz	-	Roller Rotational Frequency
120+ Hz	-	Roller -- Outer Race Frequency
143 Hz	-	Roller -- Inner Race Frequency

The following subsections describe the correlation between the high frequency diagnostic data collected during the last four test series and the condition of the bearings upon test termination.

Test C3A

This test was terminated after 200 hours of operation because the low frequency spectra of the center bearing (bearing 207) indicated the presence of a discrete frequency of 55.2 Hz at 198 hours which had not previously been present. This frequency indicated the possibility of a roller defect. Also, bearing 208 generated a discrete frequency of 120.4 - 120.8 Hz which increased steadily in amplitude throughout the test indicating the presence of an outer race defect.

Examination of these bearings following the 200-hour test revealed that bearing 207 possessed a spalled roller and bearing 208 has a spalled cup (Figure 27).

A plot of low frequency spectra of demodulated high frequency vibration data taken from bearing 207 is shown in Figure 28 and 29. The spectra shown in Figure 28 (53 hours) is typical of the spectra at all times up until the condition at 198 hours was noted (Figure 29). The two frequencies noted in Figure 28 (5.2 and 11.2 Hz) are characteristic bearing related frequencies (cage rotation and inner race rotation, respectively). Other frequencies are test rig related. Particular attention is drawn to the 120.0 Hz frequency which is caused by motor stator vibration at twice line frequency. This is not to be confused with bearing roller outer race frequency which occurs at 120 + Hz.

Figure 29 shows the presence of a discrete frequency at 55.2 Hz which is the rotational frequency of the rollers indicating the possible presence of a roller defect -- which was verified upon disassembly. (See Figure 27.)

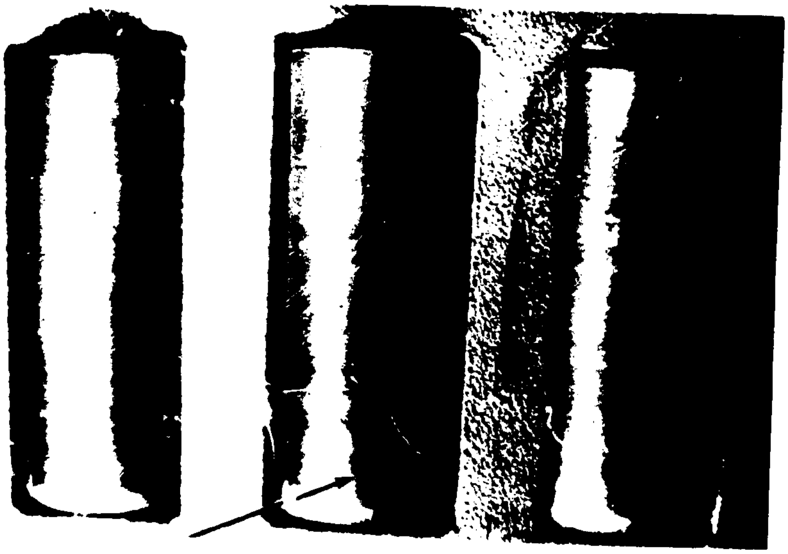

ROLLER FROM 207

CUP 208

FIGURE 27. SPALLED BEARING COMPONENTS FROM TEST C3A

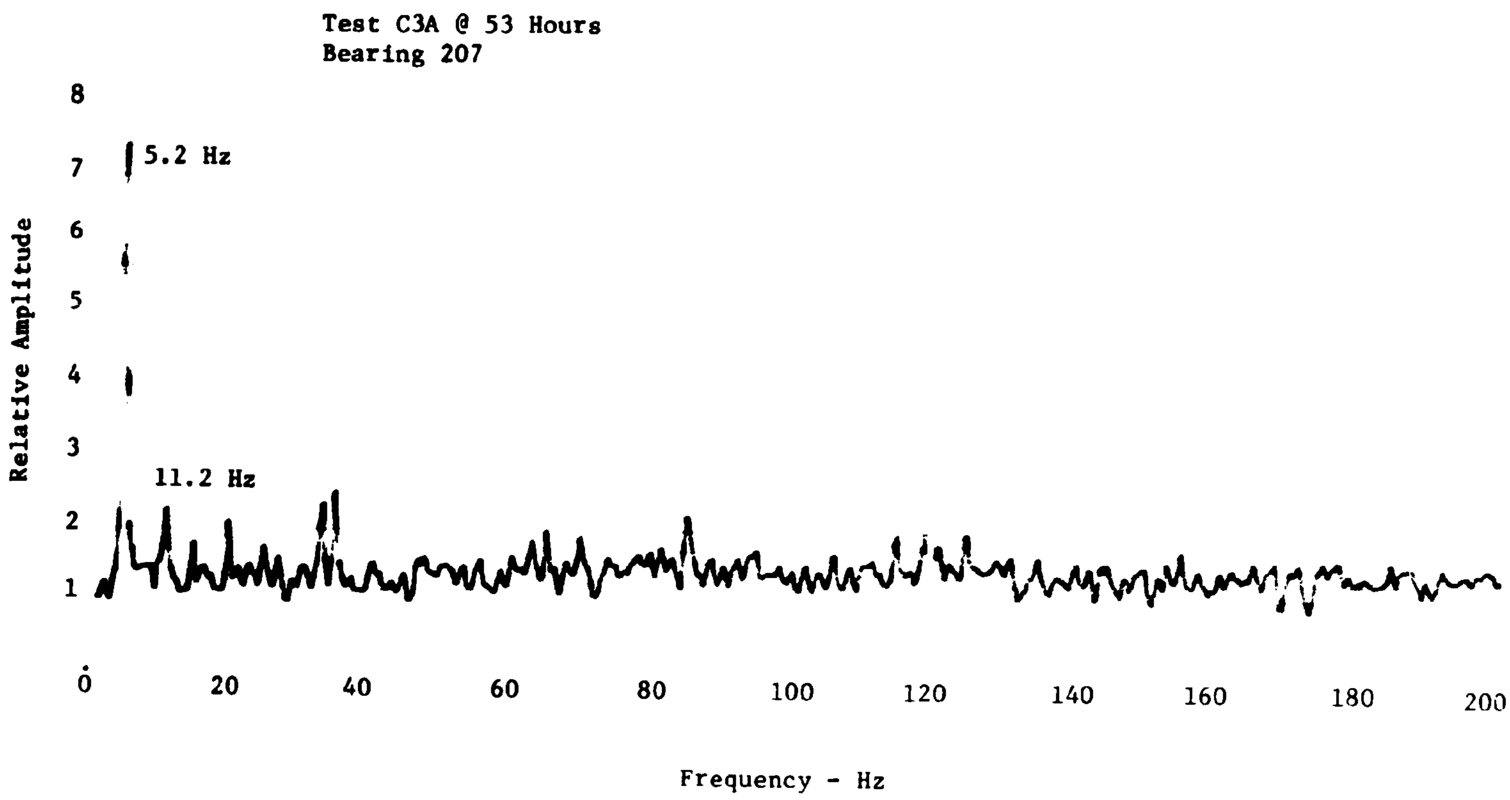

FIGURE 28. LOW FREQUENCY SPECTRA DEMODULATED FROM 39.7 kHz

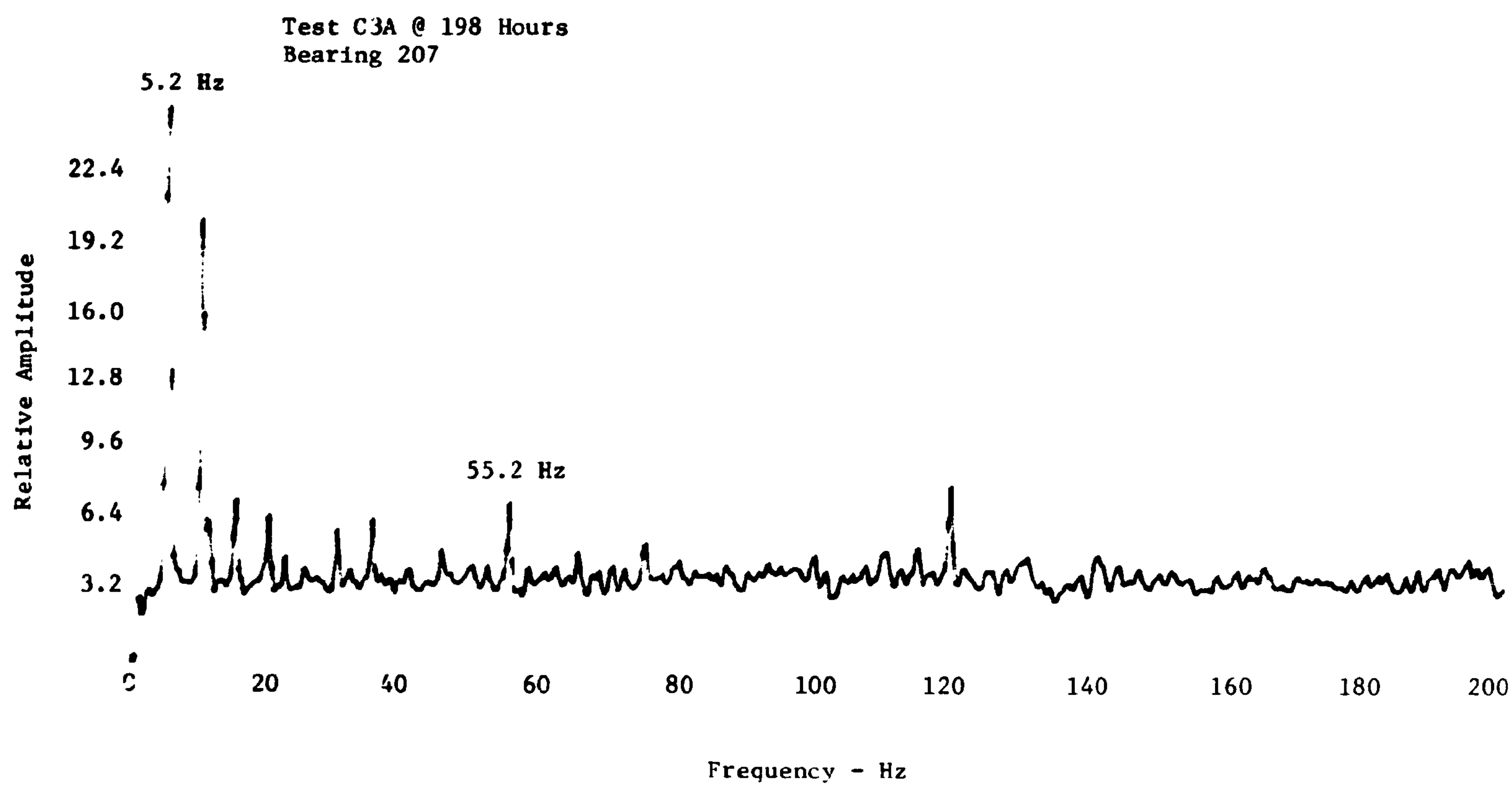

FIGURE 29. LOW FREQUENCY SPECTRA DEMODULATED FROM 37.1 kHz

It will also be noted that cage frequency is much larger at 198 h than it was at 53 h. Typically, cage frequency was dominant and tended to increase in ampiitude with time on all tests. This dominance was probably due to the poor quality of the cage (relative to other bearing components) and the increasing amplitude probably attributable to channeling and drying of the grease with time.

Also in Figure 29, harmonics of 10 Hz and 5.2 Hz side bands around 10 Hz harmonics will be noted. The 10 Hz harmonic frequency is not attributable to the bearing but is evidently rig structure related and is evident in much of the data for all the tests.

Figure 30 shows the low frequency spectra derived from bearing 208 at the beginning and end of the test. Here the only dominant frequency is 120.4 Hz, which corresponds to the roller -- outer race frequency indicating a possible outer race defect. Again this suspicion was confirmed at disassembly (see Figure 27).

For bearing 208, evidence of an outer race imperfection was present throughout the test and increased in amplitude during the course of the test, indicating a growth in imperfection size. Table 7 summarizes the 120.4 Hz amplitude with time.

TABLE 7. AMPLITUDE AND OVERALL NOISE LEVEL AT 12.04 Hz

Cumulative Test Time (h)	Relative Amplitude 120.4 Hz	Noise	Signal/Noise
6.3	2.6	1.5	1.7
23.0	5.6	3.0	1.9
53.0	7.9	2.3	2.8
198.0	10.3	3.4	3.0

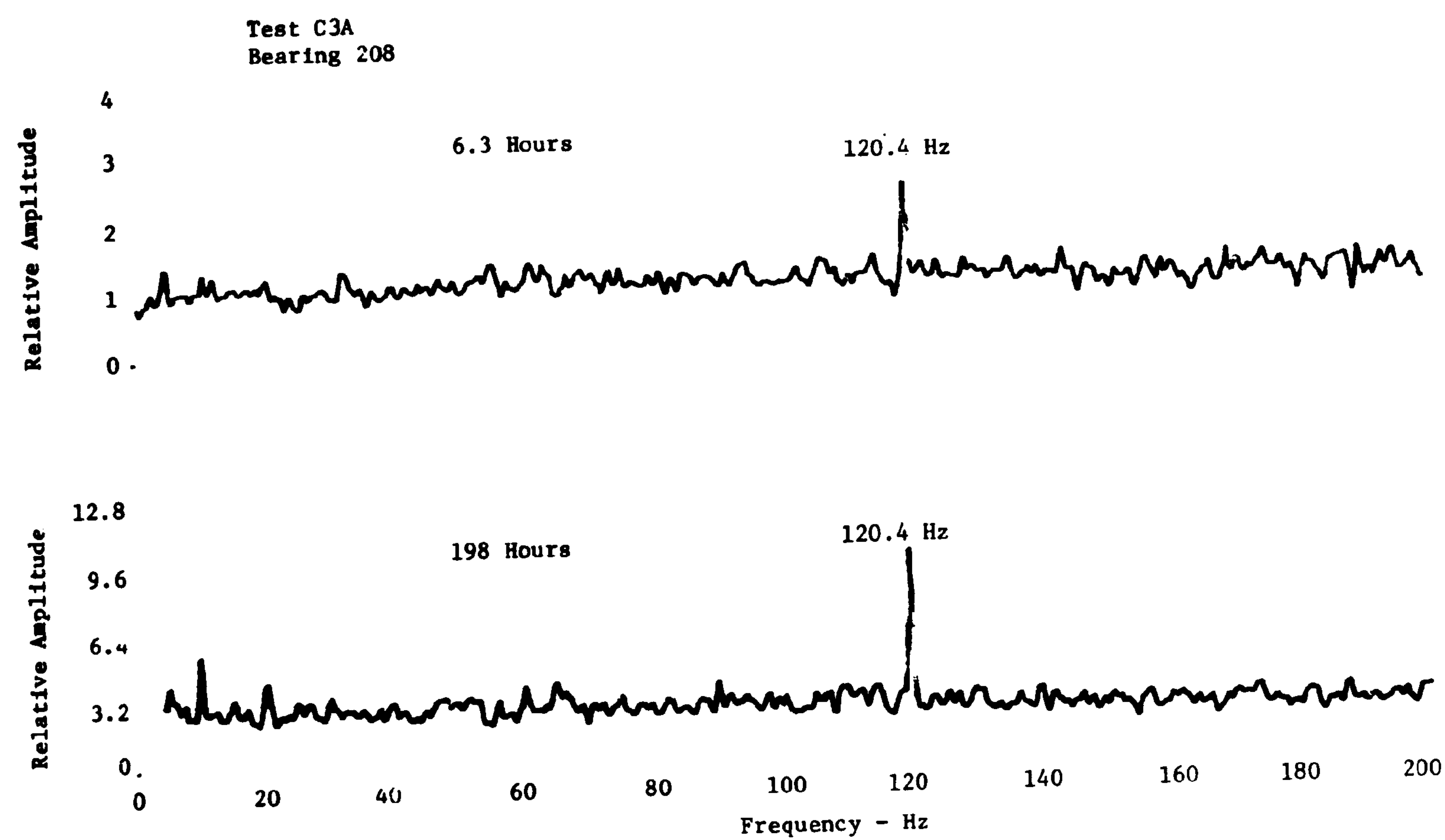

FIGURE 30. LOW FREQUENCY SPECTRA DEMODULATED FROM 10 TO 50 kHz

From Table 8, it is seen that the amplitude and the signal to noise ratio of the roller -- outer race frequency characteristic increased with time. It is unusual, however, for evidence of a defect to occur so early in the test. A probable explanation of this phenomenon is that the cup of this particular test bearing was a reground one made of modified AISI 4620 and had seen prior railroad service (approximately 10 years). Thus, a subsurface defect could easily have been present and/or the case may have been abnormally thin (from regrinding).

Test C4A

The highly loaded center bearing used during this test (number 204), had previously been run for 130.2 hours on test C2A. Upon disassembly (after C2A) one roller was found to have a long, very shallow spall -- not condemnable by AAR rules. It was decided to reassemble this bearing and subject it to further test time on test C4A to study its vibrational signature with time and to get an additional feel of the progression rate of this type of defect.

The characteristic frequency displayed for this roller defect was twice roller rotational frequency (110.8 Hz) -- one each for the roller defect impacting the inner and outer race.

Table 6 summarizes the 110.8 Hz amplitude of the demodulated 10 to 40 KHz high frequency vibration.

TABLE 8

AMPLITUDE AND OVERALL NOISE LEVEL AT 110.8 Hz

Cumulative Test Time (h)	Relative Amplitude 110.8 Hz	Noise	Signal/Noise
23	1.2	.5	2.4
69	4.9	.5	9.8
77	6.3	.5	12.6

A photograph of the spalled roller at the conclusions of test C4A (after a total accumulated time of 207.2h) is shown in Figure 31.

Test C5A

After approximately 183 h of running, it was noticed that bearing 212 produced a distinguishable vibration amplitude in the vicinity of 146 Hz which would be characteristic of an inner race defect. However, this characteristic essentially disappeared at approximately 186 h. At approximately 218 h, the 146 Hz discrete frequency reappeared with an amplitude approximately 50% larger than previously noted, and with a signal to noise ratio of about 2.5. At this point the test was terminated and the bearing inspected.

Figure 32 is a photograph of the inner race of bearing 212 which had developed a sizable spall during the test. The reason for the erratic and the relatively low amplitude vibrational behavior at the inner race defect frequency has not been fully explained to date, but is most likely related to the manner in which the spall grew. Examination of the spall reveals a crushed and rounded leading edge and evidence of a very highly loaded race surface next to the spall near the large end shoulder. It is postulated that as the spall progressed, the edge rolled away causing the load to be picked up by the roller ends, thus reducing the impact and the vibration levels. Periodically, additional material at the leading edge would break away, producing a new sharp edge and high shock levels only to have the edge rolled over again. Only on rare and coincidental occasions were the vibrational levels being monitored during periods when the edge was relatively sharp. Examination of the temperature plots indicated the cup temperature at the end where

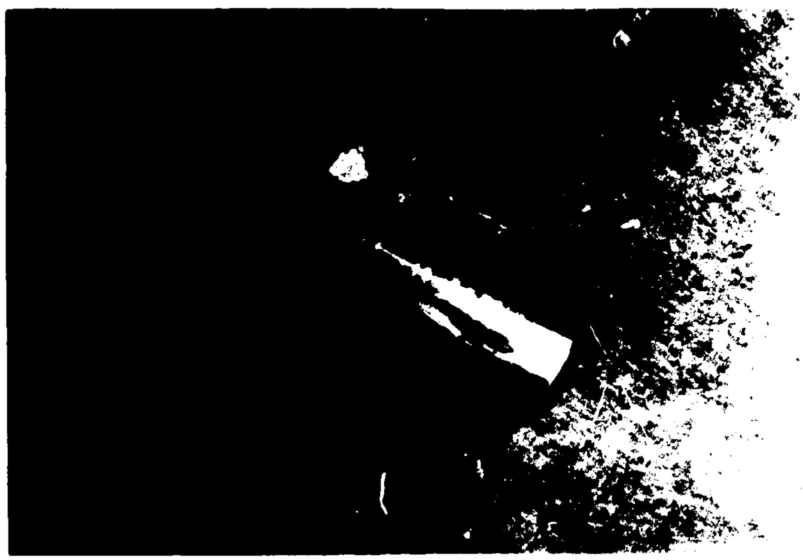

FIGURE 31. ROLLER FROM BEARING 204 FOLLOWING TEST C4A

FIGURE 32. INNER RACE FROM BEARING 212 FOLLOWING TEST C5A

the subject cone was located would periodically increase by approximately 30 to 40 degrees over a period of 3 to 4 hours and then drop to its steady state level. One of the temperature excursions commenced at about 183 hours and abruptly ended at about 186 hours. These temperature excursions were probably caused by the masticating of the broken leading edge debris. The presence of sizable wear debris was evidenced by the large size of the fragment indentations on the rolling element surfaces and severe wear bands on several rollers.

Test C4B

For this test, the same support (end) bearings that were used for test C4A were employed, while a new bearing (214) was placed in the center position to replace bearing 204 which had developed a roller spall on test C4A.

After 65 hours of operation, bearing 214 displayed the first signs of a discrete frequency in the demodulated low frequency spectra at 141.6 Hz -- indicating a possible inner race defect. The signal-to-noise ratio at this frequency was only 1.3, but it was decided to discontinue the test at this point and to inspect the bearing since this represented the minimum imperfection size that could be detected with the diagnostic equipment being utilized -- if indeed a defect was present.

Figure 33 is a photograph of one of the cones from bearing 214 showing a defect measuring approximately 0.08 inches long by 0.05 inches wide by 0.0062 inches deep. Under the microscope the defect appears as a dent with a definite spall developed at one end.

FIGURE 33. INNER RACE FROM BEARING 214 FOLLOWING TEST C4B

3.3.1.4 Railroad Wheel Shop Tests. To demonstrate the feasibility of a bearing fault detection scheme for bearings while installed on the axle -- say following a derailment or at any other convenient inspection point -- ninety 6 x 11 roller bearings were subjected to ultrasonic crack detection and high frequency fault detection tests.

The bearing cup was rotated on the axle at an equivalent speed of approximately 45 miles per hour by means of a motor-driven tired device shown in Figure 14. Vibration was measured by means of an accelerometer mounted on a clamp which was in turn bolted to the axle. A hand-held ultrasonic probe was in turn bolted to the axle. This probe was used to traverse the length of the cup to detect for cracks. Instrumentation, signal conditioning, and data recording equipment are also shown in Figure 14. The block diagram of the vibration envelope detector is shown in Figure 6.

The sequence of test operations, which consumed approximately 1-1/2 minutes per bearing, consisted of the following:

1. End cap was removed.
2. A strip about one inch wide of external dirt and rust was removed from the cup O.D. by means of an electric disk sander. (This cleaned surface was later used for crack detection.)
3. An identifying number was painted on the bearing.
4. The accelerometer mounting clamp was bolted to the axle.
5. The bearing turning device was moved in position under the bearing (moved on tracked wheels).
6. The tires were raised by means of a foot pedal and rotation was started.
7. Vibration levels were manually recorded and magnetic tape recorded for approximately 10 seconds.
8. Rotation was stopped, accelerometer removed, and turning device moved from under bearing.
9. Oil was applied to cleaned portion (strip) on cup O.D.
10. Cup was probed for cracks (visual observation on oscilloscope).

Following the tests, each bearing was removed and visually inspected. The inspection results are briefly summarized below:

Total number of bearings	90
Number of bearings for which vibration data was analyzed	80
Number of bearings having condemnable surface defects (spalls, brinells, indentations)	14
Number of bearings having either condemnable or other surface defects worth noting	43
Number of bearings having cracked or broken cups	5

The vibrational behavior of each of the 80 bearings was analyzed for correlation with surface defects identified by visual inspection. The following vibrational characteristics versus bearing condition were evaluated:

1. Peak amplitude between 10 kHz and 40 kHz
2. Peak-peak amplitude of the demodulated envelope
3. Average amplitude of the demodulated envelope
4. Peak-peak ÷ average of the demodulated envelope

It was found that the last characteristic provided the best correlation with bearing condition. Figures 34 and 35 show the proportion of condemnable bearings and the proportion of bearings with any noted defect versus the four different vibrational characteristics. Here it is seen that the last characteristic (peak-peak ÷ average) provides the better correlation with bearing condition.

Figure 36 shows the effect of rejection level on the percentage of bearings rejected and typical defects associated with various levels. For example, if a rejection level of 1.0 were selected, the following would have resulted:

1. 21% of the bearings with condemnable defects would have been accepted.

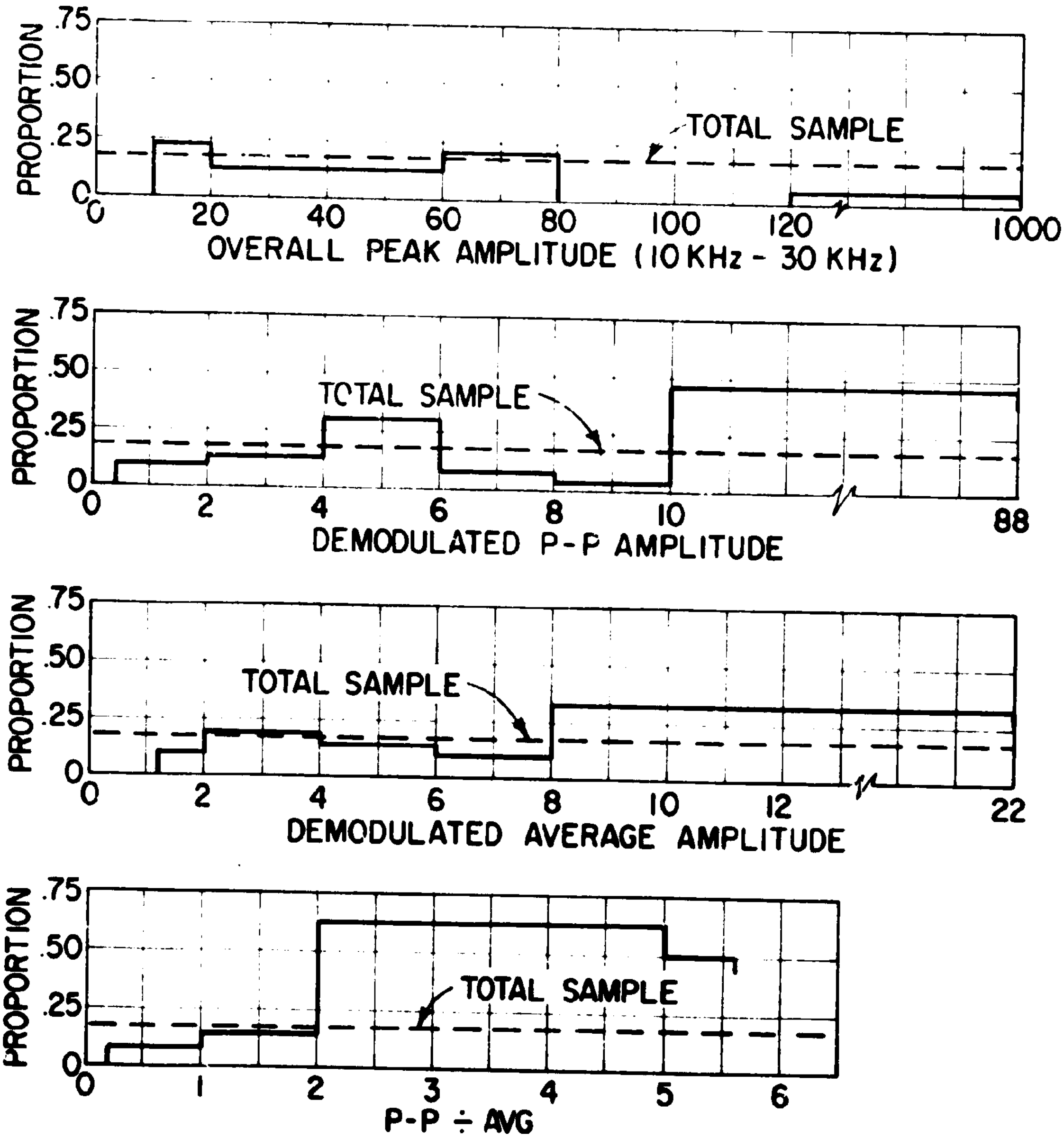

FIGURE 34. PROPORTION OF CONDEMNABLE BEARINGS VERSUS VIBRATION CHARACTERISTIC AMPLITUDE

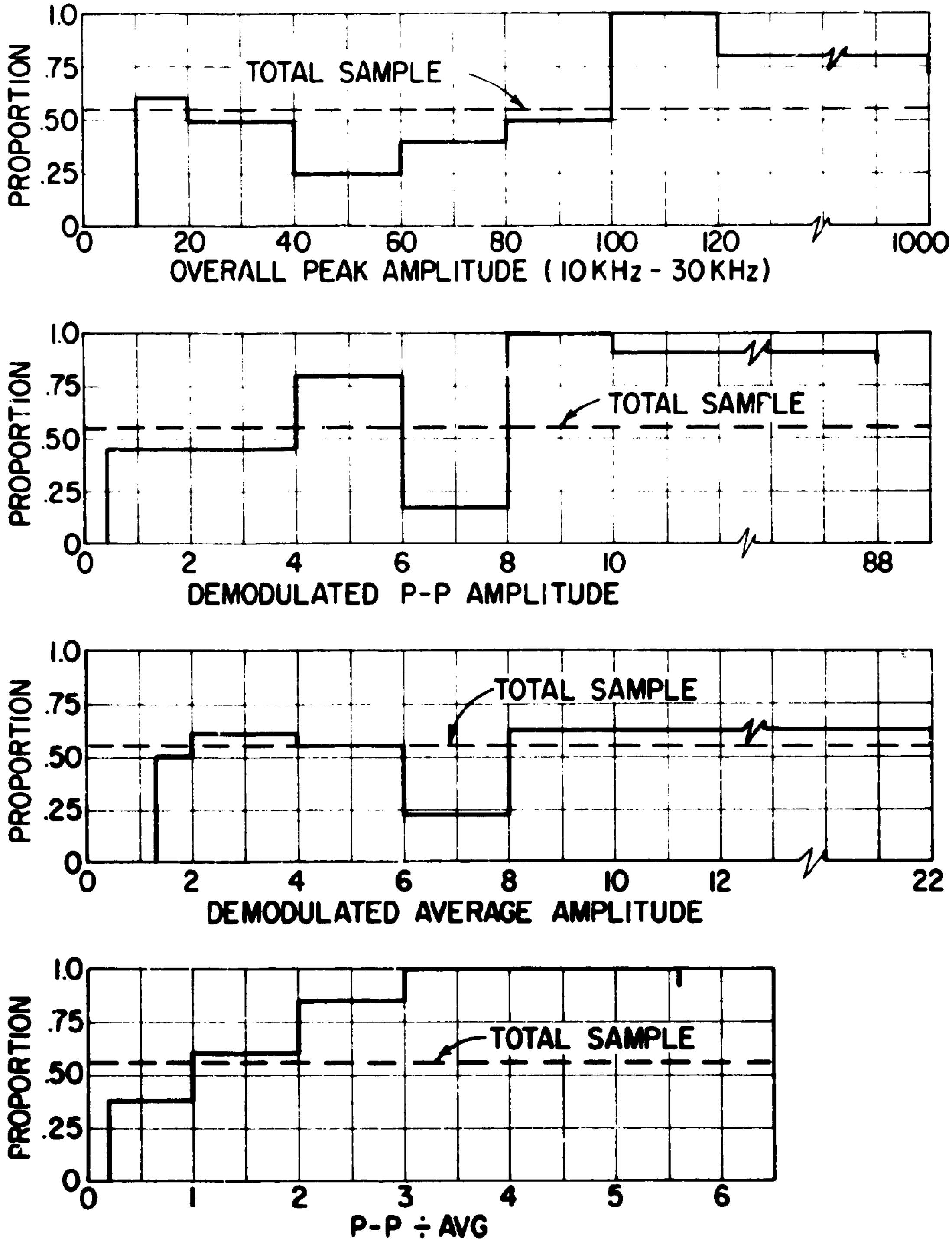

FIGURE 35. PROPORTION OF DEFECTIVE BEARINGS VS. CHARACTERISTIC VIBRATION AMPLITUDE

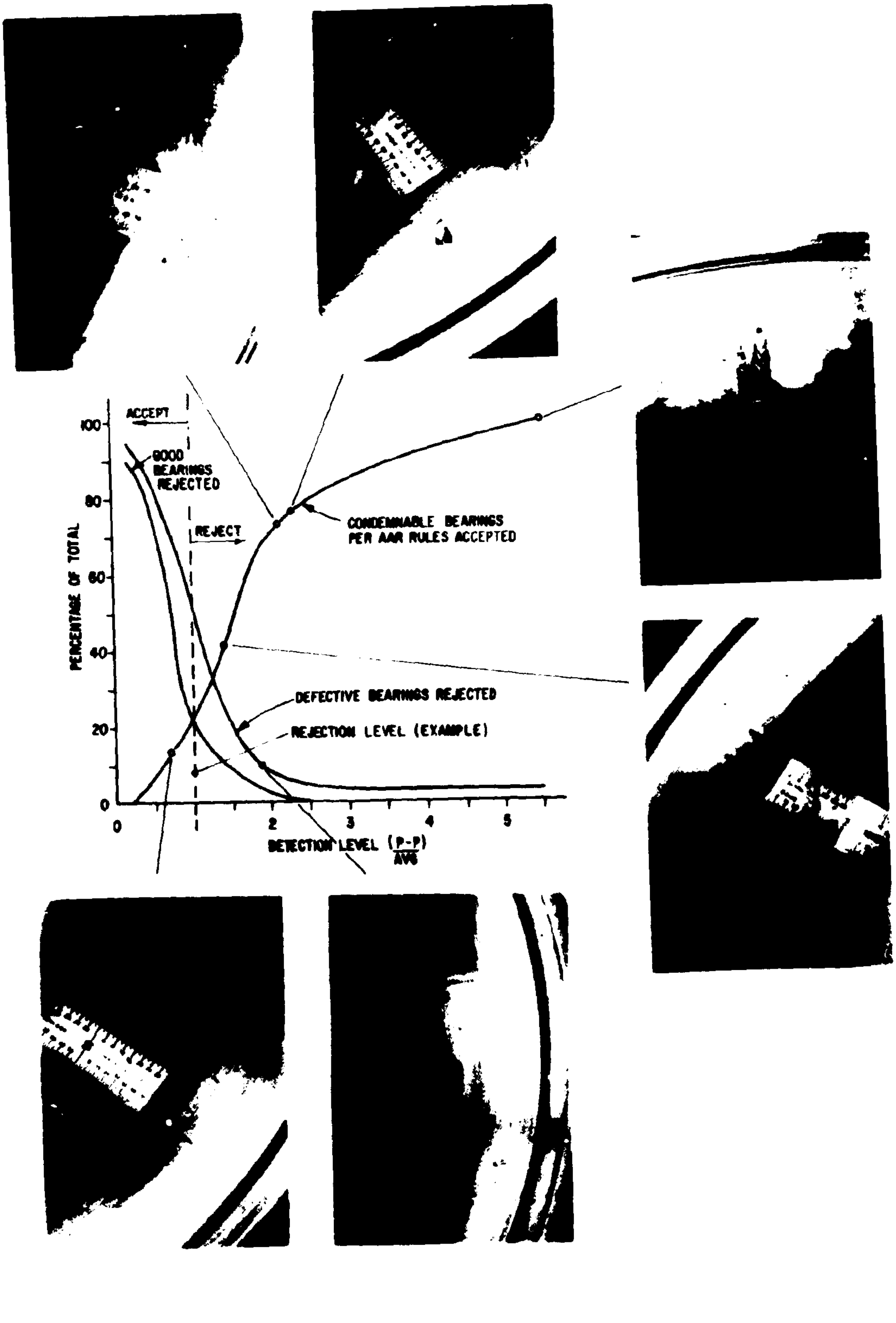

FIGURE 36. RESULTS OF TESTS AT SOUTHERN RAILROAD WHEEL SHOP SHOWING TYPICAL DEFECTS

2. 21% of the bearings with no defects would have been rejected.

3. 52% of the bearings with noncondemnable defects would have been rejected.

Considering the adverse conditions under which the subject tests were conducted, the results were extremely encouraging. The primary adverse situation was the shortness of time during which valid data could be collected.

With all the aforementioned operations that had to be accomplished, only about 10 seconds of reasonably steady-state data could be collected on magnetic tape for analysis.

It should also be noted that two of the three bearings with condemnable defects that fell below a peak-peak : average reading below 1.0 contained roller spalls and that only three bearings in the total sample had roller spalls. Thus, it appeared that the fault detection scheme tested needed improvement in the area of roller fault detection.

Following its return from the wheel shop, the bearing turning device was used to test suspected faulty bearings following certification demonstration testing (starting with test C4A) but prior to dismounting the bearings from the test shaft.

For these tests, high frequency vibration data were processed by the vibration envelope detector and then analyzed by use of the spectrum analyzer. Typical low frequency spectra for each of the faulty bearings from tests C4A, C5A, and C4B are shown in Figures 37 through 39. In each case the discrete frequency associated with a particular defect found during the subsequent inspection is quite evident. Attention should be drawn to Figure 37 which clearly shows the roller-defect-associated frequency, indicating that roller defects can indeed be detected if suitable data processing techniques are employed.

Roller Defect Produced During Certification Demonstration Testing
(207 Hours; 52,000 lbs.: 65 mph Equivalent)

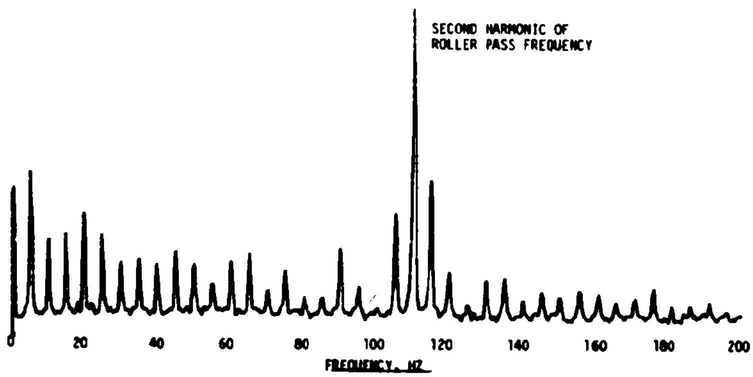

Frequency Spectra of Envelope-Detected Signal at End of
Test on Roller Bearing Test Rig
(above)
and
on Cup Turning Rig
(below)

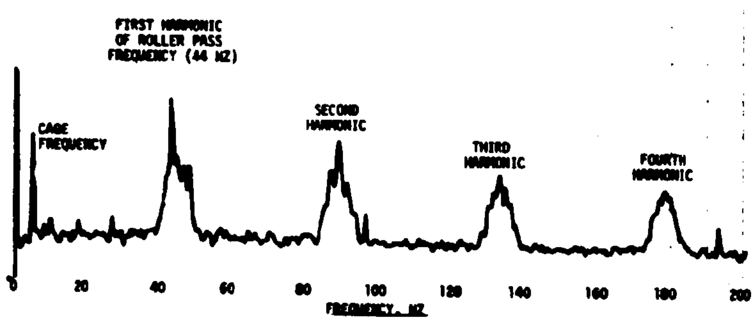

FIGURE 37. BEARING 204 DEFECT AND LOW FREQUENCY SPECTRA FOLLOWING TEST C4A

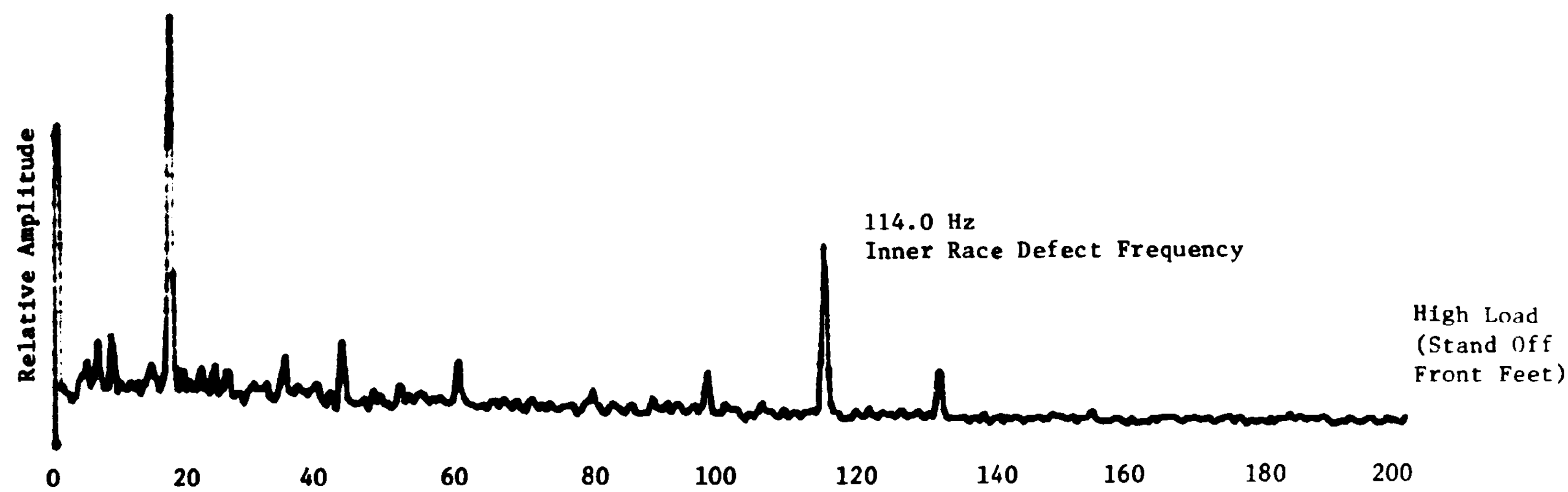

FIGURE 38. DEMODULATED LOW FREQUENCY SPECTRA FROM BEARING 212 FOLLOWING TEST C5A USING BEARING TURNING DEVICE

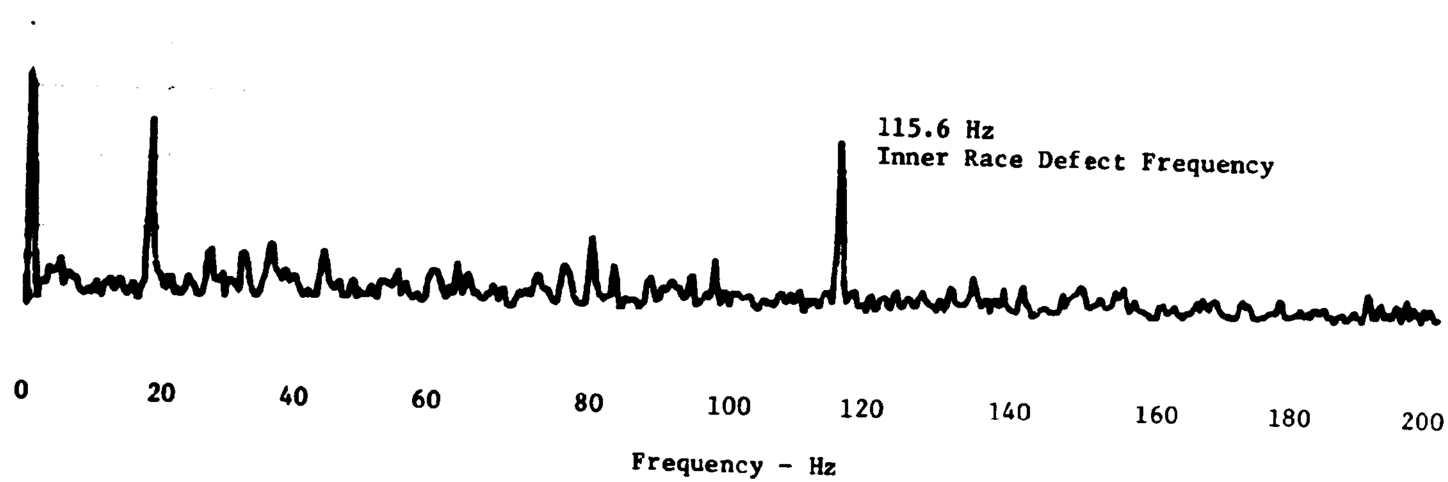

FIGURE 39. DEMODULATED LOW FREQUENCY SPECTRA FROM BEARING 214 FOLLOWING TEST C4B USING BEARING TURNING DEVICE

3.3.1.5 Summary of High Frequency Vibration Technique Results. The preceding subsections have discussed the results of various high-frequency-vibration-based diagnostic tests of defective railcar roller bearings employing a variety of test apparatus. In this subsection, we summarize the significant results of these tests and attempt to put them into an easily visable perspective.

Of the four test series previously discussed, only two approached the environment of the railcar roller bearing in terms of speed, load, lubrication process, and rotating component orientation. They were the failure progression tests (Section 3.3.1.2) and the certification demonstration tests (Section 3.3.1.3). In the case of the component tests (Section 3.3.1.1) the cup was rotating, the load was purely axial, and the bearing was oil lubricated. For the wheel shop tests (Section 3.3.1.4), the cup was also rotating and the load was very lightly (on the order of 100 lbs.) radial.

These significant differences in test condition might be expected to produce significant differences in vibrational behavior induced by the various defects. Indeed there were differences, but they were, in a sense, subtle differences. In general, the peak vibrational amplitude in the 10 to 40 kHz band fell between near zero and 50 g for all bearings on the three different test stands. The range between zero and 2 g contained bearings with no damage and moderately damaged bearings at or near the AAR defined condemning limits. Bearings producing "g" levels above two were consistently condemnable.

Figures 40 through 44 are representative of the test results. Figure 40 graphically shows where the various defective bearings fell on a scale of 0 to 20 g during the component tests described in Section 3.3.1.1.

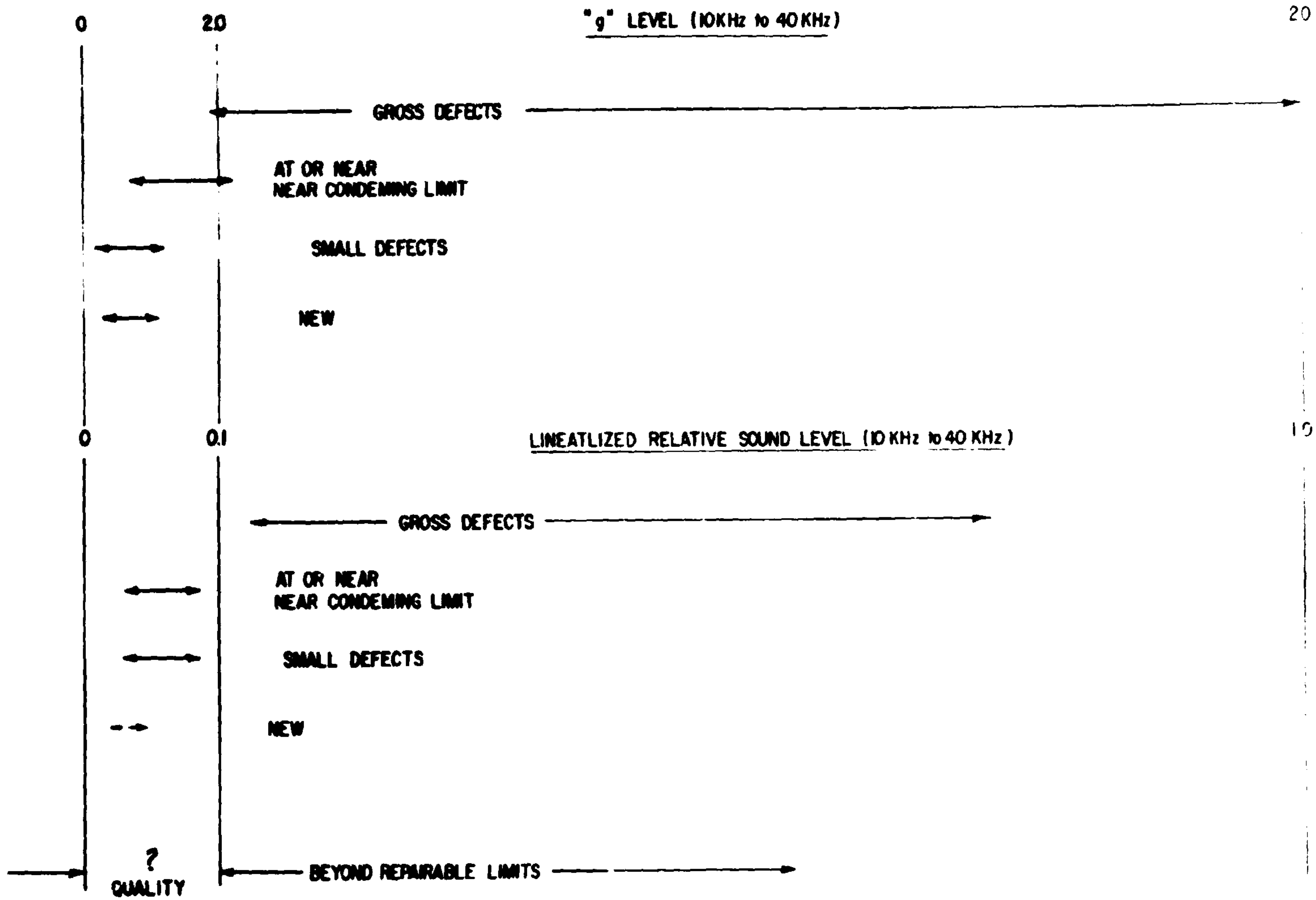

FIGURE 40. SUMMARY OF SINGLE COMPONENT TESTS

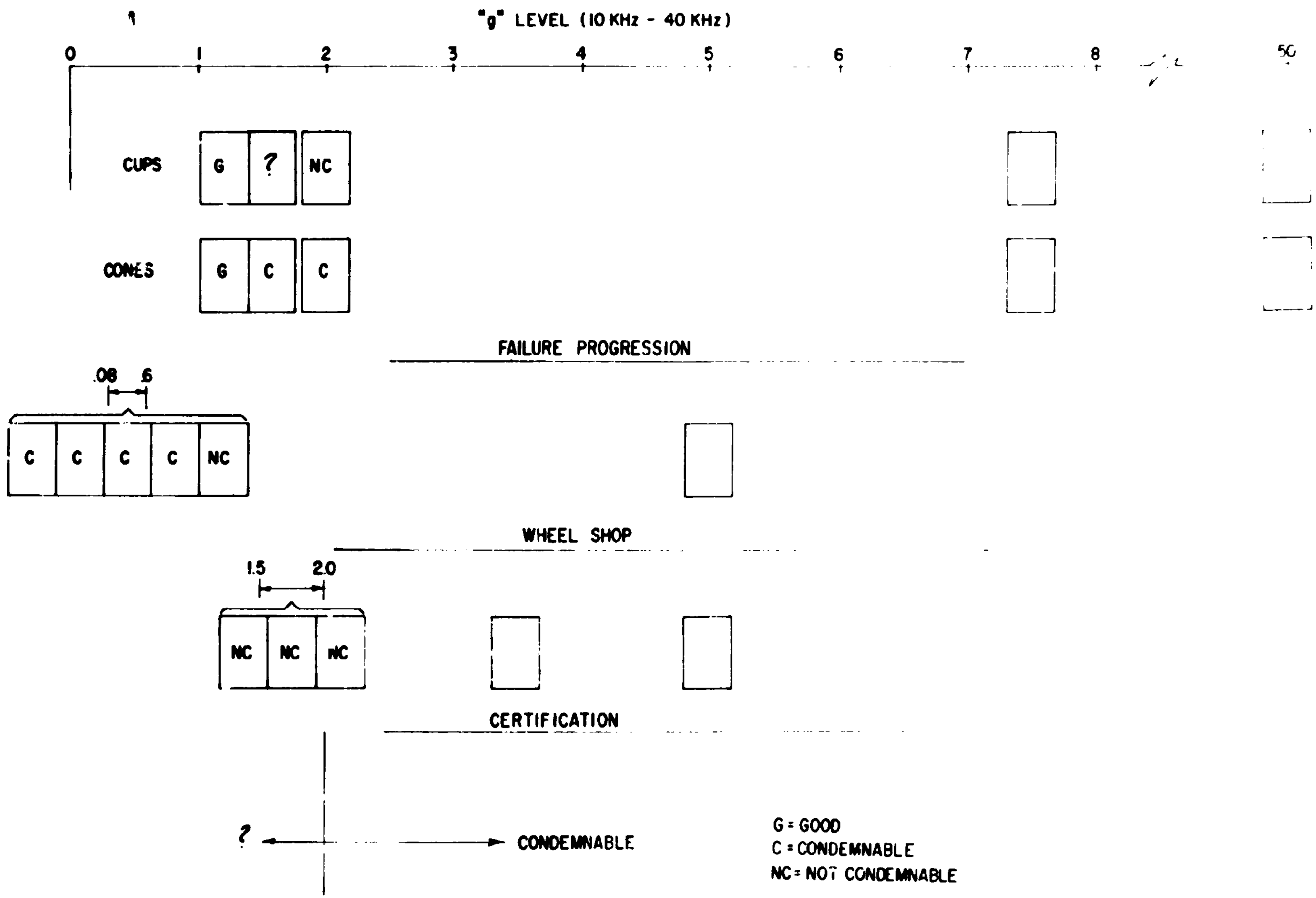

FIGURE 41. SUMMARY OF DEFECT VARIETY

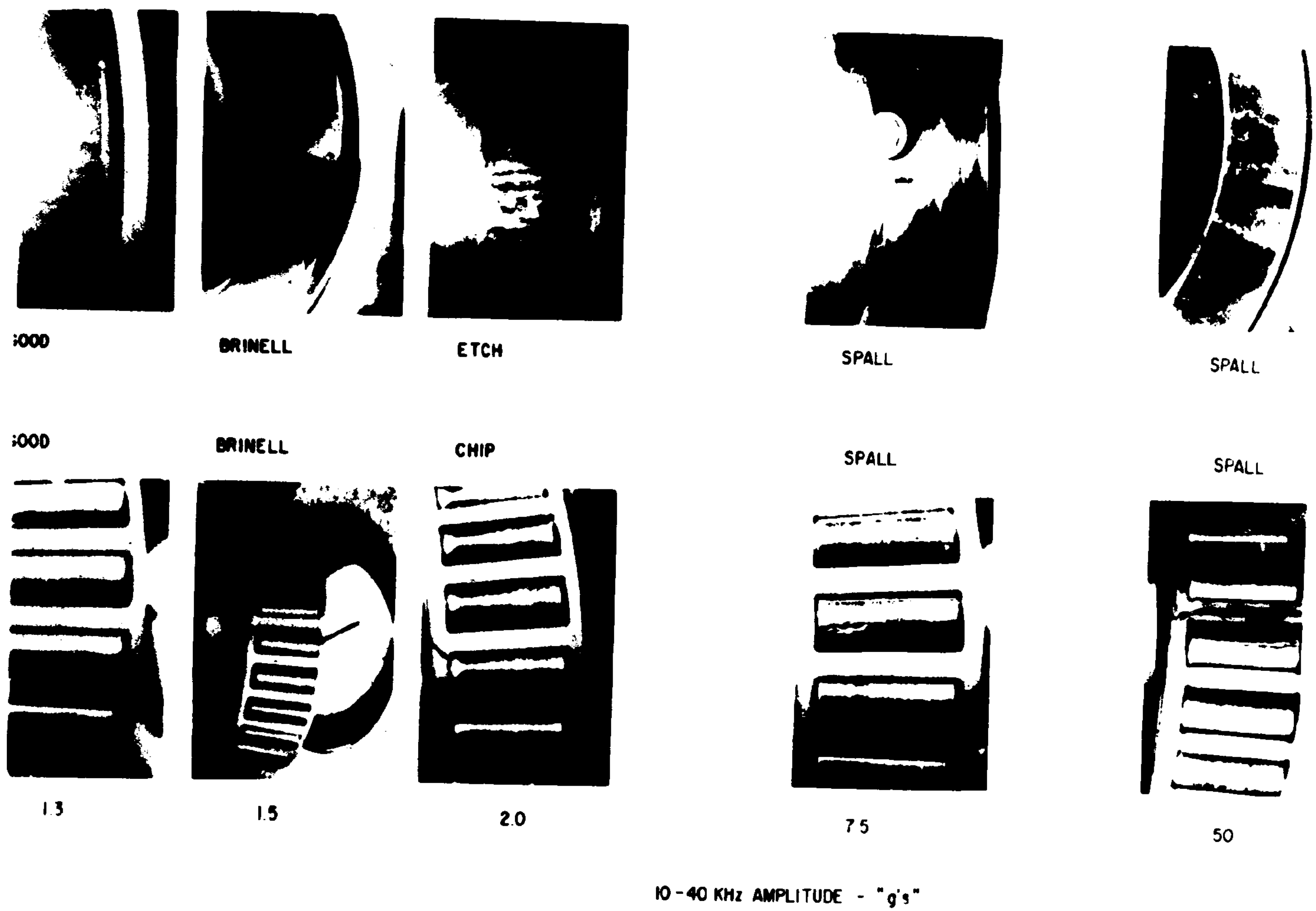

FIGURE 42. CONDITION AND AMPLITUDE-FAILURE PROGRESSION TESTS

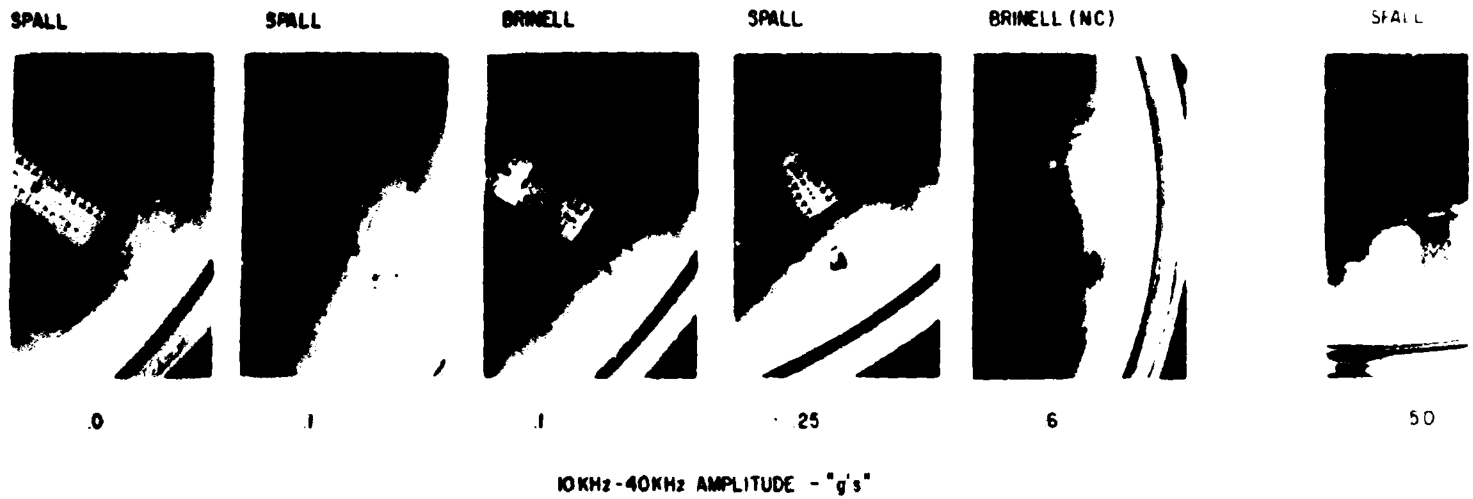

FIGURE 43. CONDITION AND AMPLITUDE-WHEEL SHOP TEST

1.5 - 2.0			3.5	5.0

10 - 40 KHz AMPLITUDE - "g's"

1.3	1.3	3.0	12.6	6.7

SIGNAL - NOISE OF DISCRETE DETECT FREQUENCY

DEMODULATED FROM 10 - 40 KHz (FROM 0-200 Hz SPECTRUM ANALYSIS)

FIGURE 44. CONDITION AND AMPLITUDE-CERTIFICATION TESTS

Figures 42 through 44 shows the condition and "g" levels of representative bearings from the other three tests as well as signal-to-noise ratio of the discrete frequency content from the certification demonstration tests (Figure 44). Figure 41, which precedes the figures containing photographs, sets the stage from an amplitude point of view for the figures that follow. The rectangles in Figure 41 depict the relative location on the "g" level scale of each of the photographs in Figures 42-44. An examination of these various photographs reveals that:

1. The severity of damage and the "g" levels are consistent between tests.
2. The severity of damage above 2 g's should be cause for concern from an operating bearing point of view.
3. Although many bearings that produced "g" levels below 2 were beyond condemnable limits, their severity of damage should not produce an imminent safety hazard.

3.3.2 Ultrasonic Crack Detection

If an ultrasonic pulse is introduced into the cup at an angle from normal incidence, Figure 45 shows that the pulse will be transmitted around the cup by reflecting from both inner and outer surfaces. The presence of a crack in the transmission path will reflect back a signal. The angle of the transducer will reduce the sensitivity to the pulse transmitted completely around the ring. Every time a reflection is made, energy is lost at the interface. The distance around the circumference that can be used is therefore a function of the angle (number of reflections) and the frequency.

Initial tests in the laboratory indicated that inspection performed at any one circumferential location on the cup would be adequate.

Tests on five cracked cups at the wheel shop showed that two locations are required. However, none of the five cracked or broken cups were detected at the wheel shop using the ultrasonic detector. Laboratory

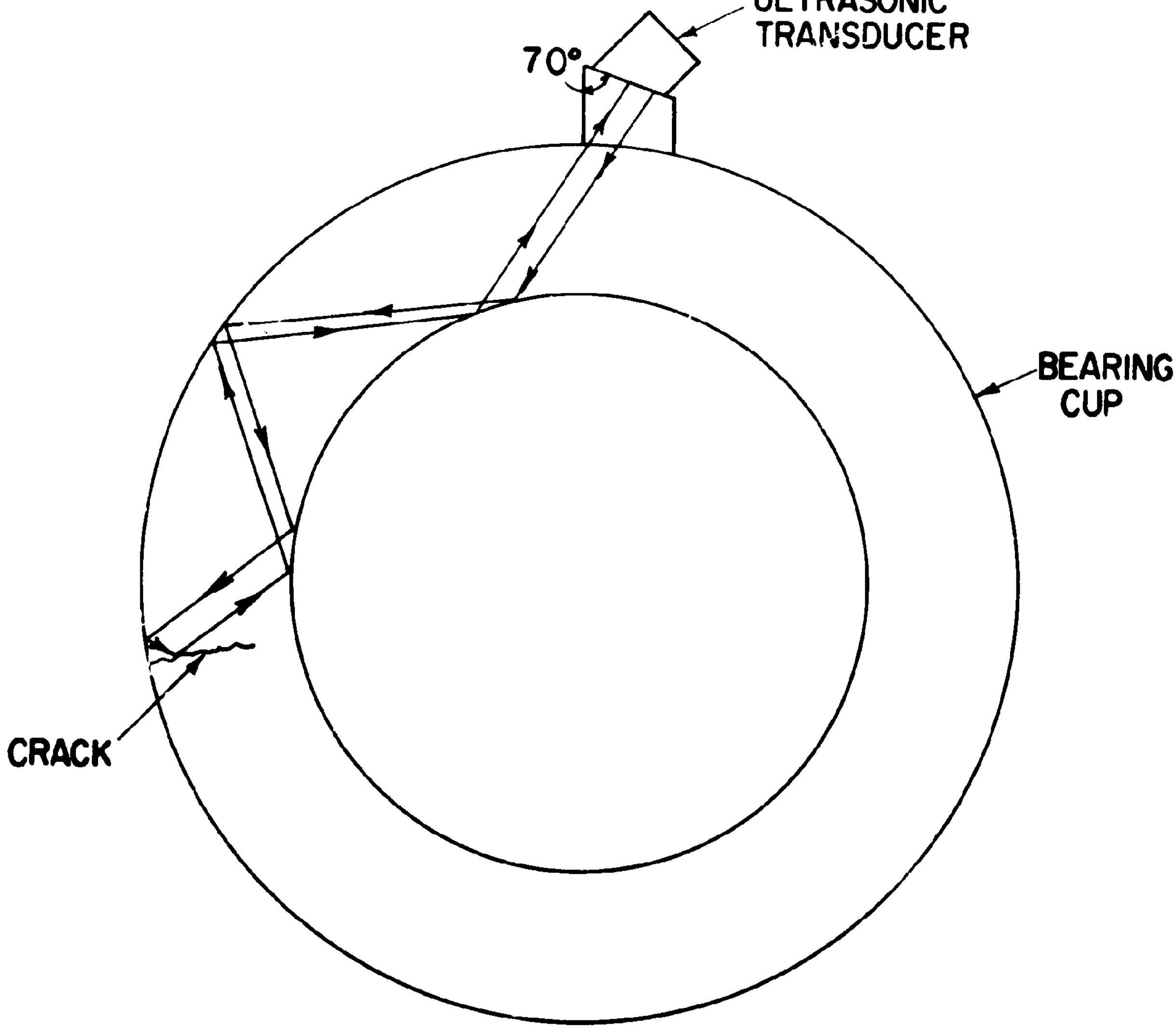

FIGURE 45. MODE OF OPERATION - ULTRASONIC CUP CRACK DETECTOR

tests conducted subsequently revealed that the wheel shop tests were performed with improper gain settings. The initial gain settings were established using an unassembled cracked cup as a standard. Unfortunately, it was found that the presence of grease and the seal case significantly attenuates the ultrasonic signal.

The subsequent laboratory tests showed that if a fully greased assembled bearing with a cracked cup is used to establish gain settings, cracks and broken cups can be repeatedly found. Figure 46 shows a typical oscilloscope trace of a cracked cup along with the method of probing. Unfortunately, we did not have a sufficient quantity of cracked cups available in the laboratory to perform a truly quantitative evaluation, but the cracked cups we were able to test demonstrated the viability of the approach.

3.3.3 Grease Ferrography

Following each of the acceptance demonstration tests (discussed in Section 6.2, Reference 3), samples of grease were collected from five different locations from each bearings. These locations were:

1. Behind grease seal -- A side
2. Cage surface -- A side
3. Spacer area
4. Cage surface -- B side
5. Behind grease seal -- B side

Five of these samples were subjected to ferrographic analysis by the Naval Air Engineering Center (NAVAIRENGCEN) to evaluate the feasibility of relating the quantity and nature of wear debris to the condition of a bearing.

The pertinent conditions associated with each of the five selected samples are summarized in the following table.

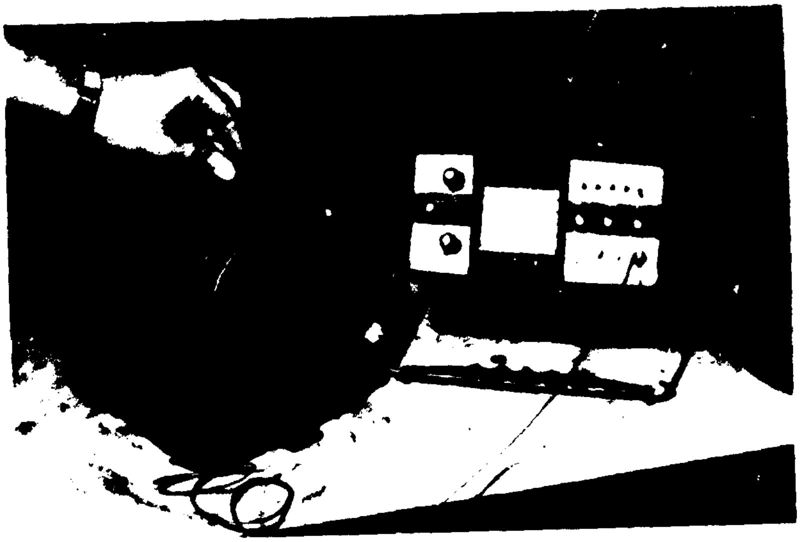

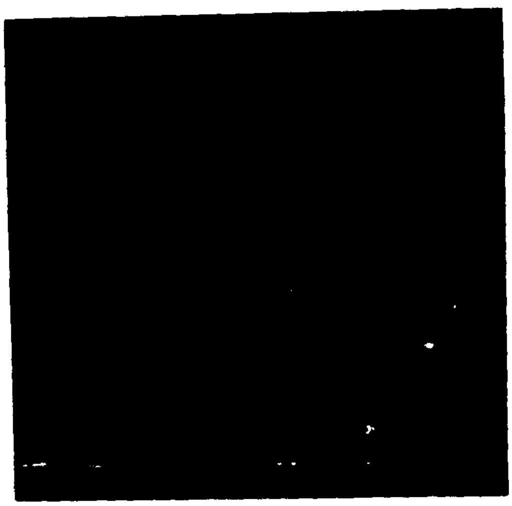

SIGNAL FROM GOOD CUP

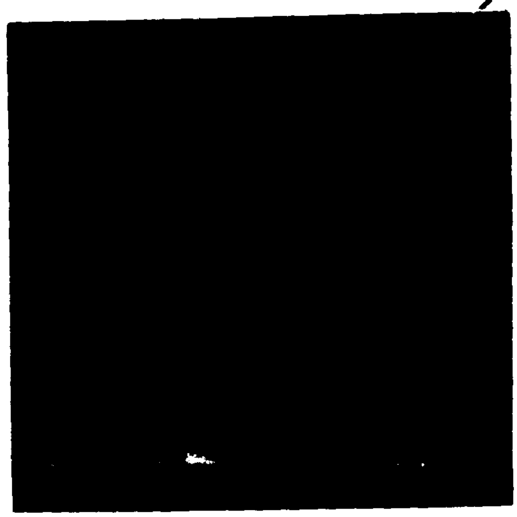

SIGNAL FROM CRACKED CUP

FIGURE 46. ULTRASONIC DETECTION OF CRACKED CUPS

Sample No.	Bearing No.	Sample Location	From Test No.	Description of Damage
38	203	3	C2A	Moderately Spalled Cone
58	209	3	C4A	Spalled Roller
63	212	3	C5A	Heavily Spalled Cone (See Figure 32)
64	212	4	C5A	
65	212	5	C5A	

Table 9 summarizes the results. The following comments summarize the observations made during the analysis.

Sample 38. Sample contained large quantities of black oxide and carbon. Temper coloration was noted on various ferrous metallic particles, indicating high operating temperatures. The amount of particles indicates that a component was in an abnormal wear mode.

Sample 58. Sample contained large quantities of black oxide and carbon. Nonferrous metallic particles were also detected in slightly greater number than other samples observed. Slight temper coloration was also observed on ferrous metallic particles.

Sample 63. Sample contained large quantities of carbon and ferrous metallic spheres which can be attributed to rolling contact fatigue. Slight coloration was observed on the ferrous metallic particles. Ferrous metallic laminar particles were of sufficient quantity to indicate roller contact fatigue.

Sample 64. Sample as received was extremely deteriorated, indicating high temperatures in the sample area. Large amounts of black oxides, carbon and polymer were observed, with temper coloration noted on the larger ferrous metallic particles. The amount of large ferrous particles compared to small ferrous particles also indicates a severe wear situation was occurring.

TABLE 9

SUMMARY OF FERROGRAPHIC ANALYSIS

WEAR MODE CHARACTERISTIC	Sample Number:	38	58	63		63	64	65
	Sample Location:	1	2	3	4	5	6	7
Beiby Particles		M	M	M		M	M	H
Fatigue Chunks (typical gear surface fatigue)		F	F	F		F	F	M
Laminar Particles (gears or rolling bearings)		M	M	M		M	M	H
Cutting Wear Particles (high unit pressure)		F	F	F		F	F	F
Spheres (fatigue cracks in rolling bearings)		F	F	H		H	F	M
Corrosive Wear Particles		F	F	M		M	N	N
Oxide Particles (includes rust)		M	F	M		M	F	F
Dark Metallic-oxide Particles (typical hard steels)		M	H	M		M	M	H
Severe Wear Particles		F	M	M		M	M	M
Nonferrous Metallic		F	M	F		F	M	M
Nonmetallic, Crystalline		M	M	M		M	H	H
Nonmetallic, Amorphous (i.e. friction polymer)		M	M	M		M	M	M
DENSITOMETER DATA (TYPE 7056) % AREA COVERED								
Reading at 54 mm		11	13	8		8	9	58
Reading at 50 mm		3	3	3		3	1	48
Reading at 10 mm		2	4	1		1	0.9	14

NONE N FEW F MODERATE M HEAVY H

Sample 65. Sample contained an extremely large quantity of particles, both ferrous and nonferrous, approximately 4 times the amount observed in the other samples. Large quantities of carbon, friction polymer and oxide spheres were present, with large ferrous metallic particles similar to those observed in Sample 64 also present. Temper coloration was very evident on ferrous metallic particles.

Based upon the work performed on the railroad roller bearing grease samples as well as work performed under the NAVAIRENGCEN Wear Particle Analysis Program, the following preliminary conclusions and recommendations have been made:

1. It is feasible to identify a severe state of wear in railroad roller bearings using grease ferrogram analysis techniques.

2. Prime indicators of railroad roller bearings wear are:

   Elemental Analysis of the Grease
   Particle Size Distribution
   Particle Morphology.

3. Particle Morphology appears to be a good indicator of railroad roller bearing wear. Particles peculiar to roller contact fatigue were found in sufficient quantities to facilitate an acceptable analysis.

4. Total particle count exhibited wide variations in reflecting wear state relative to the actual bearing condition. This may be attributed to sensitivity to sample technique and grease conditions. More samples will need to be analyzed to establish a realistic sensitivity trend.

5. Trend analysis (a series of samples from one railroad roller bearing from beginning of test to failure) as opposed to individual sample analysis (one sample from the failed bearing) as utilized in this effort, would be the best approach in the development of a grease analysis correlation effort.

6. A blue temper coloration appearing on ferrous metallic wear particles in several of the samples, coupled with the presence of black and red oxides, indicates that these samples have been subjected to extreme temperatures. Observations of some grease breakdown confirm this indication.

7. The seal cavity locations (Locations 1 and 5) appear to be the best locations for collecting grease samples.

3.3.4 Electrical Contact Resistance

This technique has been extremely useful in the analysis of the lubricant quality and surface finish of precision ball bearings. In initial tests the resistance variation across the railroad bearing was analyzed using a spectrum analyzer. The resultant spectrum closely resembles a vibration spectrum for a given bearing. The criteria for the identification of a bad bearing was postulated to be a low average resistance (small film thickness) and a high peak-to-peak variation (surface roughness). Thus for the failure progression tests described in Section 3.2.2, recording of both the average resistance value and the peak amplitude of the resistance was planned. Unfortunately, new bearings in many cases had lower average resistance than defective bearings because of their initial poor surface finish. For this reason, recording of the average resistance was discarded as being inappropriate for the subject class of bearing.

The peak resistance amplitudes recorded during the failure progression tests are summarized in Table 5. From Table 5 it is seen that the resistance amplitudes tended to increase with time but were not as consistent as the vibration levels. Part of the reason for this lack of consistency was ground (electrical) problems encountered in the mechanical test equipment. Another factor contributing to this poor correlation is thought to be the fact that the surface roughness, the bearing uniformity, and the lubricant film thickness on even new railcar roller bearings are simply not in the same class as precision ball bearings where the electrical contact resistance diagnostic technique has been successfully applied in laboratory situations.

Because of the implementation difficulties in applying the technique and the lack of correlation encountered during the failure progression tests, the electrical contact resistance technique was not pursued further.

4. COST MODELING

A technique for determining component-associated costs was developed for use in performing roller-bearing-related cost-benefit analyses. The technique, simulation cost modeling, calculates the cost per unit time required by a railroad or by the railroad industry to operate the component (roller bearing). This is accomplished by representing with a digital computer the manner in which the component is used. The emphasis is on the instantaneous behavior of the component-using system; consequently, the technique has data requirements which are relatively easy to satisfy. The technique allows sensitivity analyses and cost benefit studies to be performed easily and provides many opportunities to check the accuracy and reasonableness of the computed results. In addition, since the cost modeling is based on dynamic simulation procedures, the technique allows future cost and usage projections to be made. These projections can include the effects of introducing a new or improved component into the existing system and the effects of changing the manner in which the system employs the component.

4.1 Description of the Technique

The cost simulation technique consists of three basic pieces: the schematic diagram which represents component usage, the computer program which implements the diagram, and the set of data needed to run the program. These three pieces of the simulation technique are described in detail below.

4.1.1 Schematic Diagram

The schematic diagram is a description of how the component under consideration is used by the system. The diagram identifies the component-related parts of the system, the system interactions involving the component, and the decisions concerning the component which take place.

The schematic diagram used for the roller bearing is given in Figure 47. The parts of the railroad system which affect the bearing are the manufacturer, the field, the yard, the wheel shop, the bearing shop, and the scrap yard. These are defined as follows:

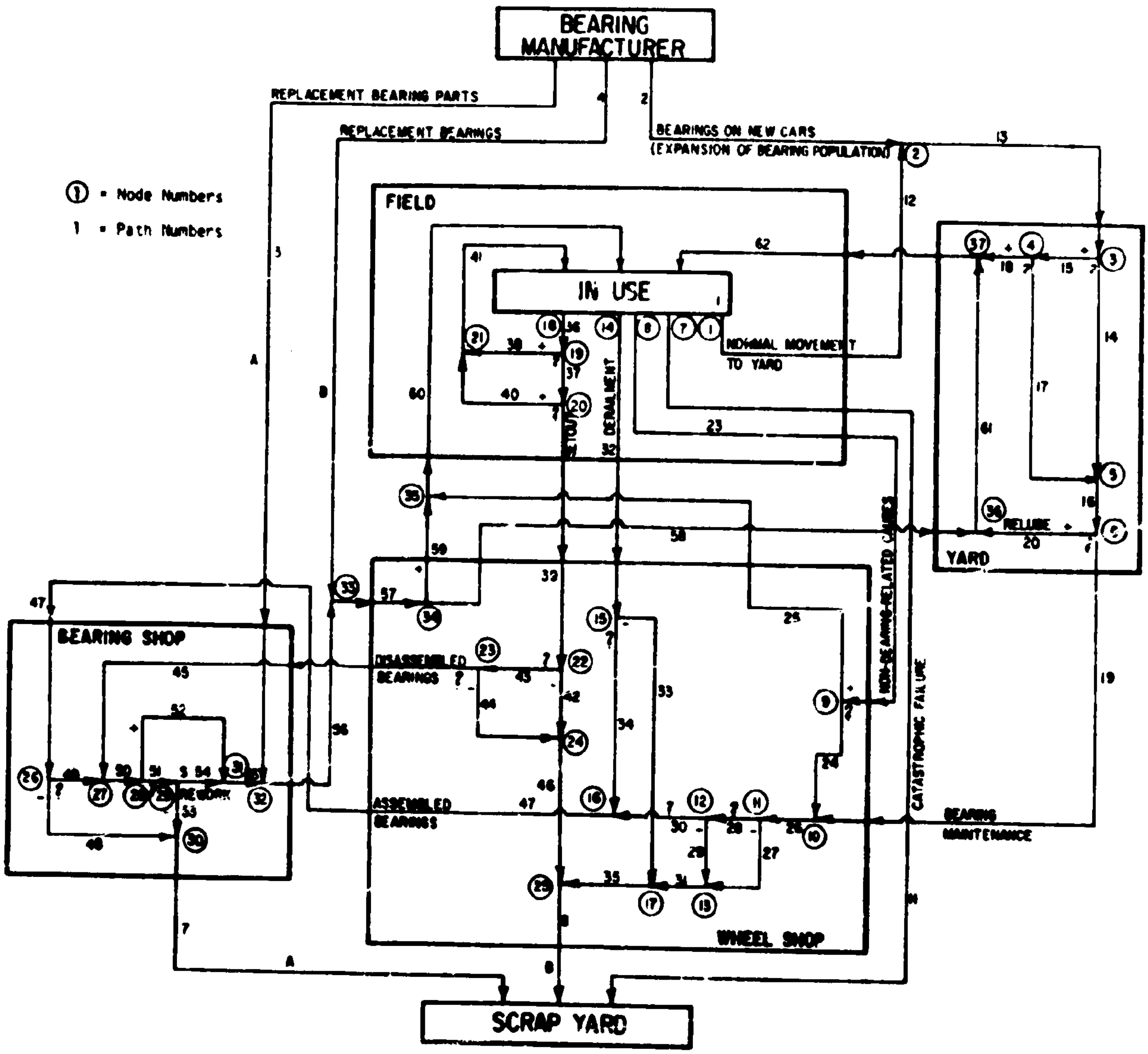

FIGURE 47. ROLLER BEARING SCHEMATIC

1. Manufacturer - the producer of the bearing.
2. Field - the part of the railroad system where the bearing is in actual use, sitting on the line, on a siding or in another location where normal maintenance would not take place.
3. Wheel Shop - the part of the railroad system where bearing removal (from the axle) and superficial bearing inspection are accomplished.
4. Bearing Shop - the part of the railroad system where detailed bearing inspection and bearing repair are accomplished.
5. Scrap Yard - the part of the railroad system where bearings that can no longer be used are discarded.

The interactions or movements of roller bearings among these six system parts are indicated by the uncircled arrowed lines or paths. Bearings can leave the field along the paths in the following ways:

1. By normal movement to the yard.
2. Because of a bearing-caused derailment (labeled "catastrophic failure"), in which event the bearing is scrapped.
3. Because of non-bearing-related causes, such as wheel maintenance, in which event no costs are assigned until the bearing is actually removed from the axle.
4. Because of a non-bearing-caused derailment requiring bearing removal (per Section 1.1 of Reference 4), in which event it is sent to the wheel ship for removal from the axle.
5. Because of a verified hot box, in which event it is sent to the wheel shop for removal and inspection.

Bearings can enter the field in the following ways:

1. By normal movement from the yard.
2. From the wheel shop.

3. From the manufacturer as a replacement for bearings scrapped due to catastrophic failure or scrapped for any reason by the wheel shop, or on a new or rebuilt car.

For the purpose of the subject model, bearings enter the yard only from the field. Although they can also enter the yard for other reasons -- i.e., on an axle after receiving wheel maintenance -- the costs associated with such events are not attributable to the bearing itself. Thus, such avenues are not considered.

Bearings leave the yard and enter the wheel shop because a bearing defect is suspected as a result of a yard inspection, in which event they are sent to the wheel shop for removal.

In addition to the avenues mentioned above, bearings are exchanged between the bearing shop and wheel shop. Bearings enter the bearing shop from the wheel shop or from the manufacturer in the form of replacement bearing parts.

The paths within each of the four areas are varied and depend upon the condition of the bearing at various locations within each area. The paths contain branch points and junction points. Each branch point is numbered (with a circled number) and is a decision point, i.e., a point where bearings considered to be good (+), questionable (?), bad (-), or reworkable (S) are separated. The junction points are those points where the bearing paths join. No decision is associated with these points. The arrowheads shown at the branches and junctions indicate from which path(s) the bearings are arriving. Paths leaving from these connection points do not contain arrowheads.

The symbol N is used to denote the total number of roller bearings in the composite bearing system. The fraction of the N bearings that leave "in use" per year in each of the five paths shown is given by C_i, where i refers to the node number. For example, if $N = 8.5 \times 10^6$ roller bearings and $C_8 = 1 \times 10^{-5}$, then $8.5 \times 10^6 \times 1 \times 10^{-5} = 86$ bearings per year associated with a catastrophic roller bearing failure. The symbol C_i is also used to denote the fraction of bearings which arrive at node i and which move in the direction of the associated arrow. For example, $C_9 = 0.9$ means that 90 percent of the bearings arriving at node 9 will move in the direction of the arrow. The fraction of bearings moving away from node i but not in the direction associated with C_i is, necessarily, $1 - C_i$.

A cost is associated with each of the paths taken by the bearings. This cost is given by c_j, where j refers to the path number. This cost is typically in dollars per bearing* and is generally composed of several contributing costs. For example, the cost for path 19 is composed of the per bearing cost to take the wheelset off the car, to ship the wheelset to the wheel shop, and to keep the wheelset out of service in the wheel shop. The total cost for any route can be obtained from the path cost. For instance, the cost associated with bearings bad-ordered in the yard and with bearings which are sent from the yard to the wheel shop is given by $c_{14}N_{14} + c_{17}N_{17} + c_{16}N_{16} + c_{19}N_{19}$, where N_j refers to the number of bearings in path j.

4.1.2 Computer Model

The computer model (which is included in Appendix A) was written to represent the bearing flow diagram and contains several features besides those described above. In the model, the value of each C and c can be specified as a known function of time, of N, or of the average age of the bearing population. Initial values of time, N, and average age must be provided for the model. The equations which describe the rate of change of N and of average age at any instant of time are solved numerically by the computer program. This solution involves the determination of all bearing flows at the time under consideration. A numerical integration procedure is then used to obtain the values of N and of average age at the next time step, at which the process is repeated.

*A nonlinear cost representation can be used if desired.

The result is a simulation of the behavior of the roller bearing composite system with time.

4.1.3 Data

The model can be used to obtain total system and path costs for either a single railroad or for the entire industry. For the purpose of this paper, it was used on an industrywide (U.S.) basis. In this manner, the results were felt to be more generally useful.

The input data for the base case analysis (described below) are tabulated in Tables 10 through 12. Clearly, the input data are not without question. Input which was not estimated was obtained from a variety of diverse sources, as noted in the tables. Furthermore, where data from only one railroad were available, the relationship of that railroad to the total industry was incorporated into the data value used. Needless to say, if the model is to be used to accurately predict costs, additional work may have to be done to gather more representative input data.

4.2 Results

The simulation cost model was first used to produce a base case analysis (based on 1975 data) for the bearing. For this, the static problem was considered, i.e., all quantities were taken to be independent of time. The results for this base case are summarized in Tables 13 and 14.

Table 13 gives the number of bearings per year that move along each of the various paths, the per bearing cost associated with each path (same as previously shown in Table 12) the total cost associated with each path, the total yearly cost of the entire system, and the path cost sensitivity. The path cost sensitivity is the proportion of the total system cost represented by any path of interest. For example, the cost of Path 2 (new roller bearings entering system on new and rebuilt cars) is approximately 74 million dollars and represents 61% of the total yearly cost of approximately 122 million dollars. The path cost sensitivity is useful in two ways: first, it allows one to see quickly which paths contribute significantly to the

TABLE 10.

INPUT DATA

Node	Description	(C) Proportion in Non + Direction	Source
1	Normal movement to yard	52	Assumed car enters yard once per week
4	Bad ordered at departure yard	0	Bearings not typically inspected at departure
12	Discarded after detailed inspection	0	Not normally done in wheel shop
15	Discarded because of obvious, serious defect	0	Only major cup and seal damage is visible and remaining components may be o.k.; thus bearings should be sent to rework
22	Discarded because of obvious, serious defect	0	Bearings currently discarded only after joint inspection
23	Discarded at joint inspection	0.2	Brenco/SBCL joint inspection data
26	Discarded after inspection of assembled bearing in bearing shop	0	Such inspection not currently done
28	Bearings with repairable defects that are separated from line	1.0	Bearings not currently seprrated
29	Bearings requiring parts replacement	0.188	Volume I of this report
34	Returned to use via rip track	1.0	Assumed all replacement wheelsets returned via rip track

TABLE 11

INPUT DATA

Path	Description	Number of Bearings on Path	Source
1	In use	8,549,080	Yearbook of Railroad Facts, 1975 edition & AAR semi-annual summation of performance reports on journal roller bearings
2	Bearings installed on new and rebuilt cars in 1975	538,920	Yearbook of Railroad Facts, 1975 edition
11	Roller-bearing-caused accidents	86	"FPA Journal Performance Report," and Quarterly Hot Box and Performance Report" for 1975
19	Defective bearings on wheelsets removed at rip track	54,512	AAR CRB data; all bearings removed in 1975 less Rule 36 Why Made Codes 11, 33, and overheated journal
20	Bearings relubricated	512,587	AAR CRB data: Rule 26
23	Bearings removed because of non-bearing-related causes	395,366	AAR CRB data: Rule 36, Why Made Code 11
25	Secondhand bearings applied	54,533	AAR CRB data: Rule 36, Applied Code 2
27	Discarded because of obvious defect	7,728	AAR CRB data: Rule 36, Why Made Codes 07, 50, 51, 95, 96
32	Bearings involved in non-bearing-caused derailments	196,164	AAR CRB data: Rule 36, Why Made Code 33
36	Involved in setouts	9,468	3 times path 42 based upon Southern Railroad experience
37	Setouts verified by train crew	6,312	2 times path 42 based upon Southern Railroad experience
39	Setouts verified by mechanical department	3,156	Two times "Quarterly Hot Box and Performance Report" for 1975 (multiplier used so as to include mate bearing)

TABLE 12. COST INPUT DATA

Path	Description	Per-Bearing Value (c)	Basis of Value: AAR Office Manual Job Code	Labor at $17.27/hr: Time Min.	Labor at $17.27/hr: Men No.	Car Per Diem at $5/Day: Number Days	Other Sources and Remarks
1	Path number not used						
2	Installed new bearing	$137.97	2812 & 2816				Average of 11" and 12" bearings
3	Replacement bearing parts	$ 33.02					Cups and cones replaced at ratio of 5 to 3. Avg. costs: $38.20 for cups, $24.39 for cones. Avg. replacement cost is (5($38.20) + 3(24.39))/8 = $33.02
4	Cost of bearing delivered to shop	$136.53	See 1	5	1		(installed cost)-(installation cost)
7	Scrap value	-$ 6.10	2821				
8	Scrap value	-$ 6.10	2821				
11	Cost of bearing caused derailment	$120,300					FRA "Journal Failure Report - 10/72". Cost escalated by 3.3 to cost of private property.
12	Zero cost path	0					
13	Receiving yard inspection	$ 0.01		1/48	2		1 minute per car assumed; 1/6 time allotted to bearings; 1/8 bearing, inspection time allotted to each bearing
14	Delay associated with sending car to rip track	0					Included in cost path 15
15	Departure yard inspection	0					Bearings not typically inspected in departure yard

TABLE 12 (continued)
COST INPUT DATA

Path	Description	Net Bearing Value (c)	Basis of Value: AAR Office Manual Job Code	Labor at $17.27/hr: Time Min.	Labor at $17.27/hr: Men No.	Car Per Diem at $5/Day: Number Days	Other Sources and Remarks
16	Bearing inspection at track	0					Minimal inspection at this point
17	Delay associated with sending car to rip track	$ 30.91		30	3	1	
19	Remove wheelset, ship to wheel shop, out of service costs, remove bearings from axle	$ 15.08		15	2	1	a) Assumed 2 men, 30 minutes to remove and replace wheelset. Divide by two -- to get equivalent per-bearing removal cost.
							b) Assumed $5.00 to ship wheelset. Divide by two -- to get equivalent per bearing cost.
				5	1		c) Assumed 5 minutes to remove bearing
20	Relube cost	$ 2.56	2550			1	1/8 job and per diem cost used to get equivalent per-bearing cost
25	Secondhand bearing cost including installation on axle	$ 68.99	2812 & 2816				Average of 11" and 12" bearings
26	Cursory inspection	0					Bearings discarded at this point have been previously bad ordered

TABLE 12 (continued)
COST INPUT DATA

Path	Description	Per Bearing Value ($)	Basis of Value: AAR Office Manual Job Code	Basis of Value: Labor at $17.27/hr Time Min.	Basis of Value: Labor at $17.27/hr Men No.	Basis of Value: Car Per Diem at $5/Day Number Days	Other Sources and Remarks
32	Remove wheelsets, ship wheelsets, remove bearings, delay	$ 15.08					Same as path 19
36	Stop train and check bearing	$172.13					1/2 hour x $688.53/train hour divided by 2 to get per-bearing cost. Train hour value derived from "Yearbook of Railway Facts"
37	Brake train, place car on siding, have mechanical department check	$[illegible]63.20				1	3/4 train hour + 1 man day at $25/hr + 1 day per diem divided by 2 to get per-bearing cost
39	Pick up car, tow to rip track, remove axle, ship, removing bearing	$614.45				2	1-3/4 train hour + path 25 + per diem divided by 2 to get per-bearing cost
40	Pick up false setout car	$258.20					3/4 train hour divided by 2
43	Bearing disassembly and joint inspection cost	$ 28.00					Typical inspection: a lot (20 brgs), 1 day, 2 engineers, 1 technician at $23.33 per hour (avg.)
45	Ship disassembled bearings to rework	$ 2.50					Trucking cost for 16 bearing pallet (650 lb.) for 100 miles
47	Shipping	$ 2.50					Same as 45
49	Rework shop disassembly cost	$ 1.80					1/10 hour at $18.00/hr

TABLE 12. (continued)
COST INPUT DATA

			Basis of Value				
				Labor at $17.27/hr		Car Per Diem at $5/Day	
Path	Description	Per Bearing Value (c)	AAR Office Manual Job Code	Time Min.	Men No.	Number Days	Other Sources and Remarks
50	Bearing inspection	$ 1.80					1/10 hour at $18.00/hr
54	Rework	$ 0.60					2 minutes at $18.00/hr
56	Reassembly	$ 11.79					Assembly (1/10 hour at $18.00/hr), grease ($0.50), seals ($6.99/pr), and shipping ($2.50)
57	Install bearings on	$ 1.44					Same as 21(c)
58	Shipping	$ 2.50					Same as 45

TABLE 13.

SYSTEM COSTS –

1975 BASE CASE

Path Number	Number Bearings	Cost/ Bearing	Path Cost	Path Cost Sensitivity
1	8549080			
2	538920	$137.97	$74354792.40	0.6097
3	110225	$ 33.02	3639645.46	0.0298
4	8359	$136.53	$ 1141284.20	0.0093
7	110225	$ -6.10	$ -672375.44	0.0055
8	8359	$ -6.10	$ -50991.23	0.0004
11	86	$120300.00	$10345800.03	0.0848
12	444552160			
13	445091080	$ 0.01	$ 4450910.80	0.0365
14	567098			
15	444523981			
16	567098			
18	444523981			
19	54511	$ 15.08	$ 822040.88	0.0066
20	512586	$ 2.56	$ 1312222.62	0.0107
23	395365			
24	340832			
25	54532	$ 68.99	$ 3762231.61	0.0308
26	395344			
27	7728			
28	387616			
30	387616			
31	7728			
32	196163	$ 15.08	$ 2958153.00	0.0242
34	196163			
35	7728			
36	9467	$172.13	$ 1629726.70	0.0133
37	6311	$363.20	$ 2292518.19	0.0188
38	3155			
39	3155	$614.45	$ 1939204.02	0.0159
40	3155	$258.20	$ 814879.12	0.0066
41	6311			
43	3155	$ 28.00	$ 88367.99	0.0007
44	631			
45	2524	$ 2.50	$ 6311.99	0.0000
46	631			
47	583780	$ 2.50	$ 1459452.40	0.0119
49	583780	$ 1.80	$ 1050805.73	0.0086
50	586305	$ 1.80	$ 1055350.37	0.0086

TABLE 13. (CONTINUED) SYSTEM COSTS

Path Number	Number Bearings	Cost/ Bearing	Path Cost	Path Cost Sensitivity
51	586305			
53	110225			
54	476080	\$ 0.60	\$ 285648.16	0.0023
55	476080			
56	586305	\$ 11.79	\$ 6912544.94	0.0566
57	594664	\$ 1.44	\$ 856317.57	0.0070
58	594664	\$ 2.50	\$ 1486662.45	0.0121
60	54532			
61	1107251			
TOTALS			\$121941504.06	1.0000

TABLE 14.

BRANCH COST SENSITIVITY —

1975 BASE CASE

Branch Number	Branch Sensitivity
1	1573.40/%
3	29359186.80/%
6	238122.50/%
7	$10284543243.53/%
8	2985394.63/%
9	-156250.27/%
11	422986.88/%
14	3629782.06/%
18	62430412.17/%
19	79265.45/%
20	27241.73/%
23	3433.47/%
29	154315.67/%

total cost, and, second, it permits one to calculate quickly the effect of any per bearing related cost. For example, a 1% change in the per bearing cost associated with Path 2 would result in a 0.6097% change in the total system cost.

From Table 13, it is seen that the four most significant paths (from a cost standpoint) are:

1. Path 2 - New roller bearings entering system on new and rebuilt cars (61% of total).
2. Path 11 - Bearings causing accidents (8.5%).
3. Path 13 - Receiving yard inspections (3.7%).
4. Path 56 - Reassembly and shipping of rebuilt bearings (5.7%).

Table 13 can be used to evaluate the effect of changing "per-bearing costs" in each path since the path cost affects the total cost directly. However, it cannot be used to evaluate the effect of changing the number of bearings in any given path because each bearing accumulates cost in several series-connected paths.

Table 14 gives the branch change sensitivity which allows one to evaluate the effect of changing the number of bearings in each path. For example, at branch point 19 the base case analysis has a train crew determination that 33% (3055 out of 9165) of the set-out bearings were falsely set out. These bearings were returned to service via Path 38. If this percentage were increased by 1% (to 34%) or by 92 bearings, the yearly saving would be $79,265.

Care must be exercised in using the values shown in Table 14 because they are based upon a 1% change in the branch split proportion. In those cases where the split proportion is small, the sensitivity shown in Table 14 appears very large. For example, the split proportion at node 7 is 1.006×10^{-5} (86 out of 8,549,030 bearings). Adding 1% (or 0.01) changes the split proportion to 1.001×10^{-2}, yielding 85,576 bearings in Path 11. This explains the apparently high sensitivity shown for this branch in Table 14.

For the node 7 example, if one wanted to evaluate the effect of increasing the number of catastrophic failures from 86 to 90 (a 4.7% increase), the effect on the total cost would be calculated as follows:

$$\text{Original split proportion } (C_o) = {}^{86}/8{,}549{,}030 = 1.0060 \times 10^{-5}$$

$$\text{New split proportion } (C_n) = {}^{90}/8{,}549{,}030 = 1.0527 \times 10^{-5}$$

$$\text{Change in percentage} = (C_n - C_o) \times 100 = (1.0527 - 1.0060) \times 10^{-5} \times 100$$

$$= 4.67 \times 10^{-5}$$

$$\text{Change in total cost} = \%\text{ change} \times \text{split sensitivity}$$

$$= 4.67 \times 10^{-5} \times \$10{,}280{,}543{,}243/\%$$

$$= \$480{,}101.$$

4.3 Examples of Cost-Benefit Analysis

4.3.1 Derailed Bearing Diagnostic System

The simulation cost model was used as a tool in performing cost-benefit studies. The motivation for such studies is based on the observation that good and defective roller bearings can be separated at various points in the railroad system. The addition of diagnostic procedures to do this causes the values of the splits at the decision points to change from their base case values. These decision point changes produce changes in the overall system cost. The difference between this new overall system cost and the base case cost is the benefit associated with use of the diagnostic system.

An example case is the cost benefit to the railroad industry from a diagnostic system to be used to test bearings that had been involved in derailments. The potential of such a system suggests itself because of the large number of bearings which enter the wheel shop as a result of derailments. The function of such a system would be to separate the good from the bad bearings. The tests might be performed at the derailment site or at a rip track. The good bearings would then be returned immediately to service, thereby saving wheel-shop/bearing-shop and associated costs. Such immediate return of derailed bearings to service is not now permitted; consequently, the example considers one effect of such a change in railroad system operation.

For this example, the cost benefit is a function of two variables -- the cost per bearing to perform the inspection and the accuracy of the diagnostic system. Accuracy is made up of two factors; the first is the accuracy of finding bad bearings and the second is the accuracy of finding good bearings. In the derailment case, the accuracy of finding bad (damaged) bearings must be 100 percent. In order to achieve this, one must expect that some good bearings will be classed as bad; i.e., the system must be designed to err on the side of safety.

Figure 48 shows the cost-benefit results for the diagnostic inspection as a function of the per-bearing inspection cost. A family of curves is drawn for the benefit as a function of the percentage of good bearings found.

The top curve indicates that if the system is infallible, it not only finds 100 percent of the bad bearings but never classifies a good bearing as bad. The curve axis at (0,0) represents current practice in which all bearings are removed. (In effect the current system finds 0 percent of the good bearings.)*

*Figure 48 was constructed by changing two parameters in the model. The value of the cost in Path 32 was changed to determine the effect on the cost benefit of the derailment inspection cost. Also, the value of C_{14} was varied. Because the number of defective bearings reaching the bearing shop depends on C_{14}, the value of C_{29} for this example depended on the value of C_{14}.

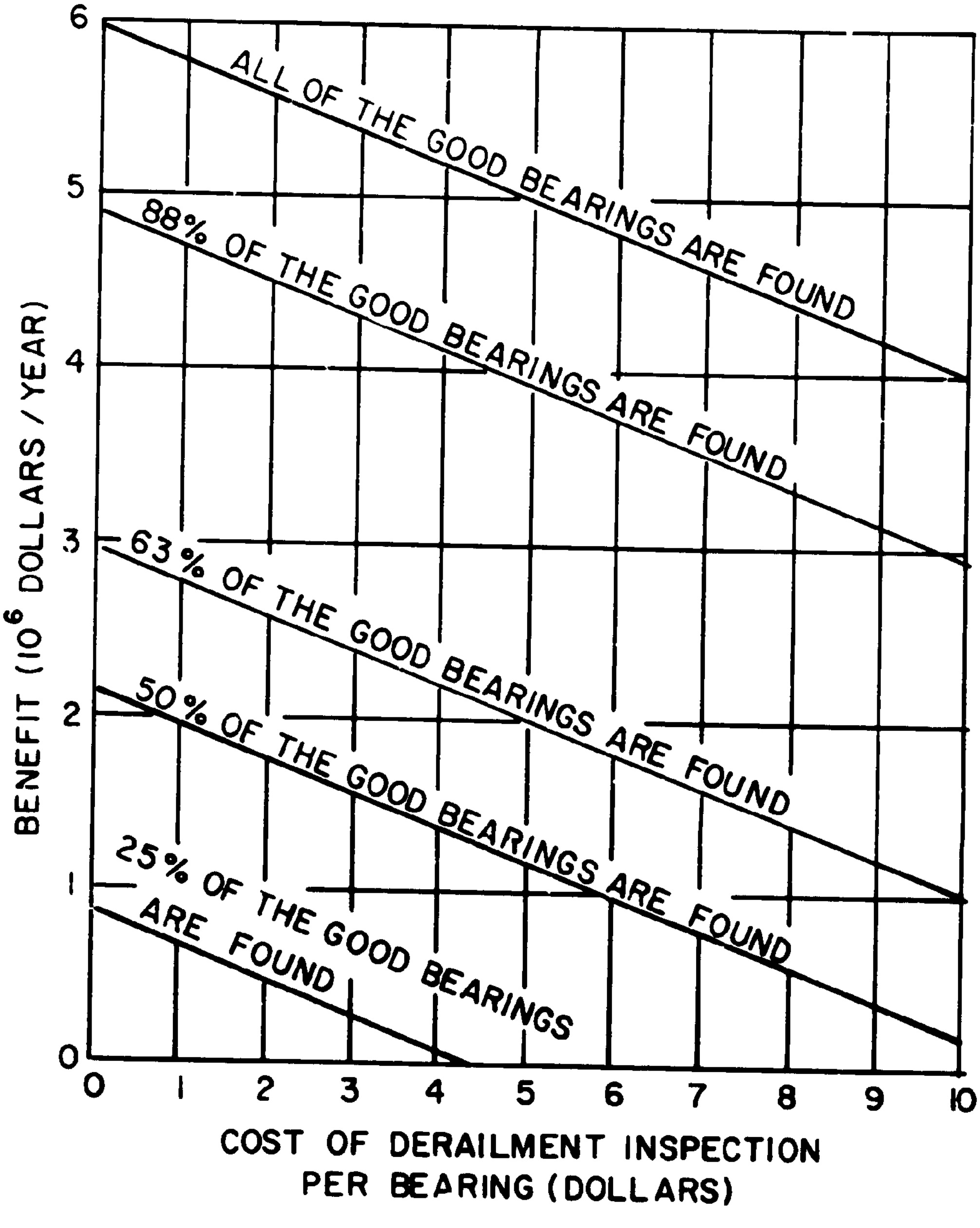

FIGURE 48. COST-BENEFIT ANALYSIS - DERAILMENT DIAGNOSTIC SYSTEM

Figure 48 shows that if 88% of the good bearings can be safely identified as good by a system that costs the railroad $4.50 per bearing at the derailment site, then the saving to the industry is 4 million dollars per year. It is clear that the savings to the industry in this area could be dramatic and that the development of a diagnostic system for this purpose might be desirable.

4.3.2 Improved Safety

To evaluate permissible implementation costs of different strategies that could be employed to improve bearing safety, the base case cost analysis was run for the 1986 situation in which it was extrapolated that virtually all of the railcar fleet would be on roller bearings.

For the 1986 case, only four input changes were made to the original (1975) base case. These were:

1. Total population (Path 1) was changed from 8,549,080 to 15,300,000.
2. Catastrophic failures (Path 11) were changed from 36 to 220 based upon the percentage increase in the number of roller bearing failures, confirmed setouts and derailments shown in Figure 36.
3. Setouts (Path 36) were changed from 9467 to 24,342 based upon the same percentage increase as in No. 2 above.
4. Expansion of the bearing population (Path 2) was changed from 538,920 to 610,000 to reflect a constant rate of population increase per No. 1 above.

All other branch node proportions and path costs were identical to those used in the 1975 base case. The results in terms of costs and sensitivities are given in Tables 15 and 16. These results were then used to estimate the future costs associated with failures (including setouts) and to evaluate the allowable costs to the industry to reduce the incidence of failures. Figure 49 shows the yearly (based upon the year 1986) saving that could be

TABLE 15.

PATH COST SENSITIVITY–

1986 BASE CASE

Path Number	Number Bearings	Cost/ Bearing	Path Cost	Path Cost Sensitivity
1	15300000			
2	610000	$137.97	$84161700.00	0.4604
3	197629	$33.02	$6525732.67	0.0357
4	15452	$136.53	$2109736.20	0.0115
7	197629	$-6.10	$-1205541.16	-0.0065
8	15452	$-6.10	$-94260.53	-0.0005
11	220	$120300.00	$26578119.60	0.1454
12	795600000			
13	796210000	$0.01	$7962100.00	0.0435
14	1014466			
15	795195533			
16	1014466			
18	795195533			
19	97514	$13.64	$1330102.73	0.0072
20	916951	$2.56	$2347395.44	0.0128
23	707573			
24	609977			
25	97595	$68.99	$6733138.97	0.0368
26	707492			
27	13829			
28	693662			
30	693662			
31	13829			
32	351068	$15.08	$5294106.61	0.0289
34	351068			
35	13829			
36	24342	$172.13	$4190040.09	0.0229
37	16228	$363.20	$5894082.18	0.0322
38	8114			
39	8114	$614.45	$4985708.69	0.0272
40	8114	$258.20	$2095060.59	0.0114
41	16228			
43	8114	$28.00	$227194.79	0.0012
44	1622			
45	6491	$2.50	$16228.19	0.0000
46	1622			
47	1044730	$2.50	$2611826.31	0.0142
49	1044730	$1.80	$1880514.94	0.0102
50	1051221	$1.80	$1892199.24	0.0103

TABLE 15. PATH COST SENSITIVITY (CONTINUED)

Path Number	Number Bearings	Cost/ Bearing	Path Cost	Path Cost Sensitivity
51	1051221			
53	197629			
54	853592	$0.60	$512155.26	0.0028
55	853592			
56	1051221	$11.79	$12393905.07	0.0678
57	1066674	$1.44	$1536011.06	0.0084
58	1066674	$2.50	$2666685.87	0.0145
60	97595			
61	1983625			
TOTALS				1.0000

TABLE 16

BRANCH COST SENSITIVITY —

1986 BASE CASE

Branch Number	Branch Sensitivity
1	$2815.86/%
3	$52519763.10/%
6	$425970.16/%
7	$18405900000.00/%
8	$5342860.05/%
9	$-279635.84/%
11	$756958.89/%
14	$6496098.47/%
18	$111729601.94/%
19	$203792.09/%
20	$70038.72/%
23	$8827.47/%
28	$0.00/%
29	$276681.57/%
34	$0.00/%

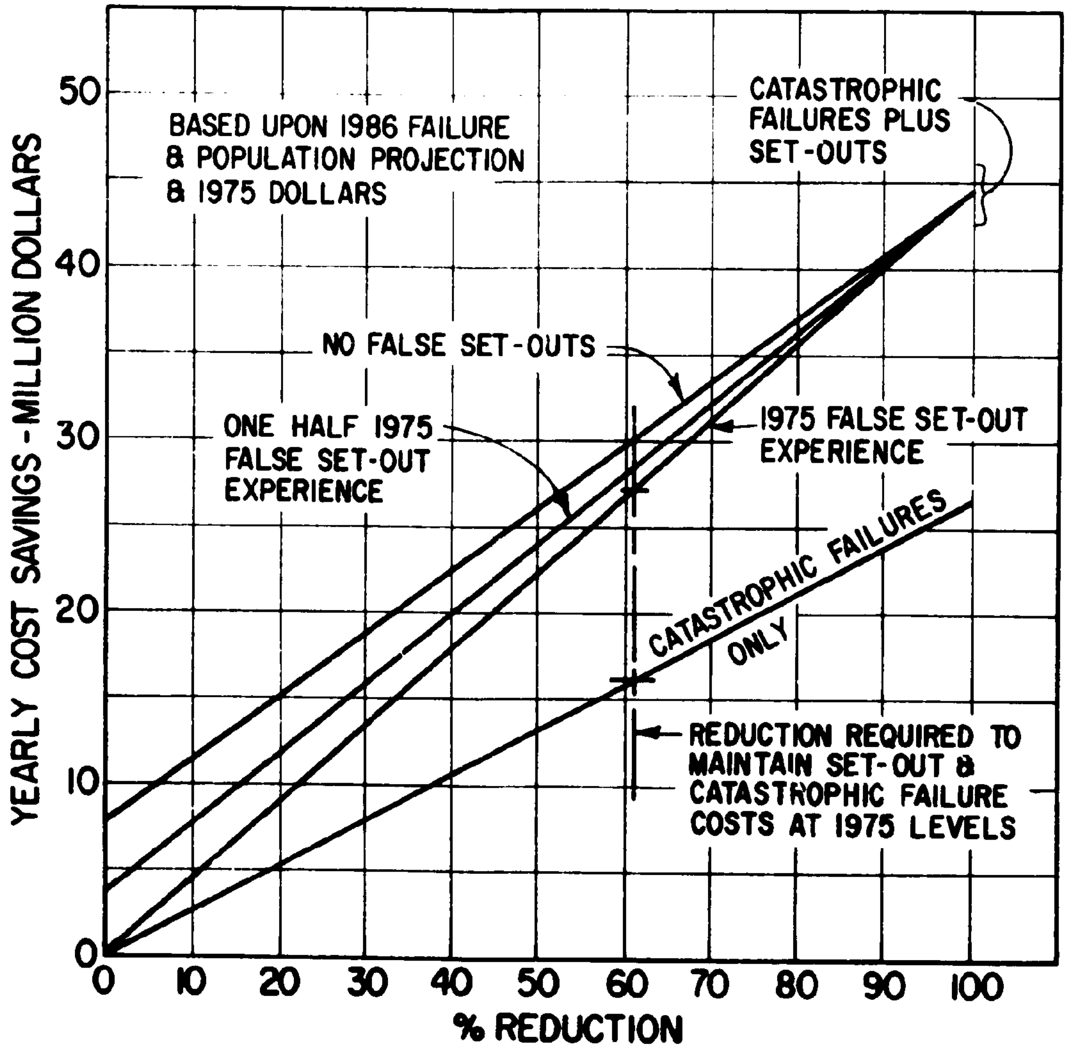

FIGURE 49. SAVING EFFECTED BY ROLLER BEARING FAILURE REDUCTION

effected by reductions in catastrophic failures and setouts and in the effect of false setouts.

Three methods (or combinations thereof) for achieving a reduction in failures can be postulated: 1) by improving bearing quality, 2) by adding a diagnostic sensor to the bearing (i.e., a heat-sensitive warning device), or 3) by deploying a number of improved wayside diagnostic sensors (i.e., an improved hot-box detector).

Figure 50 shows the cost benefit that could be achieved during the year 1986, as a function of increased bearing cost (either for improved quality or for the addition of a diagnostic sensor), for different assumed failure reduction percentages. It should be noted that this figure does not consider the investment cost accrued between the time that the "improved" bearings are introduced and 1986 -- the time that significant failure reductions are assumed to be realized.

If one were to assume that "improved" bearings were introduced as replacement bearings on parts as well as on new cars (Paths 2, 3 and 4) starting in 1977 and that "old" bearings (manufactured prior to 1977) were retired at a rate of 18.3% per year (split at node 29), 95% (approximately 14.2 million) of the population would be "improved" bearings by 1986 - see Figure 51. Thus, it is seen that the investment in the additional cost of the "improvement" could be significant.

For example, if the objective was to keep the number of and cost of failures and setouts constant at 1975 levels, then a reduction in projected failures of 61% by 1986 would be required. (See Figure 49.) If one were to assume that such a reduction would require increasing the bearing cost by $10 (either by improving quality or by adding a diagnostic sensor), the additional investment required would be at least 142 million dollars (14.2 million bearings times $10 per bearing). We say "at least" 142 million dollars because some of the 14.2 million "improved" bearings will become defective between 1977 and 1986 and would have to be replaced.

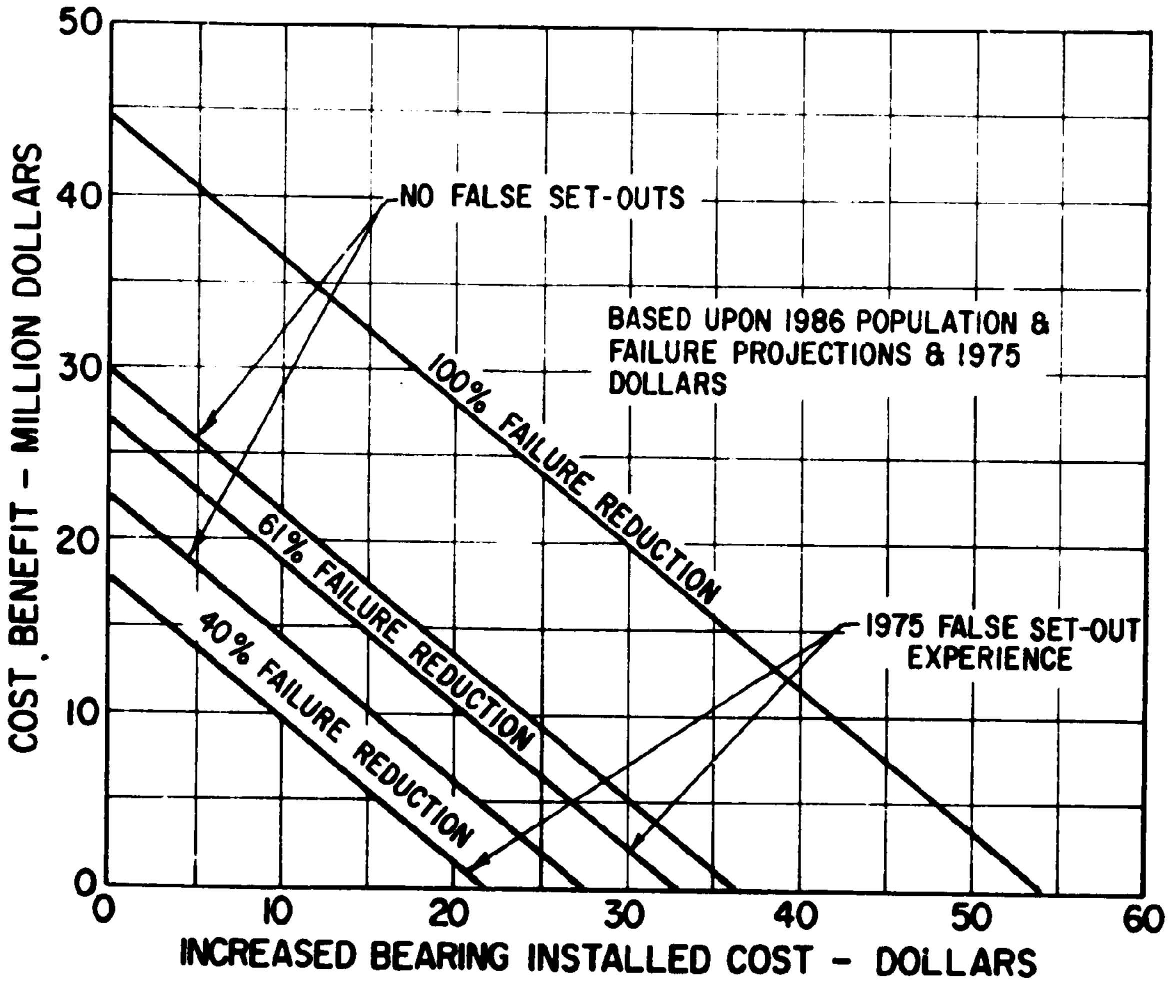

FIGURE 50. EFFECT OF INCREASED BEARING COST ON TOTAL COST SAVING FOR VARIOUS FAILURE REDUCTIONS

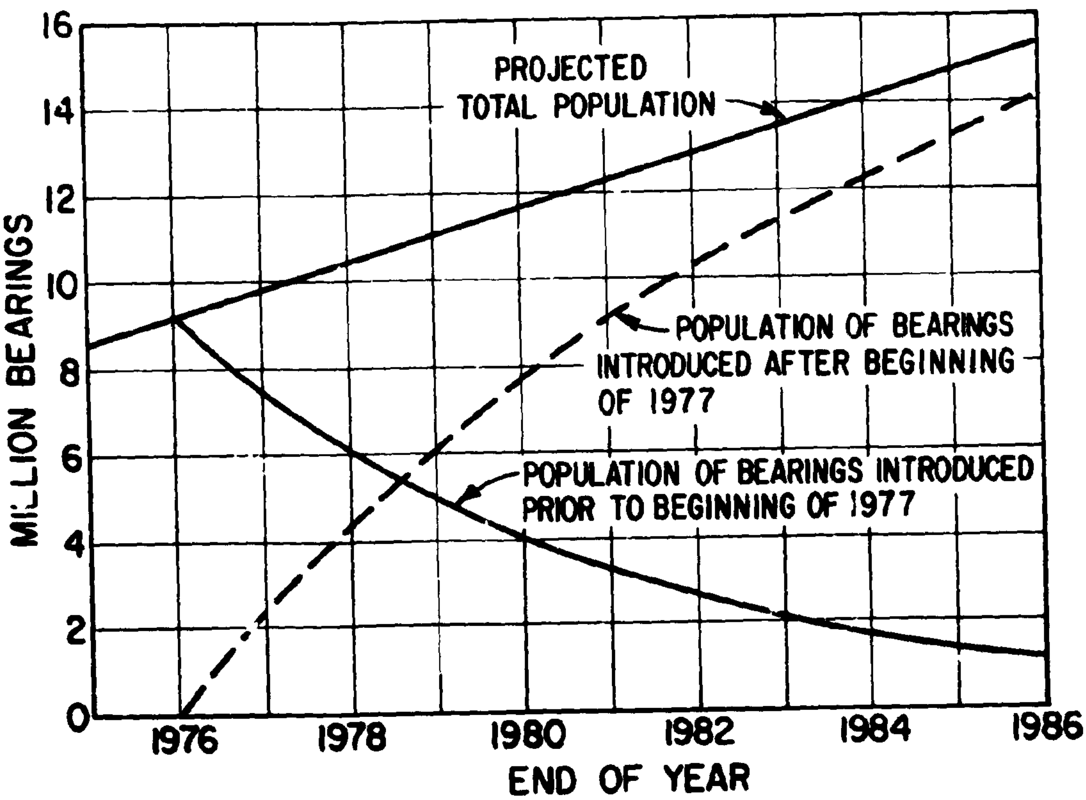

FIGURE 51. PROJECTED TOTAL POPULATION AND POPULATION OF "OLD" BEARINGS ASSUMING A CONSTANT 18.8% REMOVAL RATE

On the other hand, by 1986 the benefit derived by the 61% reduction in failures (to 1975 levels) would reach 20 million dollars per year. Depending upon how one chooses to define current value of money or other investment criteria, the 142 million dollar investment could be recovered in seven or more years.

Using the same 142 million dollar investment between 1977 and 1986 ($10 per bearing) and 20 million dollar cost benefit as an example, Figure 52 shows the tradeoff between increasing bearing costs and wayside disgnostic systems to achieve the same end. This figure shows, for example, that 2,000 wayside systems costing in excess of $70,000 each can be deployed for the same total investment as adding $10 to the cost of each bearing; or that $5, say, could be added to the cost of every bearing produced after 1977 (possibly for a primary sensor) allowing for approximately $35,000 each for 2,000 wayside detectors - each achieving the same end objective of 61% reduction in failures and a 20-million-dollar cost benefit per year by 1986.

The foregoing is but one example of how the cost model can be used to evaluate tradeoffs between two technical approaches. The example case does, however, dramatically show that thousands of wayside systems costing tens of thousands of dollars can be procured for the same investment as adding but a few dollars to the cost of the bearing.

4.4 Example of Time Dependence

The model was also exercised in its time-dependent (dynamic) mode to obtain an estimate of how the average age of the population would change with time and how the bearing shop reject rate would affect this average age.

To accomplish this, the total bearing population, all costs, and all splits (except split 29) were held constant, i.e., at the same values used in the base case. Split 29 was held at 0.188, 0.4, 0.6, and 0.8 (representing a shop reject rate of 18.8%, 40%, 60%, and 80%, respectively) for each dynamic simulation run. The results of these runs are shown in Figure 53 where it is

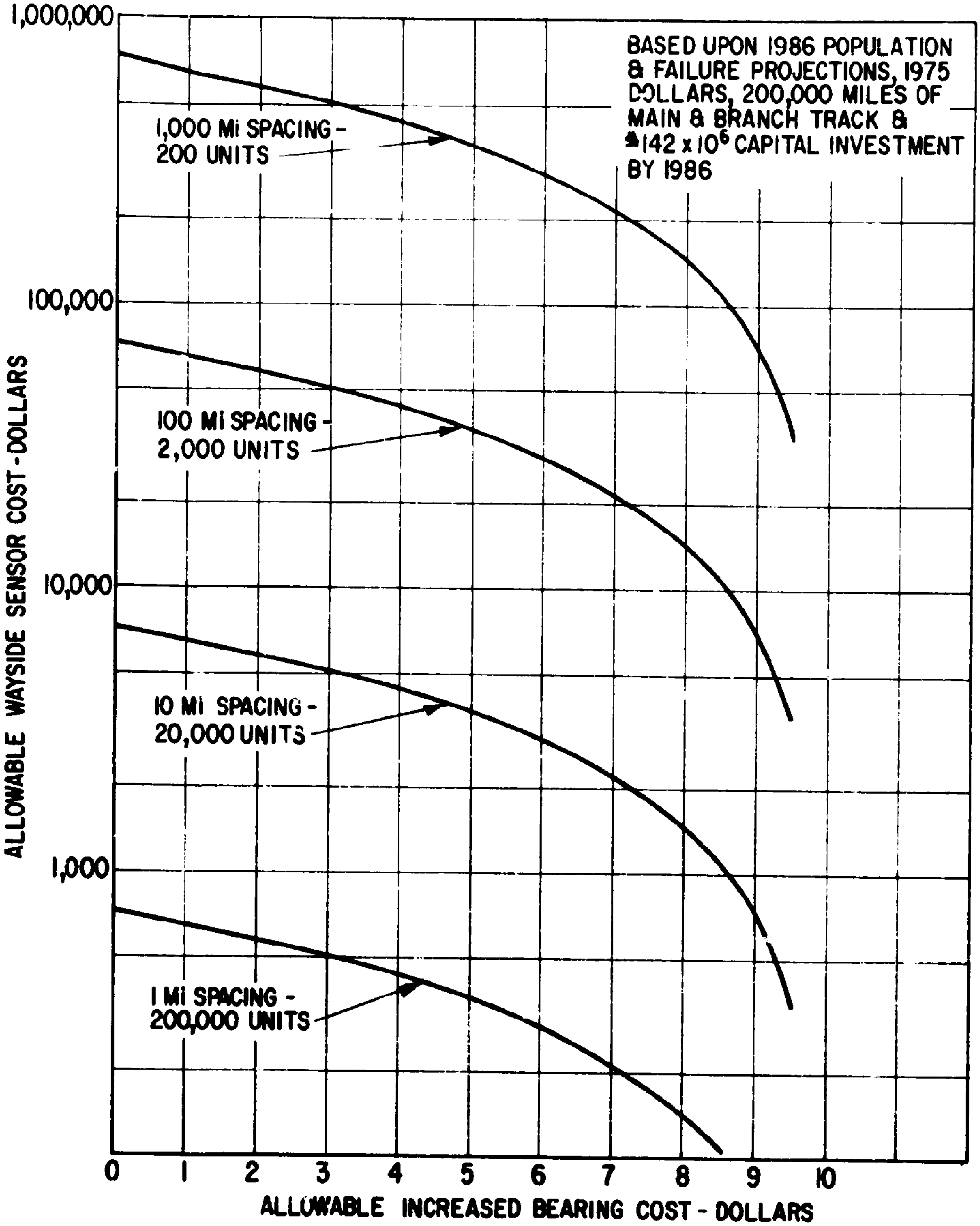

FIGURE 52. ALLOWABLE WAYSIDE SENSOR AND INCREASED BEARING COSTS TO ACHIEVE A 61% REDUCTION IN CATASTROPHIC BEARING FAILURES AND HOT-BOX SETOUTS BY 1986 AND A $\$20X10^6$ PER-YEAR COST BENEFIT BY 1986

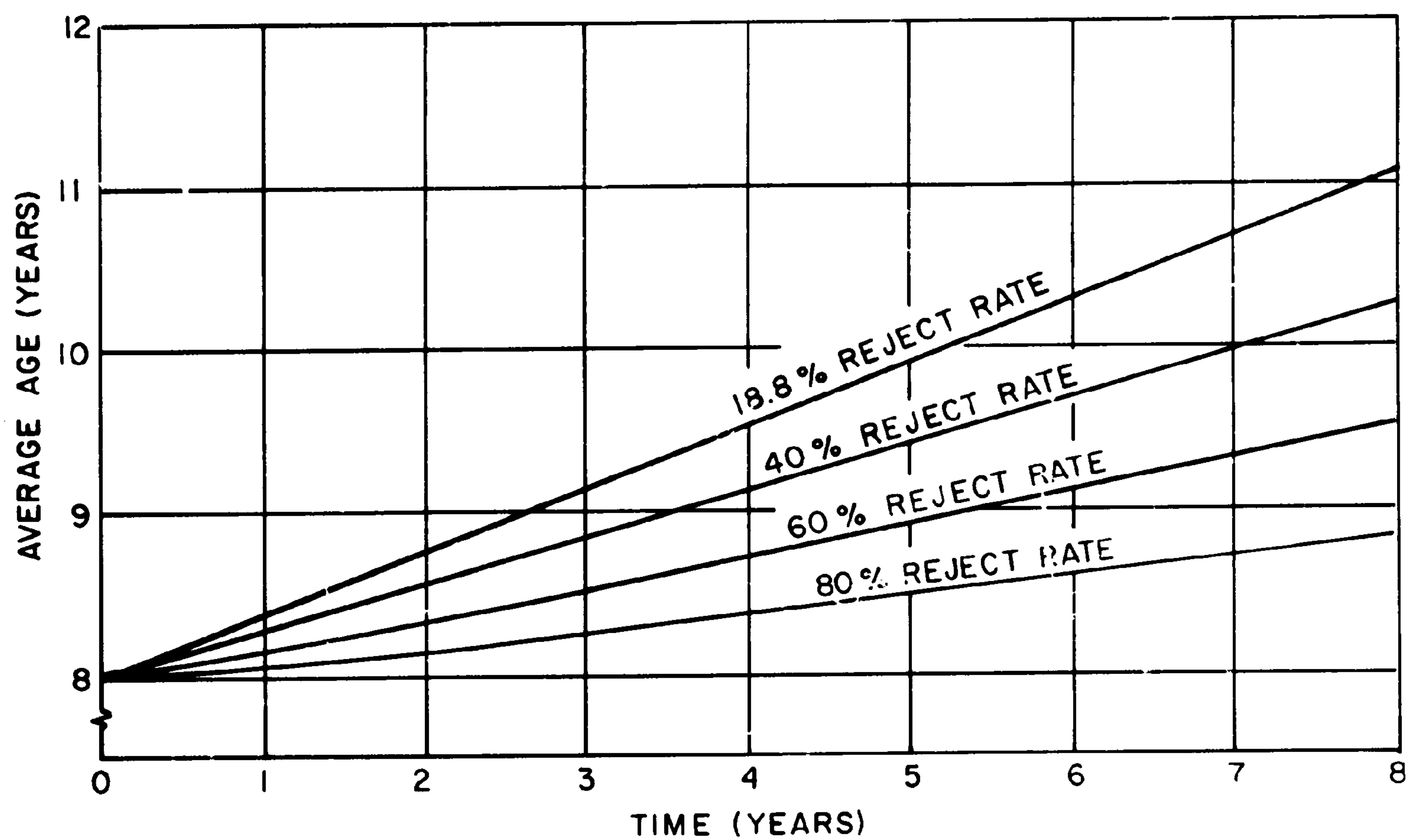

FIGURE 53. EFFECTS OF BEARING SHOP REJECT RATE ON AVERAGE AGE OF BEARING POPULATION

seen that at the current reject rate (18.8%), the average age of the population is increasing at a rapid rate. As the reject rate increases, the rate of average age increase decreases. These results are of interest because the average age of the population is related to the occurrence of bearing failures and, consequently, to the occurrence of bearing-caused derailments.

5. CONCLUSIONS AND RECOMMENDATIONS

5.1 Conclusions

The work conducted in this program has been directed toward the identification, selection, and development of diagnostic techniques for railroad roller bearings. The following are the basic conclusions drawn from the study.

5.1.1 Bearing Temperature Rise

Normal bearing temperature is a function of bearing load, the ambient temperature, the degree to which the bearing is greased, and speed. A fully loaded (26,000 lb.) and normally greased bearing (18 oz.) will run at approximately 115°F to 120°F above ambient at 60 mph. Overgreasing a test bearing (to 35 oz.) resulted in a temperature rise of 39° above the normal loaded temperature. A reduction in load of a normally greased bearing to approximately 4000 pounds resulted in a reduction in temperature of 38°F below the fully loaded condition.

5.1.2 Failure Progression

Ten bearings containing defects that were condemnable per AAR rules (4) were run under full freight car load at 65 miles per hour over an equivalent rail mileage of approximately 6000 miles. All test bearings survived the test without catastrophic failure or significant increase in temperature levels.

5.1.3 High Frequency Vibration

The high frequency vibration technique in at least one form was applied to all tests conducted. The following is a summary of results using varying analysis techniques.

Overall Amplitude (15-40 kHz)

In initial tests (Section 3.3.1.1) this technique was able to separate bearings into three categories: (1) large defects, (2) medium defects, and (3) small defects or good bearings. There was considerable overlap however in the results for categories (2) and (3). In tests using a high frequency microphone instead of an accelerometer, category 1 could still be identified but categories (2) and (3) overlapped to an extent that no claim can be made for separating these two categories.

In tests conducted at the Southern Railway Wheel Shop (Section 3.3.1.4) overall amplitude using an accelerometer was the only indicator used in real time (data was taped for later analysis). The technique was successful in identifying the one bearing out of 90 that was significantly degraded. Data from other bearings containing defects in the high end of the medium range could not be separated from small defects or good bearings as determined by subsequent teardown and inspection. While the technique in this simple implementation did pick out the worst bearing, its sensitivity did not allow the identification of other bearings that were condemnable per AAR rules.

In the failure progression tests (Section 3.3.1.2) there was a large difference in overall vibration amplitude between damaged bearings and new bearings and the amplitude increased as the defect progressed. One exception to this occurred when a damaged roller producing high level vibration locked in its cage, which actually resulted in a reduced amplitude; however, it was still significantly higher than for undamaged bearings.

The overall amplitude alone or even the trend in this amplitude could not be used to identify the presence of the first small defect in certification testing (Section 3.3.1.3). This is consistent with other results.

<u>Modified Crest Factor (15-30 kHz)</u>

This technique was employed on only one set of data. This was on the tape recorded vibration data generated at the Southern Railway Wheel Shop. Since peak amplitude alone was an unreliable indicator to select bearings near the condemning limit, a modified crest factor technique was employed. The initial tests used the peak amplitude divided by the average demodulated amplitude. Results of these tests were greatly improved and a reasonable batting average was obtained by re-analyzing the tape-recorded data. There was still overlap between good and bad bearings, however. The final results shown in Section 3.3.1.4 involved one further modification: the peak-to-peak amplitude of the demodulated data was divided by the average value. This produced a small improvement. This approach can be utilized in an inspection procedure if some bearings with a small defect can be allowed back into service along with allowing a small percentage of good bearings to be rejected erroneously.

Demodulated Spectrum Analysis

This technique consistently gave the most accurate results. During acceptance testing (Section 3.3.1.3) every time a discrete frequency appeared at a calculated defect frequency, it was correlated with an actual defect in the bearing. This allows acceptance testing to be conducted to the point of initial failure rather than for a fixed time period. In addition, if periodic inspection of roller bearings were to be conducted, this system could be automated to provide reliable inspection of the roller bearing population at a reasonable cost.

5.1.4. Ultrasonic Crack Detection

A standard ultrasonic crack detector is capable of detecting a cracked cup. Initial tests in the lab on only the cup indicated that inspection performed at any one circumferential location on the cup would be adequate. Tests with grease-packed bearings, however, showed that two locations are required due to the attenuation resulting from the grease coupling a larger amount of ultrasonic energy into the grease rather than reflecting it at the inner cup surface. This makes a test more difficult but not impossible when the adapter, side frame, and retainer key are in place.

5.1.5 Grease Ferrography

Grease samples were taken from five different locations in the 18 bearings tested during certification demonstration tests. However, time limitations permitted only five samples from three different bearings to be analyzed. The results of these analyses indicated that the technique accurately identified the failure mode and that the concentration of particles was greatest in the seal area due to the pumping action of the bearing. This would allow some method to be developed to remove the sample from this area. This point is the most accessible for an assembled bearing; however, it would still be extremely difficult to obtain samples from both seal areas.

However, because of the limited number of samples analyzed, no conclusions regarding the sensitivity of the technique to quantify the magnitude of damage can be made.

5.1.6 Bearing Electrical Contact Resistance

The resistance variation across a railroad roller bearing did not correlate with increasing bearing degradation. The criterion for identification of defective bearings was postulated to be low average resistance and a high peak-to-peak variation. New bearings in many cases had lower average resistance and higher peak-to-peak variations than defective bearings.

5.1.7 Diagnostic System Deployment

A cost modeling technique for determining roller-bearing-associated costs was developed and applied to the roller bearing problem. Using the model, it was shown that several million dollars per year could be saved if a diagnostic system could identify defective bearings at a derailment site and thus save removal and rework shop costs for those bearings not suffering derailment damage. It was also shown that if a wayside diagnostic system could be deployed in such a manner that it maintained the roller-bearing-caused derailments at current levels (approximately 86/year) instead of increasing to projected 1986 levels on the order 200/year, then tens of millions of dollars could be invested into the system and still be cost-beneficial.

5.1.8 Proposed Diagnostic System

A diagnostic system based on the high frequency vibration technique is a viable approach for deployment at a rip track or in a wheel shop. Such a system can be developed to detect condemnable bearing defects per AAR rule without removing the bearing from the axle.

5.2 Recommendations

Based upon the results and conclusions of the work reported herein, additional experimental work is recommended. Like the subject program, the experimental work should be directed at railcar roller bearing failure progression and definition of diagnostic technique. However, unlike the subject program, it is recommended that the effort be concentrated on bearings having defects at the severe end of the damage spectrum. That is to say that the subject program concentrated on bearings having damage near the AAR-defined condemning limits.

The reasons for this were many, including the effort in the certification area which implicitly is concerned with very early precursors of failure, the fact that the AAR rules provided a widely accepted definition of a defective bearing, the fact that such bearings were readily available for use as experimental vehicles, and the apparent high cost that the current AAR bearing removal rules impose upon the industry.

However, the fact remains that bearings near the condemning limit do not present an operational problem to the industry (except for the high cost of complying with the AAR removal rules) and do not represent an immediate safety hazard. This is evidenced by at least three results of the subject program:

1. Approximately 18% of the roller bearing population in the fleet are condemnable by AAR rules, yet only about 0.001% fail to the point where they cause accidents each year.
2. Only about 0.02% of the population are set out each year for cause.
3. None of the ten defective (well beyond AAR limits) bearings failed during the 6000-mile, full-load, high-speed test.

That is not to say that there is no roller bearing failure problem because the few failures that do occur are very costly and are life-endangering. Furthermore, the failure rate has been shown to be increasing because of the increasing age of the population. What it does say is that the more cost-effective solutions appear to be closer to the point of actual bearing failure. In other words, a diagnostic system designed to warn of a potential bearing failure within the next few hundred miles should be developed.

There is considerable evidence that temperature-based diagnostic systems cannot reliably provide warning of rolling element bearing failures beyond a few miles, making them questionable contenders from an economic standpoint. On the other hand, vibration-based systems do not appear to offer the potential for reliable failure detection* and disperse deployment. Thus, it is recommended that emphasis be continued on a vibration-based diagnostic system that has potential for wayside deployment.

Clearly before such a system can be developed one needs to understand the mechanism of the final failure process and the precursors of that process. This can only be gained experimentally and must involve testing of many severely damaged bearings containing a variety of failure-producing defects. Laboratory (as opposed to field) experimentation is most appropriate, at least for the initial experiments. The objectives of such an experimental program should include:

1. Obtaining a better understanding or definition of the manner in which railcar roller bearings fail,
2. Obtaining a definition of an accept-reject criterion in terms of expected miles to failure,
3. Obtaining a laboratory demonstration of the viability of a vibration-based diagnostic system to recognize the advent of a predefined "reject level" through an appropriate coupling mechanism,
4. A definition of a field test verification experiment.

---

*It should be pointed out that no system, including vibration, can predict fracture. Thus, some potential failures will always slip by.

6. REFERENCES

1. Anonymous, "Yearbook of Railroad Facts," Association of American Railroads, Washington DC, 1974.

2. Anonymous, "Journal Failure Report," Federal Railroad Administration, Washington DC, October, 1972.

3. Waldron, W.D., McGrew, J.M. and Krauter, A.I., "Improvement of Railroad Roller Bearing Test Procedures and Development of Roller Bearing Diagnostic Techniques, Volume I - Certification," DOT-TSC-FRA-81-6, I/FRA/ORD-81/28,I, March 1981.

4. Anonymous, Roller Bearing Manual, Third Edition, Association of American Railroads, May 1, 1974.

5. Letter from C.R. Kaelin, Santa Fe Railway Company, Chicago, Ill, dated November 29, 1974, File No. 96-06.55; Enclosure File No. TB-17.5.

6. "NYC's Electric Eye Detector Catches High Loads," Railway Age, June 13, 1960, p 94.

7. Ultrasonic Probe Detects Rail Flaws, Electronics and Power 17; 217 (1971).

8. "All about Signals," Kalmbach Publishing Co., (Reprint from) Trains, June-July, 1957.

9. O'Steen, J.H., "Department of Transportation System for Train Accident Reduction (DOT-STAR)," presented at the 26th Meeting of the Mechanical Prevention Failure Group, May 1977, National Bureau of Standards Publication, NBS 494.

10. Sawatari, T., Keating, P.N., and Zipin, R.B., "Experimental Analysis of Surface Flaw Detection Using Grazing Angle Illumination," Applied Optics, Volume 12: No.11, November 1973.

11. Seifert, W.W., Westcott, V.C., "A Method for the Study of Wear Particles in Lubricating Oil," Wear, 21, 27 (1972).

12. Frarey, J.L., Smith, R.L., and Krauter, A.I., "Wayside Derailment Inspection Requirements Study for Railroad Vehicle Equipment," DOT-TSC-FRA-77-5/FRA/ORD-77/18, Final Report, May 1977, PB271244.

13. Furey, J.M., "Metallic Contact and Friction Between Sliding Surfaces," ASLE Transactions 4, 1961.

14. Wilson, D.S. and Frarey, J.L., "Investigations of a Bearing Fault Detector for Railroad Bearings," Shaker Research Corporation, Ballston Lake, NY, Report No. 75-TR-14, prepared under Contract NAS8-31449.

APPENDIX A

COST MODEL COMPUTER PROGRAM

PATH NUMBER	NUMBER BEARINGS	COST/ BEARING	PATH COST	PATH COST SENS
1	8549080			
2	538920	$137.97	$74354792.40	0.6097
3	110225	$33.02	$3639645.46	0.0298
4	8359	$136.53	$1141284.20	0.0093
7	110225	$-6.10	$-672375.44	-0.0055
8	8359	$-6.10	$-50991.23	-0.0004
11	86	$120300.00	$10345800.03	0.0848
12	444552160			
13	445091080	$0.01	$4450910.80	0.0365
14	567098			
15	444523981			
17	567098			
19	444523981			
20	567098			
21	54511	$13.64	$743543.61	0.0060
22	512585	$2.56	$1312222.62	0.0107
23	395365			
24	340832			
25	54532	$68.99	$3762231.61	0.0308
27	54532			
28	54511	$1.44	$78497.27	0.0006
29	395344			
30	7728			
31	387616			
33	387616			
34	7728			
35	196163	$15.08	$2958153.00	0.0242
37	196163			
38	7728			
39	9467	$172.13	$1629726.70	0.0133
40	6311	$363.20	$2292518.19	0.0188
41	3155			
42	3155	$614.45	$1939204.02	0.0159
43	3155	$258.20	$814879.12	0.0066
44	6311			
46	3155	$28.00	$88367.99	0.0007
47	631			
48	2524	$2.50	$6311.99	0.0000
49	631			
50	583780	$2.50	$1459452.40	0.0119
52	583780	$1.80	$1050805.73	0.0086
53	586305	$1.80	$1055350.37	0.0086
54	586305			
56	110225			
57	476080	$0.60	$285648.16	0.0023
58	476080			
59	586305	$11.79	$6912544.94	0.0566
60	594664	$1.44	$856317.57	0.0070
61	594664	$2.50	$1486662.45	0.0121
63	54532			
64	1107251			
TOTALS			121941504.06	1.0000

A-2

BRANCH NODE	SENS = $/%
1	$1573.40/%
3	$29359186.80/%
4	$166724142.24/%
5	$563916.12/%
8	$238122.50/%
9	$10284543239.90/%
10	$2985394.64/%
11	$-156250.27/%
12	$16855.92/%
15	$422986.87/%
16	$414718.52/%
18	$3629782.06/%
19	$209879.46/%
22	$62430412.18/%
23	$79265.45/%
24	$27241.73/%
26	$1863.09/%
27	$3433.47/%
30	$103748.61/%
32	$0.00/%
33	$154315.67/%
38	$0.00/%

```
5 DEFFN '00"LISTS":SELECT PRINT 005
10 DIM G$(50)12,N(65),A(65),Q(65),C$(75)1
20 DIM Z(2),S(2),D(2),K(2),L(2),M(2),B1(6),B(65,3)
30 GOTO 9000
1000 DEFFN '01(X,R,S,T)
1010 ON X GOTO 1020,1030,1040,1050,1060,1070,1080,1090,1100,1110,1120,11
30,1140,1150,1160,1170,1180,1190,1200,1210,1220,1230
1020 REM B  1: A1=1:C=52                                :GOTO 1270
1030 REM B  2: A1=1:C=1.2741189E-3                      :GOTO 1270
1040 REM B  3: A1=1:C=0                                 :GOTO 1270
1050 REM B  4: A1=1:C=0                                 :GOTO 1270
1060 REM B  5: A1=1:C=9.6124309E-2                      :GOTO 1270
1070 REM B  6: A1=1:C=1.0059562E-5                      :GOTO 1270
1080 REM B  7: A1=1:C=4.6246613E-2                      :GOTO 1270
1090 REM B  8: A1=1:C=.862069576                        :GOTO 1270
1100 REM B  9: A1=1:C=0                                 :GOTO 1270
1110 REM B 10: A1=1:C=1.95475332E-2                     :GOTO 1270
1120 REM B 11: A1=1:C=0                                 :GOTO 1270
1130 REM B 12: A1=1:C=2.2945626E-2                      :GOTO 1270
1140 REM B 13: A1=1:C=0                                 :GOTO 1270
1150 REM B 14: A1=1:C=1.1074875E-3                      :GOTO 1270
1160 REM B 15: A1=1:C=.66666666                         :GOTO 1270
1170 REM B 16: A1=1:C=.5                                :GOTO 1270
1180 REM B 17: A1=1:C=0                                 :GOTO 1270
1190 REM B 18: A1=1:C=.2                                :GOTO 1270
1200 REM B 19: A1=1:C=0                                 :GOTO 1270
1210 REM B 20: A1=1:C=1                                 :GOTO 1270
1220 REM B 21: A1=1:C=.188                              :GOTO 1270
1230 REM B 22: A1=1:C=1                                 :GOTO 1270
1270 IF S7<=0 THEN 1330: IF X<>S7 THEN 1330
1280 J7=J:CONVERT STR(G$(J7),10,3) TO G7:N7=N(G7):C=C+.01
1330 Q1=1: N1=C
1350 RETURN
2000 DEFFN '02(I,N(I),A(I))
2010 IF C$(I)<>"0" THEN 2020: J=J+1: C=0: RETURN
2020 J1=I-J
2030 ON J1 GOTO 2040,2050,2060,2070,2080,2090,2100,2110,2120,2130,2140,2
150,2160,2170,2180,2190,2200,2210,2220,2230,2240,2250,2260,2270,2280,229
0,2300,2310,2320,2330
2040 REM C  1: C=N(I)*     137.97:B(2,2)=137.97        :GOTO 2340
2050 REM C  2: C=N(I)*      33.02 :B(3,2)=33.02        :GOTO 2340
2060 REM C  3: C=N(I)*     136.53 :B(4,2)=136.53       :GOTO 2340
2070 REM C  4: C=N(I)*    (-6.10):B(7,2)=-6.10         :GOTO 2340
2080 REM C  5: C=N(I)*    (-6.10):B(8,2)=-6.10         :GOTO 2340
2090 REM C  6: C=N(I)*120300.00 :B(11,2)=120300.       :GOTO 2340
2100 REM C  7: C=N(I)*        .01 :B(13,2)=.01         :GOTO 2340
2110 REM C  8: C=N(I)*      30.91 :B(18,2)=30.91       :GOTO 2340
2120 REM C  9: C=N(I)*      13.64 :B(21,2)=13.64       :GOTO 2340
2130 REM C 10: C=N(I)*       2.56 :B(22,2)=2.56        :GOTO 2340
2140 REM C 11: C=N(I)*      68.99 :B(25,2)=68.99       :GOTO 2340
2150 REM C 12: C=N(I)*       1.44 :B(31,2)=1.44        :GOTO 2340
2160 REM C 13: C=N(I)*      15.08 :B(35,2)=15.08       :GOTO 2340
2170 REM C 14: C=N(I)*     172.13 :B(39,2)=172.13      :GOTO 2340
2180 REM C 15: C=N(I)*     363.20 :B(40,2)=363.20      :GOTO 2340
2190 REM C 16: C=N(I)*     614.45 :B(42,2)=614.45      :GOTO 2340
```

```
2200 REM C 17: C=N(I)*    258.20 :B(43,2)=258.20     :GOTO 2340
2210 REM C 18: C=N(I)*     28.00 :B(46,2)=28.        :GOTO 2340
2220 REM C 19: C=N(I)*      2.50 :B(48,2)=2.50       :GOTO 2340
2230 REM C 20: C=N(I)*      2.50 :B(50,2)=2.50       :GOTO 2340
2240 REM C 21: C=N(I)*      1.80 :B(52,2)=1.80       :GOTO 2340
2250 REM C 22: C=N(I)*      1.80 :B(53,2)=1.80       :GOTO 2340
2260 REM C 23: C=N(I)*       .60 :B(57,2)=.60        :GOTO 2340
2270 REM C 24: C=N(I)*     11.79 :B(59,2)=11.79      :GOTO 2340
2280 REM C 25: C=N(I)*      1.44 :B(60,2)=1.44       :GOTO 2340
2290 REM C 26: C=N(I)*      2.50 :B(61,2)=2.50       :GOTO 2340
2300 REM C 27: C=0                                   :GOTO 2340
2310 REM C 28: C=0                                   :GOTO 2340
2320 REM C 29: C=0                                   :GOTO 2340
2330 REM C 30: C=0                                   :GOTO 2340
2340 IF S7>=0 THEN 2360: IF J1<>(-S7) THEN 2360
2350  C=C+1
2360 RETURN
3000 DEFFN'11: MAT K=D: MAT Z=(T1/2)*D: MAT Z=Z+S: RETURN
4000 DEFFN'12: MAT L=D: MAT Z=(T1/2)*D: MAT Z=Z+S: RETURN
5000 DEFFN'13: MAT M=D: MAT Z=(T1)*D: MAT Z=Z+S: RETURN
6000 DEFFN'14
6010 REM PATH 1 IDENTIFIES THE STATE VARIABLES. PATH 2 PROVIDES
6020 REM FOR EXPANSION OF THE COMPONENT'S POPULATION
6030 N(1)=Z(1): A(1)=Z(2):J=0
6040 J=J+1: PRINT J
6050 CONVERT STR(G$(J),1,3) TO X
6060 CONVERT STR(G$(J),4,3) TO R
6070 CONVERT STR(G$(J),7,3) TO S
6080 CONVERT STR(G$(J),10,3) TO T
6090 IF X=0 THEN 6120
6100 IF X>Z2 THEN 6110: GOTO 6190
6110 STOP "ERROR IN BRANCH POINT DATA"
6120 N(T)=N(R)+N(S): N3=N(T)+1.0E-25
6130 A(T)=(N(R)*A(R)+N(S)*A(S))/N3
6160 IF T<7 THEN 6180: IF T>10 THEN 6370
6170 N(T-4)=N(T): A(T-4)=0
6180 GOTO 6370
6190 GOSUB '01(X,R,S,T)
6200 IF R<>1 THEN 6220: N(S)=N1*N(R): A(S)=A1*A(R): Q(S)=Q1*Q(R)
6210 GOTO 6350
6220 N2=1-N1+1.0E-25
6230 N3=N1+1.0E-25
6240 IF N1>0 THEN 6250: N1=0
6250 IF N1<1 THEN 6260: N1=1
6260 IF A1>1 THEN 6270: A1=1
6270 IF A1<1/N3 THEN 6300: A1=1/N3
6300 N(S)=N1*N(R): A(S)=A1*A(R)
6310 N(T)=N(R)-N(S)
6320 A(T)=(1-N1*A1)*A(R)/N2
6350 IF S<7 THEN 6370: IF S>10 THEN 6370
6360 N(S-4)=N(S): A(S-4)=0
6370 IF J<>Z1 THEN 6040
6380 REM N(2)=N(11): REM CAT. FAILURE FLOW COMP. USING THIS LINE
6390 D(1)=N(2)-N(11): D(2)=1-(N(2)-N(11))*A(1)/N(1)
6400 FOR I=7 TO 11: D(2)=D(2)-A(I)*N(I)/N(1): NEXT I
```

```
6450 RETURN
7000 DEFFN'15: SELECT P0: SELECT PRINT 005
7010 IF T0<>0 THEN 7020: SELECT P2
7020 IF A=0 THEN 7030: SELECT P0: SELECT PRINT 01D
7030 IF A7=0 THEN 7040: SELECT P0: SELECT PRINT 005
7040 PRINT :PRINT :PRINT T9
7042 PRINT "NUMBER IN FIELD = ";Z(1);PRINT
7050 PRINTUSING 7070
7060 IF A7=1 THEN 7080: IF A=1 THEN 7120
7070%LIN  BRGS/YEAR LIN   BRGS/YEAR LIN   BRGS/YEAR LIN   BRGS/YEAR
7071 PRINT
7080       FOR I=1 TO Z3/4
7090 PRINTUSING 7100,I,N(I),I+16,N(I+16),I+32,N(I+32),I+48,N(I+48):FOR B
8=0 TO 63 STEP 16:B(I+B8,1)=N(I+B8):NEXT B8
7100%### ########### ### ########### ### ########### ### ###########
7110       NEXT I
7120 J=0: C0=0: PRINT
7130       FOR I=1 TO Z3
7140 GOSUB '02(I,N(I),A(I)): C0=C0+C
7150 IF A7=1 THEN 7160: IF A=1 THEN 7180
7160 PRINTUSING 7170,I,C$(I),C
7170% PATH ###;  COST PATH=#    PATH COST =$##########.##
7180       NEXT I
7190 PRINTUSING 7200,C0:PRINT
7200% TOTAL COST = $##########.##
7210 SELECT P0: SELECT PRINT 005: RETURN
8000 DEFFN'16
8010 SELECT PRINT 005: IF A=0 THEN 8020: SELECT PRINT 01D(72)
8020 IF S7<>0 THEN 8030: S7=S7+1: C7=C0: PRINT : RETURN
8030 IF S7<0 THEN 8090:R7=(C0-C7)/1
8033 CONVERT STR(G$(J7),7,3) TO B7:CONVERT STR(G$(J7),10,3) TO G7:CONVER
T STR(G$(J7),4,3) TO F7
8040 PRINTUSING 8050,J7,R7
8044 IF N(G7)=N7 THEN 8050
8045 B(B7,3)=R7*W7/C7/.01:B(G7,3)=((R7*W7/C7)*.01)/((N(G7)-N7)/N7)
8050%##           $############.##/%
8070 S7=S7+1:IF S7>Z2 THEN 8080:RETURN
8080 PRINT : S7=-1: RETURN
8090 R7=(C0-C7)/1:REM PRINTUSING 8100,-S7,R7
8100% COST PATH ###,     SENSITIVITY = $################.##/$
8110 S7=S7-1: IF S7<-Z4 THEN 8120: RETURN
8120 S7=0: T9=T0: PRINT : RETURN
9000 INIT(20) G$(): INIT(30) C$(): S7=0: T7=1
9010 REM * * * Z1 IS THE NUMBER OF NODE POINTS (BRANCH & SUM)
9020 READ Z1: DATA 41
9030 REM * * * Z2 IS THE NUMBER OF BRANCH POINTS
9040 READ Z2: DATA 22
9050 REM * * * Z3 IS THE TOTAL NUMBER OF PATHS
9060 READ Z3: DATA 64
9070 REM * * * Z4 IS THE NUMBER OF PATHS WITH ASSOCIATED COST
9080 READ Z4: DATA 26
9090 MAT REDIM G$(Z1)13: MAT REDIM N(Z3+1): MAT REDIM A(Z3+1)
9110 REM PATH Z3+1 IS 'DUMPING GROUND' FOR MANY OF THE FLOWS
9120 REM BACK TO THE 'FIELD'
```

```
9130       FOR I=1 TO Z1
9140 READ G1: CONVERT G1 TO STR(G$(I),1,3),(###)
9150 REM THIS PART OF G$() IDENTIFIES THE BRANCH/SUMMATION NODES
9160 DATA 1, 0, 2, 3, 4, 0, 0, 5, 6, 7, 8, 9, 0, 0, 10, 11, 0, 12, 13, 0
, 0,14, 15, 16, 0, 17, 18, 0, 0, 19, 0, 20, 21, 0, 0, 0, 0,22,0,0,0
9170       NEXT I
9180       FOR I=1 TO Z1
9190 READ G1,G2,G3: IF G3<>1 THEN 9200: G3=Z3+1
9200 CONVERT G1 TO STR(G$(I),4,3),(###)
9210 CONVERT G2 TO STR(G$(I),7,3),(###)
9220 CONVERT G3 TO STR(G$(I),10,3),(###)
9230 REM THIS PART OF G$() DEFINES SYSTEM TOPOLOGY. IF SUMMATION
9240 REM NODE, 1ST TWO NUMBERS ARE 'FROM PATHS' & THIRD IS 'TO'
9250 REM PATH. IF BRANCH NODE, 1ST NUMBER IS 'FROM' PATH, SECOND
9260 REM NUMBER IS 'TO-BAD' PATH, & THIRD NUMBER IS 'TO-GOOD' PATH
9270 DATA  1,12, 1,   2,12,13,   13,14,15,   15,18,19,    1,16, 1,
  14,16,17,   17,18,20,   20,21,22,    1,11, 1,    1,23, 1
9280 DATA 23,24,25,   25,26,27,   21,26,28,   24,28,29,   29,30,31,
  31,32,33,   30,32,34,    1,35, 1,   35,36,37,   33,37,50
9290 DATA 36,34,38,    1,39, 1,   39,40,41,   40,42,43,   41,'3,44,
  42,45,46,   46,47,48,   45,47,49,   38,49, 8,   50,51,52
9292 DATA 48,52,53,   53,54,55,   54,56,57,   51,56, 7,   55,57,58,
   3,58,59,    4,59,60,   60,61,62,   27,62,63,   22,61,64
9294 DATA 19,64,65
9310       NEXT I
9320 REM NOTE - THE FIVE PATHS 7-11 ARE RESERVED FOR SCRAP
9330 REM YARD PATHS. THE FLOWS IN PATHS 7-10 ARE COMPENSATED
9340 REM BY MANUFACTURERS FLOWS IN PATHS 3-6, RESPECTIVELY.
9350 REM THE FLOW IN PATH 11 IS A NON-COMPENSATED SCRAP YARD
9355 PRINT HEX(03):PRINT "0=NO     1=YES":PRINT
9360 REM FLOW.
9430 INPUT "DO YOU WANT TOPOLOGY PRINTOUT (1 OR 0)",A
9440 IF A=0 THEN 9490: SELECT PRINT 01D
9450       FOR I=1 TO Z1
9460 PRINTUSING 9470,I,STR(G$(I),1,3),STR(G$(I),4,3),STR(G$(I),7,3),STR(
G$(I),10,3),STR(G$(I),13,1)
9470%NODE ####    BN=###     FP=###     BP/FP=###     GP/TP=###     #
9480       NEXT I: SELECT PRINT 005
9490       FOR I=1 TO Z3
9500 READ A: CONVERT A TO C$(I),(#)
9510 REM C$() IDENTIFIES THOSE PATHS HAVING ASSOCIATED COSTS
9520       NEXT I
9530 DATA 0,1,1,1,    0,0,1,1,    0,0,1,0,    1,0,0,0
9540 DATA 0,1,0,0,    1,1,0,0,    1,0,0,1,    0,0,0,0
9550 DATA 0,0,1,0,    0,0,1,1,    0,1,1,0,    0,1,0,1
9552 DATA 0,1,0,1,    1,0,0,0,    1,0,1,1,    1,0,0,0
9559 PRINT HEX(03): PRINT "0 = TIME SIMULATION":PRINT "1 = SENSITIVITY A
NALYSIS":PRINT
9560 INPUT "SENSITIVITY ANALYSIS (1 OR 0)",A7
9567 PRINT HEX(03):PRINT "0 = CRT OUTPUT ONLY":PRINT "1 = SIMULATION LIM
ITED PRINTED OUTPUT":PRINT "2 = SIMULATION FULL PRINTED OUTPUT":PRINT
9570 INPUT "HARD COPY (0, 1, OR 2)",A
9580 REM ---------------- START OF COMPUTATION ----------------
9590 M1=2: MAT READ Z: DATA 5549050,5
9600 READ T0,T1,T2,N(2): DATA 10,1,1,536920
9620 T9=0: I9=T2: GOTO 9690
9630 MAT S=Z: GOSUB '14: IF I9>0 THEN 9640:GOSUB '15
9640 IF A7=0 THEN 9650:GOSUB '16:GOSUB '5: SELECT PRINT 005: IF T9=0 THE
N 9630
```

```
9650 IF T<<T0 THEN 9660:END
9660 GOSUB '11: T9=T9+T1/2: GOSUB '14: GOSUB '12
9670 GOSUB '14: GOSUB '13: T9=T9+T1/2: GOSUB '14
9680 FOR I=1TO M1:Z(I)=S(I)+T1*(K(I)+2*L(I)+2*M(I)+D(I))/6:NEXT I
9690 I9=I9+1: IF I9<T2 THEN 9630: I9=0: GOTO 9630
9700 DEFFN'5:REM PRINT ALL RESULTS:IF B1(4)<>0 THEN 9999
9710 PRINT :PRINT " PATH   NUMBER        COST/        PATH   PATH COST "
;
9720 PRINT "NUMBER BEARINGS      BEARING       COST      SENS  "
9724 PRINTUSING 9725
9725%-----------------------------------------------------
9740 PRINT :MAT B1=ZER
9750 FOR I=1 TO 65
9755 IF B(I,1)=0 THEN 9860
9760 FOR J=1 TO 5
9770 ON J GOTO 9780,9790,9800,9810,9820
9780 PRINT TAB(1):PRINTUSING 9989,I;:GOTO 9840
9790 PRINT TAB(5);  :IF B(I,1)=0 THEN 9840:PRINTUSING 9991,B(I,1);:B1(2)=
B1(2)+B(I,1):GOTO 9840
9800 PRINT TAB(16);:IF B(I,2)=0 THEN 9840:PRINTUSING 9993,B(I,2);:GOTO 9
840
9810 PRINT TAB(29);:IF B(I,2)=0 THEN 9840:PRINTUSING 9995, B(I,1)*B(I,2)
;:B1(4)=B1(4)+B(I,1)*B(I,2):GOTO 9840
9820 PRINT TAB(44);:IF B(I,2)=0 THEN 9840:PRINTUSING 9990,(B(I,1)*B(I,2)
/C7);:B1(5)=B1(5)+(B(I,1)*B(I,2)/C7)
9840 NEXT J
9841 GOTO 9860:PRINT TAB(54);:IF B(I,3)=0 THEN 9860:PRINTUSING 9990,B(I,
3);:B1(6)=B1(6)+B(I,3)
9860 NEXT I :PRINT :  PRINTUSING 9725:PRINT
9870 PRINTUSING 9880,B1(4),B1(5)
9880%TOTALS                    ############.##    #.####    #.####
9989%##
9990%-#.####
9991%##########
9993%$#######.##
9994%$#######.##
9995%$#########.##
9996%$###########.##
9998 PRINT :PRINT :PRINT : PRINT "BRANCH NODE          SENS = $/%":PRINT

9999 RETURN
```

APPENDIX B

REPORT OF NEW TECHNOLOGY

Essentially all known basic diagnostic techniques applicable to the roller bearing failure problem were reviewed, and several were identified as potentially feasible. Although conceptual adaptations of existing techniques were identified, no inventions appear to have resulted from this work.

However, this study did result in an improvement in knowledge about the experimental feasibility vibration based diagnostic approaches. Included in this work was an actual demonstration of a relatively simple diagnostic system in an actual railroad wheel shop. With minimal future development, such a system could be widely deployed to test bearings for gross defects without removing them from the axle. The experimental work is covered in Section 3.

Section 4. describes an improved mathematical model developed to perform cost-benefit analyses of innovative railcar roller bearing diagnostic approaches and procedural (operational) modifications. Included in this section are results of cost analyses which set the ground rules for allowable on-board and wayside bearing fault (diagnostic) system costs.

31 Copies

U.S. Department
of Transportation

Research and
Special Programs
Administration

Kendall Square
Cambridge, Massachusetts 02142